Atmosphere-Soil-Stream Greenhouse Gas Fluxes from Peatlands

Kerry J. Dinsmore [1,2,3]

Doctor of Philosophy

University of Edinburgh

October 2008

[1]School of Geosciences, University of Edinburgh, The King's Buildings, Edinburgh

[2]Centre for Ecology and Hydrology, Bush Estate, Edinburgh

[3]Scottish Agricultural College, The King's Buildings, Edinburgh

Declaration

I declare that this thesis and the papers within it have been composed by myself and that no part of this thesis has been submitted for any other degree or qualification. The work described is my own unless otherwise stated.

Kerry Dinsmore

October 2008

Abstract

Peatlands cover approximately 2-3% of the world's land area yet represent approximately a third of the worlds estimated total soil carbon pool. They therefore play an important role in regulating global atmospheric CO_2 and CH_4 concentrations, and even minor changes in their ability to store carbon could potentially have significant effects on global climate change. Much previous research has focussed primarily on land-atmosphere fluxes. Where aquatic fluxes have been considered, they are often in isolation from the rest of the catchment and usually focus on downstream losses, ignoring evasion (degassing) from the water surface. However, as peatland streams have been repeatedly shown to be highly supersaturated in both CO_2 and CH_4 with respect to the atmosphere, they potentially represent an important pathway for catchment GHG losses. This study aimed to a) create a complete GHG and carbon budget for Auchencorth Moss catchment, Scotland, linking both terrestrial and aquatic fluxes, and b) understand what controls and drives individual fluxes within this budget. This understanding was further developed by a short study of C exchange at the peat-aquatic interface at Mer Bleue peatland, Canada.

Significant variability in soil-atmosphere fluxes of both CH_4 and N_2O emissions was evident at Auchencorth Moss; coefficients of variation across 21 field chambers were 300% and 410% for CH_4 and N_2O, respectively. Both *in situ* chamber measurements and a separate mesocosm study illustrated the importance of vegetation in controlling CH_4 emissions. In contrast to many previous studies, CH_4 emissions were lower and uptake greater where aerenchymous vegetation was present. Water table depth was also an important driver of variability in CH_4 emissions, although the effect was only evident during either periods of extreme drawdown or when the water table was consistently near or above the peat surface. Significant pulses in both CH_4 and N_2O emissions were observed in response to fluctuations in water table depth. Despite the variability in CH_4 and N_2O emissions and the uncertainty in up-scaled estimates, their contribution to the total GHG and carbon budgets was minor.

Concentrations of dissolved CO_2 in peatland drainage waters ranged from a mean of 2.88 ± 0.09 mg C L^{-1} in the Black Burn, Scotland, to a mean of 7.64 ± 0.80 mg C L^{-1} in water draining Mer Bleue, Canada. Using non-dispersive infra-red (NDIR) CO_2 sensors with a 10-minute measurement frequency, significant temporal variability was observed in aquatic CO_2 concentrations at the 2 contrasting field sites. However, the drivers of this variability differed significantly. At Mer Bleue, Canada, biological activity in the water column led to clear diurnal cycles, whereas in the Black Burn draining Auchencorth Moss, dilution due to discharge was the primary driver. The NDIR sensor data also showed differences in soil-stream connectivity both between the sites (connectivity was weak at Mer Bleue) and across the range of conditions measured at Auchencorth Moss i.e. connectivity increased during periods of stormflow.

Compiling the results from both the terrestrial and aquatic systems at Auchencorth Moss indicated that the catchment was functioning as a net sink for GHGs (382 kg CO_2-eq ha^{-1} yr^{-1}) and a net source of carbon (143 kg C ha^{-1} yr^{-1}). The greatest flux of GHGs was via net ecosystem exchange (NEE). Terrestrial emissions of CH_4 and N_2O combined returned only ~5% of CO_2-equivalents captured by NEE to the atmosphere, whereas evasion of CO_2, CH_4 and N_2O from the stream surface returned ~40%. The budgets clearly show the importance of aquatic fluxes at Auchencorth Moss and highlight the potential for significant error in source/sink strength calculations if they are omitted. Furthermore, the process based understanding of soil-stream connectivity suggests the aquatic flux pathway may play an increasingly important role in the source-sink function of peatlands under future management and climate change scenarios.

Acknowledgements

I would like to thank my supervisors Mike Billett, Ute Skiba and Bob Rees for their support, guidance and encouragement throughout my PhD. I would also like to thank everyone at the 'Centre for Ecology and Hydrology' (CEH) Edinburgh for their ongoing support and advice, and for their open and friendly attitudes to me, to my work and to my never-ending string of questions. In particular, thanks to Frank Harvey and Robert Storeton-West for helping me set-up and run my field studies, Lucy Sheppard and Ian Leith for support and advice during all stages of the project and especially to Julia Drewer, Esther Vogt, Rebecca McKenzie and Jan Dick who all braved the Scottish weather and helped me collect and analyse field data. I'd also like to thank John Parker from the 'Scottish Agricultural College' for his help in the laboratory.

I am extremely grateful to everyone who helped me during my time at Mer Bleue, Canada. In particular Tim Moore who provided advice and support throughout my stay, and to Mike Dalva and Alison DeYoung for assistance with field work and laboratory analysis.

Finally a special thanks to my parents, my brothers, my sister-in-law, my beautiful nephew, my closest friends and my Paul for always supporting me and for keeping me smiling.

This PhD was funded by the Natural Environment Research Council through an algorithm PhD studentship grant

Contents

1. Introduction

Peatlands are characterised by having not only the high water table, poorly oxygenated soils and specialised biota of typical wetlands but also a thick layer of undecomposed plant material. Depleted oxygen levels and acidic conditions caused by prolonged periods of water logging, along with low temperatures, inhibit decomposition and promote the accumulation of organic matter. Peatlands cover only a small proportion of the earth's surface, estimated as between 2-3% (Gorham, 1991; Charman, 2002), yet represent a huge store of soil carbon, approximately 461 Gt in subarctic and boreal peatlands alone (Gorham, 1991). This represents approximately a third of the worlds estimated total soil carbon pool (1576 Gt). In Scotland the contribution of peats is even greater, with peats representing almost two thirds (65 %) of the estimated Scottish soil carbon pool and almost half (46 %) of the soil carbon in Great Britain as a whole (Milne *et al.*, 1997). It has also been claimed that *Sphagnum* mosses, the main constituent of peatland vegetation, contain more carbon in their dead and living tissues than any other plant genus (Clymo *et al.*, 1982). In addition, Northern peatlands are thought to be responsible for approximately 9% of all natural methane emissions (Bartlett *et al.*, 1993).

As precipitation patterns across peatlands change and temperatures increase, water tables are likely to drop. Having lost the conditions favourable for peat formation and carbon accumulation, what was once a large sink for atmospheric carbon may become a significant source. However, lowered water tables may also reduce peatland CH_4 emissions, counteracting the potential increased CO_2 emissions in terms of net GHG exchange. Another important consequence of climate change is the thawing of northern permafrost, the climatic feedback of which is uncertain. Although the subsequent activation of previously dormant peat layers and increase in microbial activity is likely to result in a net loss of carbon from the soil (Fray *et al.*, 2005), the development of thaw-water ponds and the successional processes of terrestrialization may lead to greater carbon uptake (Payette *et al.*, 2004). This study however focuses only on active northern peatlands and does not consider the permafrost regions further. Recent studies have found significant increases in the

volume of dissolved organic carbon exported from streams and rivers in the UK and across large areas of Europe and North America (Hejzlar *et al.*, 2003; Stoddard *et al.*, 2003; Worrall *et al.*, 2004; Skjelkvåle *et al.*, 2005), possibly indicative of an increase in carbon loss from soil reservoirs (Worrall *et al.*, 2004). It is therefore becoming increasingly important to understand and predict the biospheric feedbacks of peatlands to climate.

The availability of eddy covariance techniques allowing for long term, high frequency measurements of net ecosystem exchange have meant that many peatland budgets focus primarily on CO_2 exchange and almost exclusively on land-atmosphere fluxes (Syed *et al.*, 2006; Ball *et al.*, 2007; Miglietta *et al.*, 2007; Nagy *et al.*, 2007). However, recent work has shown that ignoring fluxes through the aquatic pathway can lead to significant underestimation of total catchment carbon losses (Hope *et al.*, 2001; Richey *et al.*, 2002; Billett *et al.*, 2004; Cole *et al.*, 2007; Jonsson *et al.*, 2007). Our knowledge of catchment fluxes is based primarily on isolated studies which focus on either the terrestrial or the aquatic system. Very little is known about the export and evasion of N_2O from peatland drainage waters which, with a global warming potential of 298 (IPCC, 2007), may be important to the catchment greenhouse gas (GHG) budget. Studies such as those carried out in the Hubbard Brooke experimental forest (Likens, 1985) have shown the advantages of a whole-watershed approach in understanding complex interactions and cause-effect relationships in natural ecosystems. They illustrate the limitations of isolated landscape studies when trying to gain a complete functional understanding of full ecosystem processes.

It is important to quantify both the carbon and the GHG budget of a catchment. Considering only the catchment carbon budget ignores the form of carbon gained or lost and hence takes no account of the radiative properties or global warming potential of gaseous fluxes. Furthermore, the carbon budget ignores fluxes of N_2O, a GHG with a global warming potential 298 times stronger than CO_2 (IPCC, 2007). Considering only the GHG budget ignores the lateral export of dissolved carbon which could potentially be released to the atmosphere as a GHG downstream of the study site. Hence to gain a true understanding of the biospheric significance of

peatlands to global climate, both budgets need to be quantified and examined individually.

This thesis therefore aimed to use this whole-watershed approach to both quantify and understand what controls fluxes of GHGs and carbon through the atmosphere-soil-stream system in peatland catchments. Specific aims were:

- To identify what controls variability in soil-atmosphere CH_4 and N_2O emissions (Papers I and II)
- To quantify annual emissions of CH_4 and N_2O from Auchencorth Moss (Paper I)
- To understand soil-stream connectivity in peatlands by considering two contrasting catchments (Papers III and IV)
- To investigate temporal variability in aquatic fluxes and to identify drivers of variability where it exists (Papers III and IV)
- To calculate a complete peatland flux budget and identify whether it acts as a sink or source of GHGs and of carbon on an annual scale, and to quantify the relative contribution of aquatic fluxes to these budgets (Results and Discussion).

2. Scientific Background

Analysis of near surface air temperature has revealed a global temperature increase of 0.74 ± 0.18°C over the 20th century (IPCC, 2007). Figure 1 illustrates the change in global near-surface temperatures since 1850. Although significant variability can be seen from year to year, the upward trend is clearly visible. Changes in many biological and physical systems are already being seen in response to climate warming such as glacier shrinkage, permafrost thawing, sea level rises and changes in growing seasons and animal migrations (Stendel *et al.*, 2002; Su *et al.*, 2002; Meehl *et al.*, 2005; Beaumont *et al.*, 2006; Linderholm, 2006).

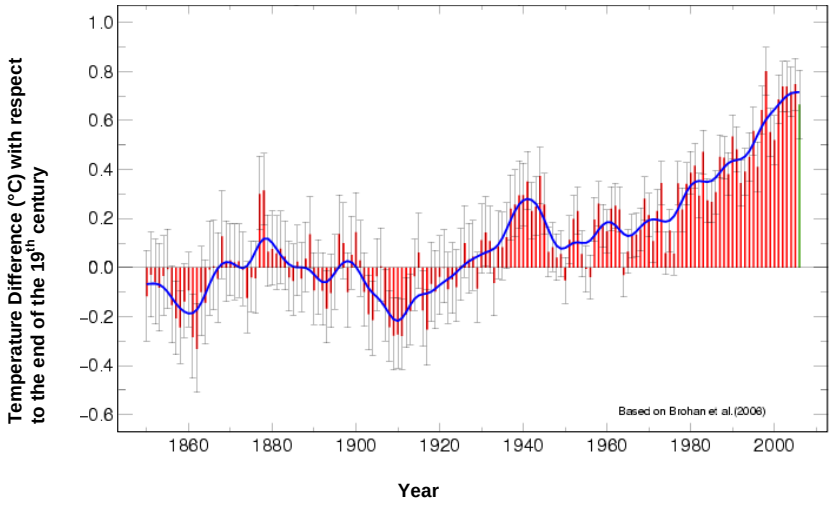

Figure 1. Global average near-surface temperatures from 1850 until 2006 expressed as the difference in °C from temperatures in the last decade of the 19th century. The blue line represents a smoothed trend. (http://www.met-office.gov.uk/research/hadleycentre/CR_data/Monthly/Hadplot_globe.gif).

In addition to increases in surface temperature the latest research suggests an increase in the frequency of extreme events such as heat waves and heavy precipitation and a general increase in precipitation in northern latitudes (IPCC, 2007). An extensive body of research clearly shows that almost all ecosystems are sensitive to environmental change and that factors such as temperature and precipitation heavily influence the internal cycling and fluxes of carbon and of many naturally occurring GHGs (IPCC, 2007 and references therein). Peatlands are particularly vulnerable due to the very specific set of conditions that restrict complete decomposition, and the importance of precipitation and hydrology in their

functioning. Increased temperatures are likely to increase both respiration and photosynthesis, lower water tables may alter CH_4 production and emission, and increased run-off associated with increased precipitation may increase carbon export through the drainage system; the outcome of these changes on the total carbon or GHG budgets are still uncertain. Furthermore, as warming is predicted to be greatest at high latitudes, the geographical position of many northern peatlands is likely to expose them to the extremes of climate change. The loss of peatlands as a carbon sink could lead to important changes in the global GHG budget; the shift in peatland functioning from sink to source represents an important positive feedback to global warming and could have potentially huge effects on the global climate

2.1. Greenhouse gases

Greenhouse gases include naturally occurring atmospheric components such as water vapour, carbon dioxide (CO_2), methane (CH_4), nitrous oxide (N_2O) and ozone (O_3) as well as some primarily industrially produced halogenated substances such as chlorofluorocarbon (CFC), hydrochlorofluorocarbon (HCFC), hydrofluorocarbon (HFC), perfluorocarbon (PFC) and sulphur hexafluoride (SF_6).This study will focus on fluxes of CO_2, CH_4 and N_2O, the most important in peatland ecosystems. Either changes in the atmospheric concentration of these gases or their addition to the atmosphere can alter the balance of radiative transfer between the earth surface, atmosphere and space by absorbing out-going radiation and causing heat to become trapped in the earth-atmosphere system. Differences in the radiative properties of the various greenhouse gases alter the degree of warming they produce. To quantify the different absorption capacities, an index of global warming potentials has been created which scales the warming potential of each gas relative to that of carbon dioxide.

Table 1 Global warming potentials (GWP) for CO_2, CH_4 and N_2O (IPCC, 2007)

Gas		Lifetime (years)	Global warming potential (GWP)		
			20 years	100 years	500 years
Carbon dioxide	CO_2	5-20	1	1	1
Methane	CH_4	12	72	25	7.6
Nitrous oxide	N_2O	114	289	298	153

2.2. Soil-atmosphere exchange

Undisturbed peatlands are generally regarded as a sink for atmospheric CO_2 and a source of CH_4 (Walter *et al.*, 2000; Smith *et al.*, 2004; Sottocornola *et al.*, 2005) though inter-annual variability can be extremely large. Other natural sources of CH_4 include non-peat wetlands, oceans, forest, animals, natural gas seepage in sedimentary basins and geothermal/volcanic CH_4 (IPCC, 2007). In the absence of oxygen and when redox potentials reach levels more negative than -200 mV, methanogens complete the degradation of organic matter (Segers, 1998) and as a by-product, release CH_4. Only a limited number of substrates can support methanogens, with acetate (CH_3COOH) and hydrogen thought to be the initial substrate for approximately 95% of CH_4 production in fresh water systems (Segers, 1998). Alternative substrates include CO_2, CO, formate (HCOOH) and compounds containing a methyl group ($-CH_3$). Oxidation of CH_4 within the soil is carried out by methanotrophic bacteria in the oxic surface soil layer or the aerobic microenvironments of the rhizosphere; these bacteria can utilise CH_4 as a substrate and respire CO_2. Of the total CH_4 assimilated by methanotrophs in a boreal bog, Whalen and Reeburgh (2000) found that approximately 71% was respired as CO_2.

The development of aerenchyma is an adaptation to waterlogged conditions found in many vascular wetland species. Where such species are present, they can act as gas conduits, allowing GHGs produced in the anoxic layer to be transported to the atmosphere with minimal oxidation and can increase emissions by up to an order of magnitude (MacDonald *et al.*, 1998; Minkkinen *et al.*, 2006). However, roots also exert a negative control on CH_4 fluxes. Vascular plant transport provides roots with O_2, some of which leaks into the surrounding soil. This creates oxic conditions in the rhizosphere which can both inhibit production and stimulate the oxidation of CH_4 (Joabsson *et al.*, 1999). Vegetation heterogeneity is therefore likely to lead to significant spatial variability in GHG uptake and emissions over relatively small distances. In addition, the microtopographic pattern of raised hummocks and depressed hollows, common across many peatlands, leads to variation in water table depth, which determines the depth of the oxic/anoxic boundary and redox level within the soil, further enhancing the spatial variability in fluxes.

Soil N_2O production is usually the consequence of one of two processes, aerobic nitrification or anaerobic denitrification. Denitrification is thought to be the dominant production process in soils with water filled pore space greater than 60% (Davidson, 1991; Russow *et al.*, 2000; Wolf *et al.*, 2000; Ruser *et al.*, 2006). Due to the close proximity of aerobic and anaerobic sites within the soil, nitrate produced in an aerobic zone can be utilised in the nearby anaerobic zone by denitrifying bacteria, linking the processes through a common nitrate pool (Russow *et al.*, 2000). N_2O is only an intermediate product of denitrification, total reduction of NO_3^- leads to the production of N_2. Therefore where the site of denitrification allows N_2O to diffuse easily into an oxygenated pore space, further reduction will be prevented and the N_2O may be released to the atmosphere. Hence the release of N_2O from the soil surface via denitrification requires a complex arrangement of anaerobic microsites set within an aerobic network of soil pores (Smith *et al.*, 2003).

Due to the number of processes, controlling factors, interactions between controlling factors and the non-linearity in many of the responses, the study of N_2O emissions is extremely complex. The spatial variability of N_2O emissions, even over very small scales, is often extremely high. Nitrification is dependent primarily on the availability of NH_4^+, O_2 and an adequate supply of CO_2. The availability of these substrates is dependent upon plants and roots through exudation, mortality, nutrient uptake and respiration, the rate of organic matter mineralization or immobilisation, the diffusion properties of the soil and the rate of microbial respiration (Hutchinson, 1995). The same factors along with the rate of nitrification itself, and hence the supply of NO_3^-, also control the rate of denitrification. The high spatial variability in surface fluxes reflects a similarly high variability across small scales within the soil. Due primarily to substrate limitation, N_2O fluxes from peatlands are generally considered to be small. However, where peatlands are located either in areas of high atmospheric nitrogen deposition or in close proximity to agriculture, fluxes may be higher.

2.3. Aquatic fluxes

The acrotelm-catotelm model of peat hydrology considers the peat profile as two distinct zones, an upper aerated layer with fluctuating water table (acrotelm), and a permanently saturated lower layer consisting of highly humified peat (catotelm) (Holden, 2005b). Water movement through the acrotelm is generally considered to be rapid in comparison to the catotelm where water movement is much slower. This has led to the common assumption that runoff production and solute transfer occurs primarily in the near-surface peat. However, due to the much greater depth of the catotelm in the majority of peatlands, despite low hydraulic conductivities the runoff contribution is still likely to be great.

Beckwith *et al* (2003) showed that in many cases lateral water movement was more important than vertical in peat soils, confirming the results of Chason and Siegel (1986) who similarly found a greater horizontal than vertical hydraulic conductivity. The low vertical conductivity results in a build up of dissolved and gaseous solutes in the peat pore water which is then transported to surface water courses via lateral throughflow or macropores/soil pipes (Holden, 2005a). Both the importance of lateral movement and the sheer volume of water contained within peat, suggest strong linkages will be apparent between soil composition and stream water chemistry.

There are 3 forms of carbon commonly identified in streamwater; (i) particulate carbon often associated with turbulence disturbing the stream bed and increased peat erosion following rainfall events (ii) dissolved, i.e. dissolved organic carbon (DOC), bicarbonate (HCO_3^-) or carbonate ions (CO_3^{2-}) or (iii) gaseous such as free CO_2 or CH_4 (Dawson *et al.*, 2004). Although gaseous CO_2 and CH_4 are a form of dissolved inorganic carbon (DIC), for clarity they have been separated throughout the thesis due to the different methods of calculating concentrations and fluxes; therefore any reference to DIC in the remainder of the text does not include CO_2 or CH_4. Peatlands represent a large pool of organic carbon, hence peatland streams are associated with very high levels of allochthonous DOC, especially in catchments where soils are consistently saturated and throughflow primarily occurs in surface organic horizons (Aitkenhead *et al.*, 1999; Billett *et al.*, 2004). Inorganic carbon (DIC) is primarily

derived from the products of carbonate dissolution and weathering of silicate materials (Hope *et al.*, 2004). Gaseous CO_2 and CH_4 concentrations represent either the terrestrially-derived products of soil and root respiration, transported to the drainage system via water movement, or are the product of in-stream or sediment processing. Similarly where N_2O is present in catchment soils it can be transported to surface waters via throughflow, produced in-stream by denitrification in hypoxic or anoxic water and sediments, or by nitrification in well oxygenated surface waters.

As peatland streams and rivers are often highly supersaturated in CO_2 and CH_4 with respect to the atmosphere (Dawson *et al.*, 1995; Hope *et al.*, 2001; Billett *et al.*, 2004; Billett *et al.*, 2008), degassing (evasion) may represent an important conduit for losses of GHGs from the catchment. Very little work has been done considering N_2O concentrations due primarily to the low concentrations expected. However with a GWP of 298 (Table 1) even very low concentrations may have a significant influence on the total GHG budget. The relative importance of N_2O is likely to be extremely site specific, depending on the nitrogen inputs to the catchment from atmospheric deposition and agricultural fertilization.

Gaseous fluxes from water surfaces are the result of disequilibrium between air and water gas concentrations. When streams are supersaturated there will be a net flux to the atmosphere. Supersaturation can result from inputs of water with high dissolved gas concentrations, changes in stream temperature, salinity (Frankignoulle *et al.*, 1998), pH, or in-stream gas production. Stream water pH, through its influence on the carbonate equilibria system, controls the proportion of free CO_2 in the water. As many headwater streams are fed predominantly by shallow ground water inputs which flow through deep peat deposits, low pH values are common hence much of the inorganic carbon is in the form of CO_2.

Other non-biological influences are exerted by temperature and pressure. Henry's law states that the mass of a gas that dissolves in a definitive volume of liquid is directly proportional to the pressure of the gas provided the gas does not react with the solvent. This gives rise to Equation 1 below, where C_{gas} is the concentration of dissolved gas, k_h is the Henry's law constant for that particular gas species and P_{gas} is the partial pressure of gas above the solution. The value of k_h is temperature

dependent, increasing with increasing temperature. Therefore with increasing temperature the solubility of gases decrease and the rate of dissolution increases.

Equation 1 $$C_{gas} = k_h P_{gas}$$

Turbulence is important as it determines the rate at which water at the degassing interface is recharged with water deeper in the profile where gas concentrations are more representative of the stream as a whole (MacIntyre *et al.*, 1995). It also causes physical disturbance which increases the rate at which gas can travel across the water-atmosphere boundary. Turbulence can be a major cause of spatial variation within streams, with highly turbulent areas becoming degassing hot spots (Billett *et al.*, 2008). Similarly wind speed controls the rate at which air is removed from near the water surface and helps to maintain the concentration gradient. In many systems turbulence itself is a function of wind speed, though this dependence is likely to be weaker in small streams where steep banks shelter the channel. In these cases other factors such as gradient, stream bed roughness and discharge may exert a greater control over turbulence.

3. Overview of Thesis

This study was based at 2 separate peatland sites. The main study aims were to a) create a complete GHG and carbon budget for Auchencorth Moss, Scotland, and b) to understand what controls and drives the individual fluxes within this budget. As such the primary study site was Auchencorth Moss. However, to fully understand the link between catchment and drainage system, and to understand what drives temporal variability in evasion, aquatic fluxes at Auchencorth Moss were compared to a contrasting site at Mer Bleue peatland, Canada. Both Auchencorth Moss and Mer Bleue are the sites of long-term environmental monitoring under a number of European and North American projects (see sections 4.1.1 and 4.1.2.).

The thesis is composed of four individual papers. Paper I describes the spatial and temporal variability in CH_4 and N_2O emissions measured *in situ* at the primary study site, Auchencorth Moss. Monthly measurements were made across 21 static chambers, including a range of microtopographic and vegetative ecotopes, to investigate the controls on spatial variability. On 9 of the 21 chambers, measurement frequency was increased to fortnightly, this dataset, alongside auxiliary measurements, was used to examine temporal variability *in situ*.

To compliment the work being carried out at the field site, and to gain further insight into what controlled variability in soil-atmosphere emissions, cores were collected from Auchencorth Moss for use in a mesocosm study (Paper II). Cores were collected from both hummocks and hollows, and from patches dominated by distinct vegetation communities (predominantly mosses; grasses and sedges; *Juncus effusus*). The mesocosms were then exposed to either a high or low water table treatment in a factorial design. After ~14 weeks, the water table treatments were switched and the response to draining and rewetting examined.

Paper III focuses on aquatic CO_2 fluxes at Auchencorth Moss. Specifically it examines the sources of aquatic carbon during storm-flow conditions, an important part of the hydrological regime at Auchencorth Moss previously unstudied at high temporal resolution. Change in CO_2 concentration during storm events due solely to

the effect of dilution was calculated and compared to the actual change over each individual time step. This allowed the inputs and losses of CO_2 to be investigated, which were then compared to both in-stream and catchment variables, and to CO_2 concentrations in the adjacent peat. The study also examined hysteresis in the concentration-discharge relationship giving further insight into the sources of stream CO_2.

Paper IV again focuses on the sources of aquatic carbon and also calculates losses to the atmosphere via surface water evasion and compares this to catchment NEE. The study is based at Mer Bleue peatland, Canada, a site which contrasts to Auchencorth Moss both in climate, seasonality and precipitation/runoff regime. Therefore, in addition to the findings described in Paper IV, it provided an interesting comparison to the Black Burn which is described in the 'Results and Discussion' section of the thesis.

Measurements of CO_2, CH_4 and N_2O, alongside POC, DOC, DIC, NO_3^- and NH_4^+ in the Black Burn, Auchencorth Moss, were also made on an approximately weekly basis throughout the full study period. Using this data, and in the case of CO_2 the results from Paper III, surface water evasion and downstream export from the Black Burn was calculated and compared to terrestrial emissions of CH_4 and N_2O (Paper I) and to catchment NEE (Helfter, unpublished data, 2008). These results are displayed and collated in the 'Results and Discussion' section of the thesis and will provide the basis for a further publication to be prepared at a later date.

The thesis concludes by examining the state of Auchencorth Moss in terms of a net 'sink' or 'source' of the GHGs CO_2, CH_4 and N_2O, and describes whether the catchment is gaining or losing carbon on an annual basis.

Tables and figures are labelled sequentially throughout the thesis with the exception of the individual papers (Sections 5, 6, 7 and 8) where tables and figures are labelled as they will appear in the final published articles.

4. Materials and Methods

4.1. Study sites

4.1.1. Auchencorth Moss

Auchencorth Moss is a low-lying ombrotrophic peatland located approximately 17 km south west of Edinburgh, Scotland (55º47'34N; 3º14'35W). The overall peatland is estimated to cover ~1214 ha, with peat depths up to 9.5 m and an estimated total volume of ~50 million m^3 of peat (Mitchell and Mykura, 1962). This study focuses specifically within the ~335 ha watershed of the Black Burn (Figure 2) which drains NE into the North Esk. Peat depth in the catchment ranges from <0.5 m to <5 m; elevation ranges from approximately 250 to 300 m (Billett *et al.*, 2004). The majority of the study site is used for low-intensity sheep grazing; to the south west there is an area (~170 ha) of peat extraction, part of which falls in the Black Burn watershed. An area of the peatland also forms part of a Site of Special Scientific Interest (SSSI) designated by Scottish Natural Heritage (SNH). The site has been designated as a 'supersite' under the 'European Monitoring and Evaluation Programme' (http://www.emep.int), a 'level-3' site under the 'NitroEurope' project (http://www.nitroeurope.eu) and a 'UK Carbon Catchment' for 'Centre for Ecology & Hydrology (www.ceh.ac.uk).

The Black Burn is fed from a number of small tributaries close to its source, one of which originates from the area of peat extraction, and from the surrounding catchment via both below-ground flow and through a series of overgrown drainage ditches. The drainage ditches are regularly spaced and parallel, forming a "herring-bone" pattern across the catchment. Histosols (peats) cover approximately 85% of the catchment; Gleysol (9%), Humic Gleysol (3%) and Cambisol (3%) occur along the catchment margins (Billett *et al.*, 2004).

a)

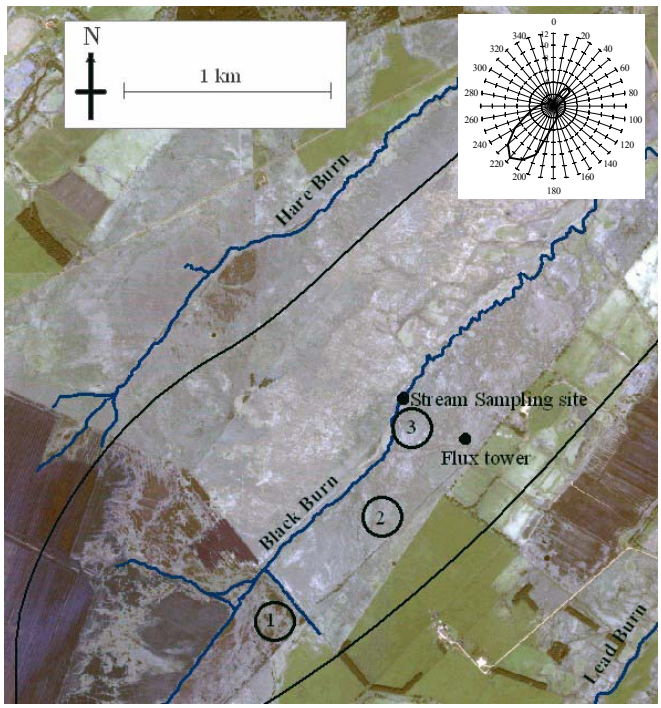

b)

Figure 2 a) Quickbird© image of Auchencorth Moss with graphics added to illustrate the drainage network (blue), an approximate watershed for the Black Burn (black) and the locations of the stream sampling site, the flux tower and the approximate locations of sites 1, 2 and 3 (circled) as defined in Paper I. The insert in the top right illustrates the prevailing wind direction at the site from 2005-2007. b) Photograph of Auchencorth Moss

The vegetation consists of a patchy mix of grasses and sedges (Figure 2b) covering a primarily *Sphagnum* base layer on a typical peatland hummock/hollow microtopography. Hummocks are typically small (~40 cm diameter, ~30 cm height) and dominated by either a mix of *Deschampsia flexuosa* and *Eriophorum vaginatum*, or *Juncus effusus*. Hollows (also referred to as depressions) are dominated primarily by mosses and a thinner layer of grass; depressions may become submerged after periods of intense rainfall but very few permanent pools of standing water exist. A more complete list of bryophytes, grasses and sedges is given in Table 2. Shrubs such as *Calluna vulgaris, Erica tetralix* and *Vaccinium myrtillus* are also present primarily within the SSSI to the south west of the catchment.

Table 2 List of common Bryophytes, Grasses and Sedges at Auchencorth Moss (Flechard, 1998)

Bryophytes	Grass	Sedge
Polytrichum commune	*Deschampsia flexuosa*	*Eriophorum vaginatum*
Polytrichum formosum	*Molinia caerulea*	*Eriophorum angustifolium*
Brachytecium spp.	*Festuca ovina*	*Juncus effusus*
Sphagnum tenellum	*Festuca rubra*	*Carex ovalis*
Sphagnum papillosum	*Agrostis stolonifera*	*Carex nigra*
Sphagnum compactum	*Anthoxanthum odoratum*	*Juncus squarrosus*
Sphagnum cupsidatum	*Nardus stricta*	*Scirpus cespitosus*
Polytrichum urnigerum	*Trichophorum cespitosum*	
Rhytidiadelphus squarrosus		
Aulacomnium Palustre		

Temperature and precipitation data for the field site over the course of this study are shown in Figure 3 below (Coyle, unpublished data, 2008). Mean annual temperature and precipitation are 8.1ºC and 1016 mm, respectively (Coyle, unpublished data, 2008). Water table at the site generally ranges from the peat surface to approximately 20 cm depth during most of the year, though it can be drawn down to >50 cm during summer droughts. The mean water extractable DOC from 5-30 cm below the peat surface is 312 ± 15.9 (SE) μg C g^{-1} dry soil and KCl extractable NO_3^- and NH_4^+ are 4.45 ± 0.48 (SE) and 21.8 ± 1.85 (SE) μg N g^{-1} dry soil, respectively (Dinsmore, unpublished data). Total N and S deposition at the site are 16.5 kg N ha^{-1} yr^{-1} and 6.9 kg S ha^{-1} yr^{-1}, respectively (Smith, personal communication, 2008).

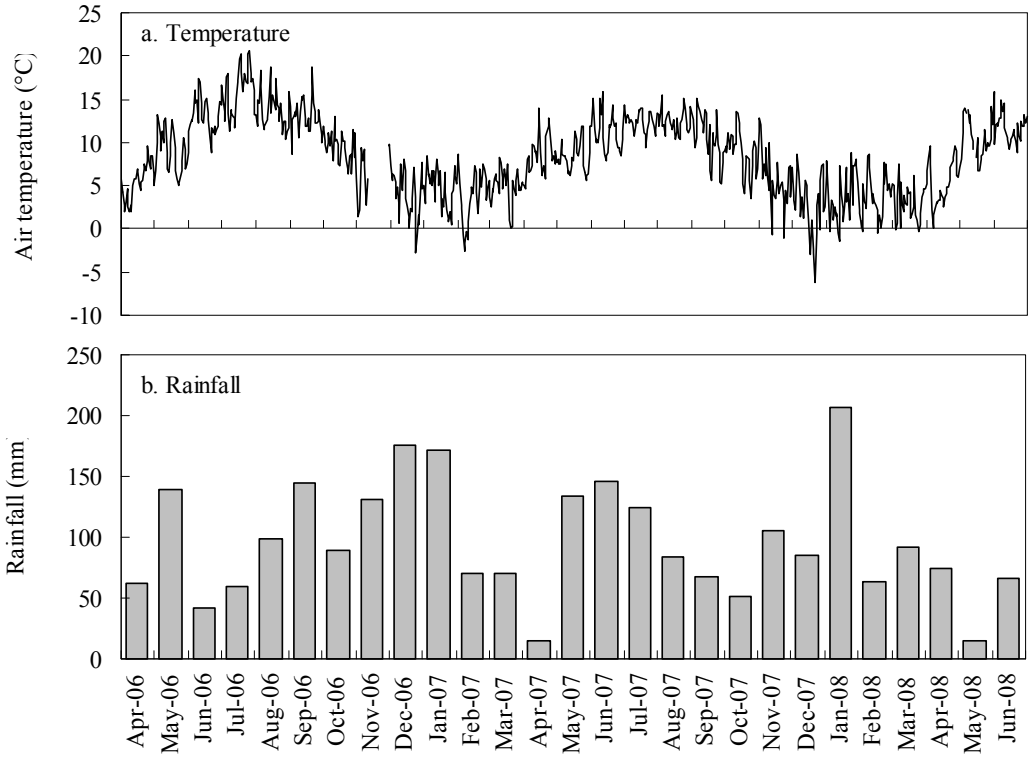

Figure 3 Daily mean temperature (a) and monthly total rainfall (b) at Auchencorth Moss

4.1.2. Mer Bleue

Mer Bleue is an ombrotrophic peatland with an average elevation of ~69 m, located approximately 10 km east of Ottawa, Ontario (45º24'33N; 75º31'7W). It is the site of the Eastern Peatland flux station for Fluxnet Canada (http://www.fluxnet-canada.ca, 2008); the site therefore provided both an existing level of infrastructure and measurement equipment, and a widely cited basis of scientific literature on catchment carbon dynamics. The bog consists of peat made up primarily of partially decomposed *Sphagnum* spp. (1-2 m near the edges to 5-6 m closer to the centre) overlying a continuous layer of marine deposits.

a)

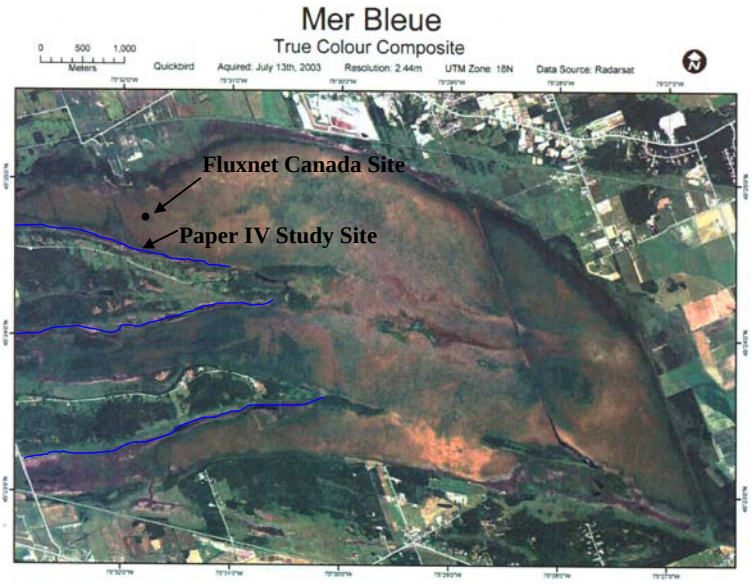

b)

c)

Figure 4 a) True colour composite image of Mer Bleue Peatland, Canada. Primary drainage channels have been highlighted in blue (image supplied by T. R. Moore, 2007). b) Image of pond site (supplied by M. F. Billett, 2007) and c) image of Mer Bleue vegetation.

Surface vegetation is primarily vascular ericaceous and deciduous shrubs and sedges, with an understorey of *Sphagnum* mosses on typical hummock/hollow microtopography (Figure 4b). The dominant vegetation consists of *Chamaedaphne calyculata, Ledum groenlandicum, Kalmia augustifolia, Vaccinium myrtilloides* and *Eriophorum vaginatum* (Moore, personal communication, 2007). Trees such as *Picea mariana*, *Larix laricina* and *Betula populifolia* occur in patches across the bog. At the peatland margin, where it abuts gravel and sand ridges, the drainage system forms a series of interconnected beaver ponds with inundated zones of *Typha latifolia* and floating mats of mosses and sedges (Figure 4c). A series of raised peat domes has led to the formation of 3 distinct drainage 'fingers', which drain the catchment from east to west into the Ottawa river valley. This study focuses specifically on the Northern drainage finger, close to the flux tower site.

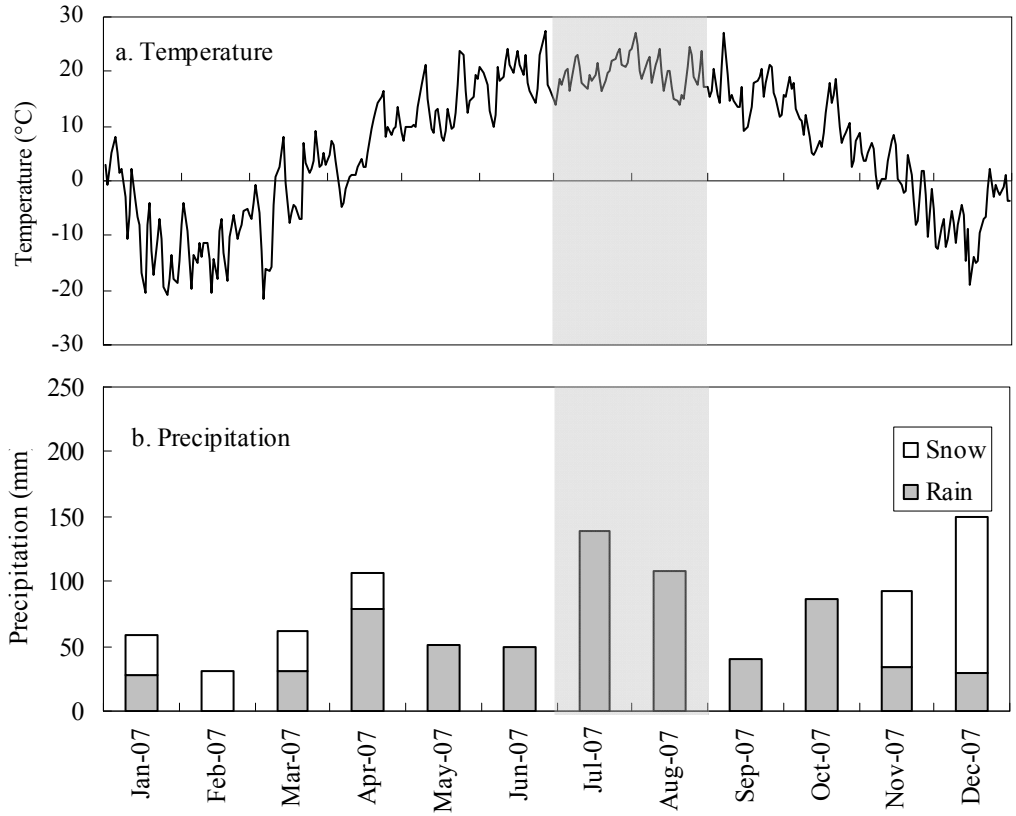

Figure 5 Mean daily temperature (a) and precipitation (b) at Ottawa International Airport during 2007 (http://www.climate.weatheroffice.ec.gc.ca/). Shaded months indicate study period (Paper IV).

The climate at Mer Bleue is classified as mid-continental cool. Mean annual temperature and precipitation are 5.8ºC and 910 mm, respectively, and the growing

season lasts from approximately May until September. Mean daily temperatures and precipitation are shown in Figure 5. The mean combined July and August temperature in 2007 was 0.4ºC cooler than the 29-year average for the region and the catchment received ~80 mm more rainfall than is usual for that time of year (http://www.climate.weatheroffice.ec.gc.ca/). The precipitation/runoff ratio at Mer Bleue is 0.4, with >55% of annual runoff occurring during spring snowmelt (Roulet *et al.*, 2007).

4.2. Methods

At Auchencorth Moss a variety of methods were employed to calculate soil-atmosphere emissions of CH_4 and N_2O *in situ*, alongside a series of auxiliary measurements to help explain variability across the site (Paper I). In addition to this, soil cores from Auchencorth Moss were extracted and used in a mesocosm study (Paper II). A combination of spot measurements, which are referred to in the 'Results and Discussion' section of this thesis, and continuous CO_2 measurements (Paper III) were made in the Black Burn (Auchencorth Moss). Continuous measurements of dissolved CO_2, alongside auxiliary data, were made in the drainage waters of Mer Bleue peatland. Whilst specific details of individual methods are given in each of the papers, summaries of the variables studied and the methods used throughout the thesis are given in Table 3 and Table 4. The underlying theory behind methods of particular importance to this thesis are described in more detail below, along with the methods used to calculate evasion and downstream export from the Black Burn (see also Appendix A).

Table 3 Variables measured in terrestrial environment and methods used. 'D' indicates the Results and Discussion chapter of the thesis.

Variable	Field Method	Laboratory Method	Paper I	II	III	IV	D
Measured							
CH_4 and N_2O emissions	Static chambers [2]	Gas chromatography	x	x			
Net ecosystem exchange	NEE chamber [2]	-------		x			
Soil respiration	Static chamber	-------	x				
Soil temperature	Temperature probe	-------	x	x			
Soil moisture	Theta probe	-------	x	x			
Soil pH	Sampling with soil auger	Solution with deionised water/pH meter					
Soil extractable DOC	Sampling with soil auger	Extraction with H_2O/TOC analyser [3]	x	x			
Soil extractable NO_3^- and NH_4^+	Sampling with soil auger	Extraction with KCL/colorimetric analyser [3]	x	x			
Soil solution DOC and DIC	Samples from dip wells	TOC analyser	x	x		x	
Soil solution NO_3^- and NH_4^+	Samples from dip wells	Colorimetric analyser	x	x		x	
Soil atmosphere CO_2, CH_4 and N_2O	Acurrel tubing© [2]	Gas chromatography	x	x		x	
Water table depth	Dip well	-------	x	x		x	
Supplied from flux tower sites							
Net ecosystem exchange	Eddy Covariance [1]	-------	x	x		x	x
Soil temperature	Humitter [1]	-------	x		x		
Air pressure	Analogue barometer [1]	-------	x				
Water table depth	Pressure transducer [1]	-------			x		
Rainfall	Tipping bucket gauge [1]	-------	x		x	x	x
Soil CO_2 concentration	NDIR sensors [1]	-------				x	

[1] Sensors connected to datalogger, therefore quasi-continuous measurement frequency
[2] Method described in more detail in following text
[3] Method described in more detail in Appendix A

Table 4 Variables measured in aquatic environment and methods used. 'D' indicates the Results and Discussion chapter of the thesis.

			Paper				
Variable	Field Method	Laboratory Method	I	II	III	IV	D
Dissolved CO_2	NDIR sensor [1, 2]	-------			x	x	
Dissolved CO_2, CH_4 and N_2O	Headspace sampling [2]	Gas chromatography				x	x
POC	Water sample	Loss-on-ignition (Dawson, 2000) [3]				x	x
DOC and DIC	Water sample	TOC analyser				x	x
NO_3^- and NH_4^+	Water sample	Colorimeter					x
Discharge/Stage height calibration [4]	Dilution gauging	-------			x		x
Stream temperature	Temperature/conductivity sensor [1]	-------			x	x	X
Stream conductivity	Temperature/conductivity sensor [1]	-------			x	x	X
Stream pH	pH sensor [1]	-------			x	x	
Stage height	Pressure transducer/data logger [1]	-------			x	x	x
Gas transfer coefficient [4]	Conservative tracer method	-------					x

[1] Sensors connected to datalogger, therefore quasi-continuous measurement frequency
[2] Methods described in more detail in following text
[3] Method described in more detail in Appendix A
[4] Results provided by Billett (unpublished data)

4.2.1. CH_4 and N_2O emissions

Fluxes were measured using the static chamber method described in Livingston and Hutchinson (1995). The soil-atmosphere flux is calculated by measuring the change in concentration over time in a known volume of air inside an enclosure. To calculate a valid flux rate the enclosure must be designed and employed in a way that limits interference with either production, consumption or transport processes. Both chamber design and measurement protocol vary considerably across the literature (e.g. Clayton *et al.*, 1994; Butterbach-Bahl *et al.*, 1997; Bubier *et al.*, 2002; Laine *et al.*, 2007), with such differences often leading to considerable variation in calculated emission estimates (Raich *et al.*, 1990; Pumpanen *et al.*, 2004). Design variations include chamber volume, material (i.e. flexible or rigid, light-penetrating or dark), and consideration of temperature control, air circulation and pressure equilibration (i.e. venting). The researcher also has to consider how long the chamber will be closed for and how many samples will be collected within this time. The enclosure time must be long enough to ensure the concentration change is greater than the analytical detection limit, though still short enough to prevent significant changes in the temperature of the enclosed air. Furthermore, as the concentration increases within the chamber, the concentration gradient across the soil-atmosphere boundary weakens and the diffusive flux is reduced, causing the concentration to level off; the calculations assume the increase over time is linear (Figure 6). Further considerations include the number of chambers to be employed, the layout across the study site, the frequency measurements are made, the time of day measurements are made and the approach to anomalies and non-linearity.

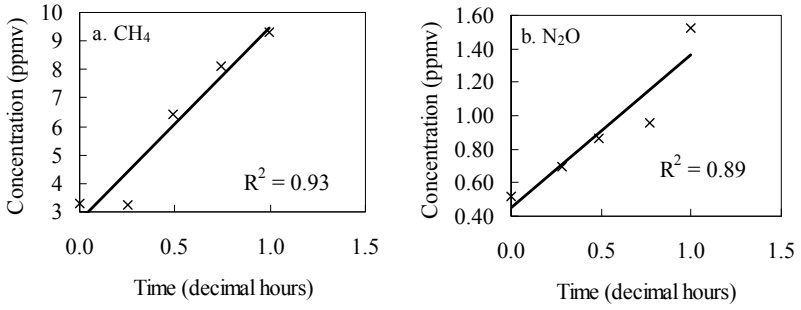

Figure 6 Example of results from linearity test in the field, illustrated for the chamber showing the greatest flux of a) CH_4 and b) N_2O

The chambers used in this study (Figure 7) are based on the design of Clayton *et al.* (1994), described in MacDonald *et al.* (1996); more details about chamber design and enclosure time can be found in the relevant papers within this thesis (Papers I and II).

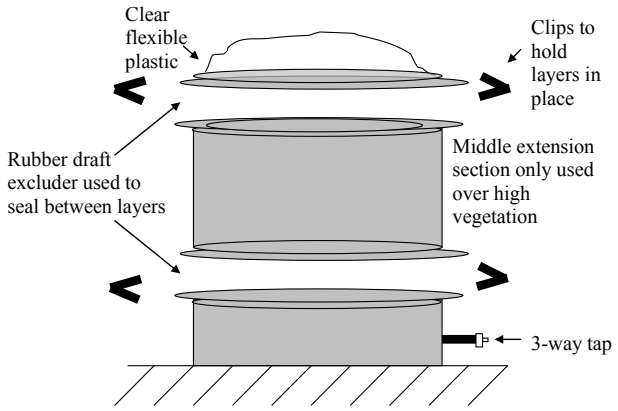

Figure 7 Illustration of static chamber design used in *in-situ* field study (Paper I).

The chamber volume was calculated by injecting a known concentration (4.75 ppb) and volume of the tracer gas SF_6 into the individual chambers. A fan was placed inside the chamber prior to closing to circulate and mix the internal air. A sample of internal chamber air was collected after 5 minutes and the concentration of SF_6 determined using gas chromatography with an electron capture detector. The volume of the chamber was calculated using Equation 2 below where V is the volume of either the gas injected or the chamber itself, and C is the concentration injected or sampled from the chamber. The SF_6 was stored at atmospheric temperature and pressure prior to use.

Equation 2 $$V_{chamber} = \frac{V_{injected} \times C_{injected}}{C_{chamber}}$$

In the field study (Paper I) 1000 ml of SF_6 was injected into each chamber and in the mesocosm study (Paper II), only 500 ml of SF_6 was used per chamber; this volume was based on both the detection limit of SF_6 and the estimated range of chamber volumes. This method overcame problems associated with measuring the volume of vegetation and the volume of hummock inside the chamber, as it measured specifically the volume in which air could easily mix and circulate.

Volumes calculated using traditional ruler estimates and the SF_6 method were strongly and significantly correlated ($r = 0.84$, $p < 0.01$), though the ruler method overestimated the chamber volume by an average of 15.5 %.

4.2.2. Net ecosystem exchange (NEE)

NEE from the individual mesocosms in Paper II was measured using the chamber theory explained in section 4.2.1, and using the chamber displayed in Figure 8. In contrast to the method in section 4.2.1., the chamber was connected to an infra-red gas analyser (IRGA) which determined the CO_2 concentration of the internal air every 4 seconds without the need to manually extract an air sample. The temperature and humidity of the internal air was also monitored continuously via a sensor placed within the chamber. Due to the larger size of the NEE chamber, a fan was also required to ensure circulation and mixing of the internal air.

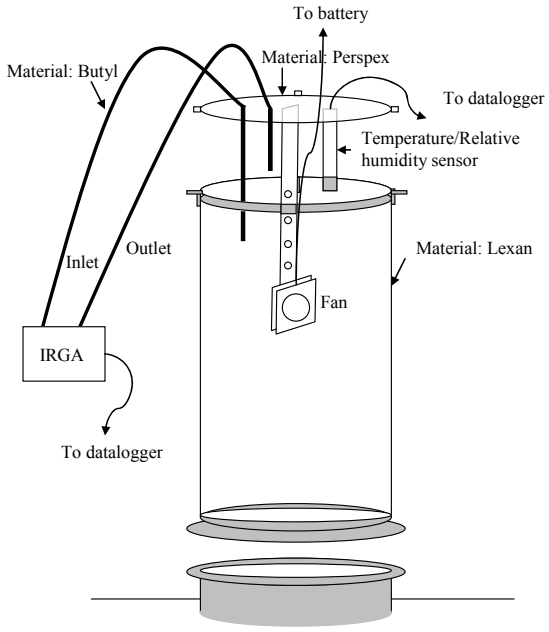

Figure 8 Illustration of NEE chamber design used in mesocosm study (Paper II)

4.2.3. Soil atmosphere CO_2, CH_4 and N_2O

Soil atmosphere wells were created using Accurel© gas-permeable, air-tight tubing (Gut *et al.*, 1998). The Accurel© was buried below-ground either beside the field chambers (Paper I), within the mesocosms (Paper II) or along a transect (Paper IV).

The Accurel© was sealed to gas-impermeable tubing which was extended to the soil surface and closed off with a 3-way tap that allowed air samples to be withdrawn when required. Samples (~5ml) were collected, either into Tedlar bag or air-tight syringes (see specific papers) and returned to the laboratory for analyses using gas chromatography.

4.2.4. Dissolved CO_2, CH_4 and N_2O – headspace method

The headspace technique is a widely cited direct method used to calculate the concentration of gas dissolved in a liquid (Kling *et al.*, 1991; Billett *et al.*, 2004; Hope *et al.*, 2004; Billett *et al.*, 2008). A known volume of water was equilibrated with a known volume of ambient atmosphere or gas standard in a luer-lock syringe with attached 3-way tap. In the Black Burn 40 ml of stream water was equilibrated with 20 ml of headspace; at Mer Bleue where concentrations were significantly higher, 20 ml of water was equilibrated with 20 ml of headspace. The syringe was shaken vigorously underwater for one minute, equilibrating the headspace and water at stream temperature. The headspace was then transferred to a gas-tight syringe for later analysis using gas chromatography. A sample of ambient air was also collected in a gas-tight syringe.

The concentration of CO_2, CH_4 and N_2O was then used to calculate the original concentration in the stream water based on Henry's law; see Equation 3 below (Dawson, 2000). $[CO_2]_{(aq)}$ is the original gas concentration in the water sample (µmol L^{-1}), P_f is the final partial pressure of the gas in the syringe (atm) (Equation 4), P_i is the initial partial pressure of the equilibration gas (atm) (Equation 5), P_{wa} is the total ambient pressure (atm) at the depth of sampling, P_{atm} is the ambient atmospheric pressure (atm), Y_f is the concentration in the equilibrated headspace (ppmv), Y_i is the concentration of the headspace prior to equilibration (ppmv), K_H is the Henry's law constant, V_{hs} is the headspace volume (L), V_w is the water volume (L), r is the universal gas constant (0.082057) and T is the stream temperature (ºK).

Equation 3 $$[CO_2]_{(aq)} = \left[P_f \times \left(K_H + \left(\frac{V_{hs}}{V_w} \right) \times \left(\frac{1}{r} \right) \times T \right) \right] - \left[P_i \times \left(\frac{V_{hs}}{V_w} \right) \times \left(\frac{1}{r} \right) \times T \right]$$

Equation 4 $$P_f = Y_f \times P_{wa}$$

Equation 5 $$Pi = Yi \times P_{wa}$$

4.2.5. Dissolved CO_2 –NDIR sensor

Vaisala CARBOCAP©, transmitter series GMT220, non-dispersive infra-red absorption (NDIR) CO_2 sensors were enclosed within water-tight, gas-permeable membranes and connected to Campbell Scientific CR1000 dataloggers (Johnson *et al.*, 2006). Measurements were made automatically once per minute and 10-minute averages recorded. Once protected from water damage the sensors could be employed both below the water table in the soil and in the water column itself. Unlike the headspace method, NDIR sensors are automated and therefore provide a significantly better temporal resolution than any other direct measurement method currently available. To avoid systematic error in the sensor output (CO_2 ppmv) the concentrations were corrected for variations in temperature and pressure using the method described in Tang *et al.* (2003). A fuller description of the method used and a comparison between NDIR and headspace concentrations at Auchencorth Moss, Mer Bleue and a number of other catchments are described in a paper by Johnson *et al.* (in preparation for Limnology and Hydrology Methods, 2008).

4.2.6. Downstream export

In order to interpolate between widely spaced concentration measurements and calculate annual loads of POC, DOC, DIC, NO_3^- and NH_4^+ in the Black Burn, 'Method 5' of Walling and Webb (1985, described in Hope *et al.*, 1997b) was used. The method estimates annual loads based on both instantaneous discharge rates corresponding to each concentration measurement, and the mean of the continuous discharge data supplied by a pressure transducer and data logger. As continuous discharge data was only available from March 2007 until June 2008, average annual loads were also calculated from the mean of the instantaneous loads, these spanned a longer period from March 2006 until December 2007. Method 5 is described below in equation 6, where K is a conversion factor to scale units to annual catchment

values, C_i is the instantaneous concentration associated with instantaneous discharge Q_i, Q_r is the mean discharge for the full period and n is the number of instantaneous samples analysed.

Equation 6 $$Load = K \times Q_r \times \frac{\sum_{n}^{i=1}[C_i \times Q_i]}{\sum_{n}^{i=1} Q_i}$$

To calculate the standard error of flux estimates based on 'Method 5', equation 7 was used (Hope *et al.*, 1997b), where F is the total annual discharge and C_F is the flow-weighted mean concentration.

Equation 7 $$SE = F \times \mathrm{var}(C_F)$$

The variance of C_F ($\mathrm{var}C_F$) is estimated from equation 8 (Hope *et al.*, 1997b), where Q_n is the sum of all the individual Q_i values.

Equation 8 $$\mathrm{var}(C_F) = \left[\sum (C_i - C_F)^2 \times Q_i / Q_n\right] \times \sum Q_i^2 / Q_n^2$$

4.2.7. Evasion flux calculation

Two different methods are used to calculate evasion fluxes from the water surface. In Paper IV the method described is based on established relationships between wind speed and gas transfer velocity (Wanninkhof, 1992; MacIntyre *et al.*, 1995). This method is based on evasion from lake or ocean surfaces and is not applicable to fast flowing streams such as the Black Burn where stream banks shelter the water surface and turbulence is generated primarily from stream-bank and stream-bed friction. Evasion from the Black Burn is therefore calculated using the reaeration flux equation of Young and Huryn (1998) with gas transfer coefficients (k) calculated using the deliberate tracer method (MacIntyre *et al.*, 1995; Hope *et al.*, 2001). This involved the co-injection of conservative solute (NaCl) and volatile gas (Propane) tracers (Billett, unpublished data, 2008). The concentration of the volatile tracer decreases down the study reach due to both dispersion and evasion. Dispersion is calculated from the decrease in concentration of the conservative solute tracer; therefore evasion can be deduced and the gas transfer coefficient calculated. The gas

transfer coefficient of propane can then be converted to that of other gases using either gas diffusion coefficients or Schmidt numbers (MacIntyre *et al.*, 1995; Hope *et al.*, 2001). The gas transfer coefficient of propane ($k_{propane}$) was calculated along a 20 m stream reach, including the sampling location used in this study, on 4 different occasions in 2006 (Billett, unpublished data, 2008).

The reaeration equation used to calculate flux is shown below in Equation 9 where F is the flux in μmol m^{-2} s^{-1}, ΔC is the difference between the reach streamwater concentration and the atmospheric equilibrium concentration (μmol L^{-1}), k_x is the gas transfer coefficient of the gas in question (min^{-1}), T is the reach travel time (min), Q is the discharge (L s^{-1}) and A is the reach surface area (m). The gas transfer coefficient increases with discharge and therefore rather than calculate fluxes based on a mean k value, it was preferable to model k based on discharge. Both T and A are specific to the $k_{propane}$ value measured on each sampling date therefore rather than specifically calculating k based on discharge, Equation 9 was rearranged (Equation 10) and the latter section modelled as one value (Figure 9). This value could then be converted to the gas specific equation using the diffusion coefficients or Schmidt numbers as described above.

Equation 9 $$F = \frac{\Delta C \times k_x \times T \times Q}{A}$$

Equation 10 $$F = \Delta C \times Q \times \left[\frac{K_x \times T}{A} \right]$$

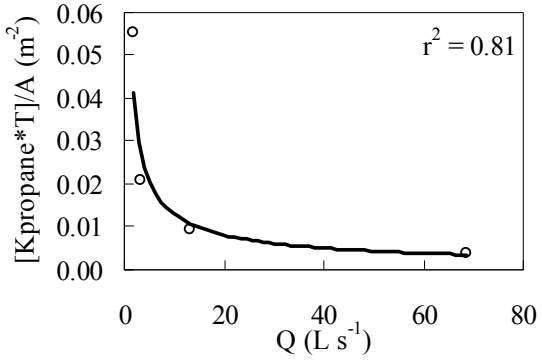

Figure 9 Relationship between kT/A and discharge on 4 separate occasions at stream sampling location used in this study

5. Paper I

Spatial and temporal variability in CH_4 and N_2O fluxes from a Scottish ombrotrophic peatland; implications for modelling and upscaling

Kerry J. Dinsmore, Ute M. Skiba, Michael F. Billett, Robert M Rees, Julia Drewer

Accepted for publication in 'Soil Biology and Biochemistry'

Spatial and temporal variability in CH_4 and N_2O fluxes from a Scottish ombrotrophic peatland; implications for modelling and upscaling

Kerry J. Dinsmore, Ute M. Skiba, Michael F. Billett, Robert M Rees, Julia Drewer

Greenhouse gases, Variability, Peatlands

Abstract

Peatlands typically exhibit significant spatial heterogeneity which can lead to large uncertainties when catchment scale greenhouse gas fluxes are extrapolated from chamber measurements (generally <1 m^2). Here we examined the underlying environmental and vegetation characteristics which lead to within-site variability in both CH_4 and N_2O emissions. We also consider within-site variation in the drivers of temporal dynamics. Net annual emissions (and coefficients of variation) for CH_4 and N_2O were 1.06 kg ha^{-1} a^{-1} (300%) and 0.02 kg ha^{-1} a^{-1} (410%), respectively. The riparian zone was a significant CH_4 hotspot contributing ~12% of the total catchment emissions whilst covering only ~0.5% of the catchment area. In contrast to many previous studies we found smaller CH_4 emissions and greater uptake in chambers containing either sedges or rushes. We also found clear differences in the drivers of temporal CH_4 dynamics across the site, e.g. water table was important only in chambers which did not contain aerenchymous plants. Temporal dynamics were less well predicted for N_2O due to the extremely high coefficient of variation. We suggest that depending on the heterogeneity of the site, flux models could be improved by incorporating a number of spatially distinct sub-models, rather than a single model parameterized using whole-catchment averages.

Introduction

Northern peatlands are currently thought to act as net sinks of CO_2 (Gorham, 1991). However, due to the prevalence of waterlogged conditions, they represent a significant net source of CH_4 (Bartlett and Harriss, 1993; Huttunen *et al.*, 2003) and in some cases a net source of N_2O (Huttunen *et al.*, 2002; Regina *et al.*, 1996). In order to calculate a realistic global warming potential for peatland systems, all three of the aforementioned gases need to be accurately quantified and upscaled. It is also becoming increasingly important to understand what drives variability in the sink/source strength of the various greenhouse gases (GHG), in order to predict the biospheric feedback of peatlands in response to changes in peatland management and global climate.

The availability of micrometeorological techniques has greatly improved our understanding of the temporal variability in CO_2 emissions, revealing significant patterns in annual and inter-annual fluxes (Lafleur *et al.*, 2003; Lund *et al.*, 2007). Furthermore, the availability of near-continuous datasets has led to a much greater understanding of the drivers of CO_2 emission and uptake, allowing emission predictions to be made under different climate change scenarios (Griffis and Rouse, 2001). Similar micrometeorological techniques for the measurement of CH_4 and N_2O are not widely used, with most current flux estimates from peatlands based on a series of enclosed chamber measurements (e.g. Laine *et al.*, 2007; MacDonald *et al.*, 1998; Roulet *et al.*, 2007; Whalen and Reeburgh, 2000). However, with many studies repeatedly reporting high variability in fluxes both within and between sites (Bartlett and Harriss, 1993; Bubier *et al.*, 1993; Waddington and Roulet, 1996), the uncertainty associated with up-scaled estimates of annual catchment budgets is often extremely large.

The hummock/hollow microtopography typical of many peatlands can cause significant variation in soil environmental conditions at scales not picked up by single chamber measurements (Nungesser, 2003). The preferential colonisation of hummocks or hollows by distinct plant communities reinforces differences due to topography alone by influencing the quantity and quality of soil organic substrate,

and altering the aerobic capacity of the peat by transporting O_2 to the rhizosphere. Plants containing aerenchymous tissue can also provide a direct pathway for many GHGs to the atmosphere, bypassing the aerobic peat horizon, and greatly increasing soil-atmosphere fluxes (Minkkinen and Laine, 2006; Ström *et al.*, 2003; Whiting and Chanton, 1996). A clear understanding of the major sources of variation within a site is essential both during the set-up of a study, when choosing where to place individual chambers, and during the up-scaling process so that individual chamber fluxes can be correctly weighted in the final estimate.

Both temperature and water table have repeatedly been shown to be strong drivers of temporal variability in surface CH_4 and N_2O fluxes; however studies often disagree as to their relative importance (Daulat and Clymo, 1998; Hargreaves and Fowler, 1998; Updegraff *et al.*, 2001). It is likely, given the degree of within-site variability often observed, that the primary drivers of temporal variability are not consistent across typical peatland sites. By examining how these drivers vary spatially this study aims to improve our understanding of the underlying processes that control surface emissions, and in doing so, aid the design of future chamber studies to achieve the best possible up-scaled emission estimates.

Materials and Methods

Site description

Auchencorth Moss is a relatively flat, low lying, acid peatland, located approximately 17 km south of Edinburgh, Scotland (55º47'34 N; 3º14'35 W). The site is designated as a 'supersite' under the 'European Monitoring and Evaluation Programme' (EMEP) and a 'level-3' site under the 'NitroEurope' project. Total nitrogen and sulphur deposition rates at the site are 16.5 kg N ha^{-1} y^{-1} and 6.9 kg S ha^{-1} y^{-1}, respectively (Smith, personal communication, 2008). The land-use is primarily low-intensity sheep grazing with an area of peat extraction at the western edge of the catchment. Histosols (peats) cover approximately 85% of the catchment with areas of Gleysol (9%), Humic Gleysol (3%) and Cambisol (3%) occurring at the catchment margins; peat depth ranges from <0.5 m to >5 m (Billett *et al.*, 2004). Mean annual rainfall (1995-2006) at the site is 1016 mm (*Coyle*, unpublished data,

2008); maximum and minimum monthly mean temperatures (1971-2000) are 19ºC in July and 0.7ºC in January, respectively (www.metoffice.gov.uk). The vegetation consists of a patchy mix of grasses, sedges and soft rush covering a base layer of moss on a typical peatland hummock/hollow microtopography. The dominant vascular species include *Deschampsia flexusa*, *Molinia caerulea*, *Festuca ovina*, *Eriophorum angustifolium*, *Eriophorum vaginatum*, *Juncus effusus*, *Juncus squarrosus* and *Calluna vulgaris*; bryophytes are dominated by *Sphagnum* and *Polytrichum* species.

Experimental design

The full study area was separated into 3 sites approximately 0.4 miles apart to cover the full range of soil-plant conditions; site 1 was located in the west of the catchment where drainage was better and patches of *Calluna vulgaris* were present, site 2 was located roughly in the middle of the catchment with an even mix of hummocks dominated by grasses and sedges, hummocks dominated by *J. effusus* and hollows, site 3 was located in the riparian zone dominated by *J. effusus*. Site 3 is often referred to as the 'riparian zone' throughout the text. In total measurements were made from 21 chambers; 9 within site 1, 9 within site 2, and 3 within site 3.

The full study area was also separated into distinct microtopographic/vegetative classes: plots dominated by *C. vulgaris* (Calluna), hummocks dominated by sedges and grasses (Sedge/Hummock), hummocks dominated by *J. effusus* (Juncus/Hummock), and hollows dominated by mosses (Hollow). Within site 1, 3 chambers were positioned on each of Calluna, Sedge/Hummock, and Juncus/Hummock; within site 2, 3 chambers were positioned on each of Sedge/Hummock, Juncus/Hummock and Hollow; the 3 chambers within site 3 were all placed upon Juncus/Hummocks (Table 1).

Table 1 Chamber layout and number of chamber types within spatially separated sites. Site 3 is often referred to in the text as 'Riparian zone'.

	Site 1	Site 2	Site 3
Calluna	3	---	---
Hollow	---	3	---
Sedge/Hummock	3	3	---
Juncus/Hummock	3	3	3

Flux measurements were made on all 21 chambers monthly from April 2006 until October 2007. An additional monthly measurement was made from each of the 9 chambers within site 2 from August 2006 until October 2007, leading to a fortnightly sampling frequency on 9 of the total 21 chambers, thus providing a better resolution for examining temporal variability. Alongside flux measurements, soil temperature, moisture, water table depth and soil respiration were recorded and samples of soil atmosphere and soil water collected. Soil samples were collected monthly, though not on the same day as flux measurements.

Flux measurements

Flux measurements were made using the static chamber method described in Livingston and Hutchinson (1995). Polypropylene chamber bases were inserted into the soil to a depth of approximately 5 cm; the chamber bases remained in situ for the duration of the study. Lids consisted of a flexible, transparent dome of polyethylene affixed to a polypropylene flange which could be securely attached to the chamber base during measurements (MacDonald *et al.*, 1996). The total enclosed volume was approximately 30 litres for chambers containing *J. effusus* and approximately 17 litres for all other chambers. Enclosure time generally ranged between 1-2 hours. As fluxes tended to be low, and direct sunlight or high temperatures rarely a problem at the site, up to 2 hours were required to collect gas at a sufficiently high concentration for accurate analysis. No significant levelling off of emissions was observed in the chambers with the highest recorded fluxes. Ambient air samples were collected at time zero with a further two samples of chamber air collected at the mid-point and end of the enclosure period. Air samples were stored in tedlar bags for up to a week prior to analysis using an HP5890 Series II gas chromatograph (detection limits: CO_2 < 199 μl l^{-1} (ppmv), CH_4 < 1.26 μl l^{-1}, N_2O < 0.2 μl l^{-1}) with electron capture (ECD) and flame ionisation detectors (FID) for N_2O and CH_4, respectively. Fluxes were calculated as the observed rate of concentration change times the enclosure volume to ground surface area ratio.

Auxiliary measurements

Soil temperature and moisture (mean of three theta probe readings from surface 5-10 cm) were recorded adjacent to each chamber during flux measurements. Soil respiration measurements were made using a PP-systems SCR-1 respiration chamber attached to an EGM-4 infra-red gas analyser. The chamber was attached to a plastic collar inserted ~5 cm into the soil to achieve an airtight seal and allow repeated measurements to be made in the same place. Soil atmosphere wells were created by inserting Accurel© water tight, gas permeable tubing (Gut *et al.*, 1998) into the soil from 10 to 40 cm adjacent to each individual chamber before the study began. Air samples were then drawn from the Accurel each time chamber measurements were made and analysed for CO_2, CH_4 and N_2O; CO_2 was measured on the same gas chromatograph as CH_4 and N_2O using the FID with attached methanizer. Water table depth was measured and water samples collected from dip wells consisting of perforated pipes (4 cm diameter) inserted adjacent to each chamber. Water samples were analysed for DOC and DIC on a Rosemount-Dohrmann DC-80 total organic carbon analyser (detection range 0.1 to 4000 mg l^{-1}), using ultraviolet oxidation and sparging with N_2 to remove acidified inorganic carbon; NO_3 and NH_4 were analysed on a dual channel CHEMLAB continuous flow colorimetric analyser (detection range NH_4-N: 0.25 to 3.0 mg l^{-1}; NO_3-N: 0.25 to 5.0 mg l^{-1}).

Soil was collected from approximately 5 to 30 cm below the surface using a soil auger; 3 samples from within 0.5 m of each chamber were combined. A sub-sample of soil was analysed for pH and the remainder frozen within 24 hours of collection for later extraction with KCl and water for NO_3, NH_4 and DOC. Extracts were analysed alongside the soil solution samples. Percent moss, grass, sedge and rush were visually estimated for each individual chamber at the end of the study period.

In addition to the above manual measurements, continuous measurements of air temperature, soil temperature at 5, 10, 20 and 40 cm, air pressure (mb), photosynthetically active radiation (PAR, µmol m^{-2} s^{-1}) and net radiation (W m^{-2}), were measured in the catchment at the EMEC flux tower site (Coyle, unpublished data, 2008) and utilised in temporal regression models.

Statistical analysis

Monthly measurements of all 21 chambers (plus auxiliary data) were used in the analyses of spatial variability. The data was separated prior to analysis into 3 periods: growing season 2006, winter period 2006-2007 and growing season 2007 (Figure 1). The growing season was from April until October. Mean daily CH_4 and N_2O fluxes were calculated by integration over each season. The seasonal arithmetic mean was used to describe temperature, soil respiration, pH, water table depth, soil moisture and soil extractable NO_3, NH_4 and DOC. However, due to the skewed distribution of the data, the geometric mean was used to describe soil solution NO_3, NH_4, DOC and DIC, and soil atmosphere CO_2, CH_4 and N_2O concentrations. Where mean values are quoted, ± refers to the standard error of the mean unless otherwise stated.

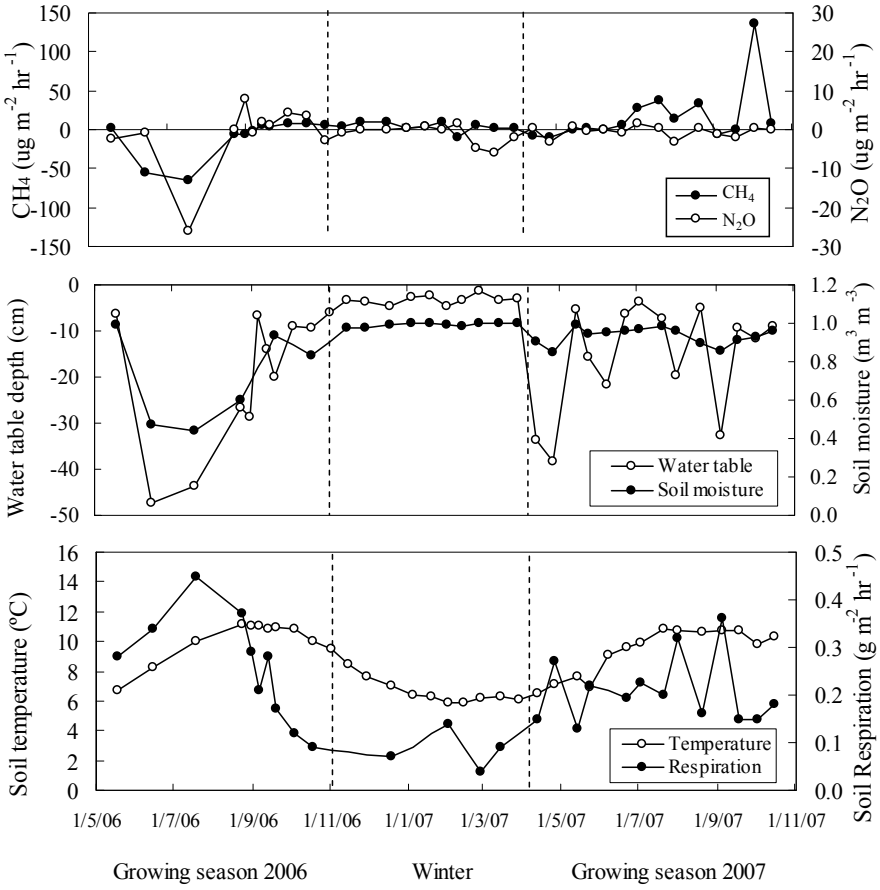

Figure 1 Time series of a) median CH_4 and N_2O fluxes from 9 chambers at site 2, b) water table depth and soil moisture and c) soil temperature and respiration over the study period. The dashed lines separate the study into growing season 2006, winter period and growing season 2007, respectively.

As the CH_4 fluxes from Juncus/Hummock chambers in the riparian zone (site 3) were highly and significantly different from the Juncus/Hummock chambers in both site 1 and site 2 ($F = 18.6$, $p < 0.01$), they were separated into a distinct class (Riparian). Chamber types (Calluna, Hollow, Sedge/Hummock, Juncus/Hummock and Riparian) were then compared using ANOVA tests after transformation to fit the normal distribution. Quoted test results refer to Pillai's test statistic (Townend, 2002) unless otherwise stated. Correlations were tested using Spearman's rank correlation. A combination of best subsets and backward selection stepwise regression analyses were used to model CH_4 and N_2O fluxes using the full list of auxiliary data. Log transformations were performed to normalise positively skewed data; an arcsine transformation was applied to soil moisture values. Variables with $p > 0.05$ were allowed to remain in the final model if their exclusion resulted in a significant rise in the full-model p-value.

Fortnightly measurements of the 9 chambers within site 2 (plus auxiliary data) were used for the analysis of temporal variability. The data were separated prior to analyses by chamber type (Hollow, Sedge/Hummock, Juncus/Hummock). As before, best-fit models for both CH_4 and N_2O emissions were created using a combination of best-subsets and backward selection stepwise regression.

Results

Over the full study period the mean of the integrated CH_4 fluxes within the groups Calluna, Hollow, Sedge/Hummock, Juncus/Hummock and Riparian were 8.12, 20.61, 2.30, 4.73 and 586 $\mu g\ m^{-2}\ hr^{-1}$, respectively (Table 2). Mean N_2O fluxes across the same groups were 1.52, -1.18, 2.02, -0.68 and 3.87 $\mu g\ m^{-2}\ hr^{-1}$, respectively (Table 2).

Table 2 Mean ± SE of data from full study period, separated by chamber type. P-values from ANOVA's testing for significant between group differences are indicated by asterisks where *, ** and *** refer to $p < 0.10$, $p < 0.05$ and $p < 0.01$, respectively. Extractable NO_3, NH_4 and DOC refer to concentrations extracted from the soil samples.

	Calluna	Hollow	Sedge/ Hummock	Juncus/ Hummock	Riparian
CH_4 flux (μg m^{-2} hr^{-1})	8.12 ± 5.77	20.6 ± 24.3	2.30 ± 6.47	4.73 ± 6.52	586 ± 311
N_2O flux(μg m^{-2} hr^{-1})	1.52 ± 3.34	-1.18 ± 1.49	2.02 ± 1.97	-0.68 ± 1.36	3.87 ± 1.35
Soil respiration (g m^{-2} hr^{-1})	0.29 ± 0.04	0.24 ± 0.01	0.28 ± 0.02	0.37 ± 0.11	0.45 ± 0.06
Soil pH ***	3.74 ± 0.01	4.54 ± 0.09	4.03 ± 0.12	4.41 ± 0.07	5.83 ± 0.28
Water table depth (cm)*	-20.7 ± 0.89	-18.5 ± 2.65	-27.2 ± 2.25	-27.8 ± 2.88	-23.4 ± 8.1
Soil moisture (m^3 m^{-3})	0.85 ± 0.04	0.88 ± 0.02	0.85 ± 0.02	0.85 ± 0.02	0.88 ± 0.04
Extractable NO_3 (μg N g^{-1})	5.08 ± 0.90	3.14 ± 1.05	4.38 ± 0.91	3.61 ± 0.45	4.57 ± 2.41
Extractable NH_4 (μg N g^{-1})***	42.9 ± 0.95	18.0 ± 3.31	21.7 ± 2.76	18.9 ± 0.73	24.8 ± 10.5
Extractable DOC (μg C g^{-1})**	595 ± 56	301 ± 57	410 ± 59	239 ± 11	247 ± 154
Soil solution NO_3 (mg N l^{-1})*	0.17± 0.02	0.12 ± 0.02	0.12 ± 0.01	0.14 ± 0.01	0.15 ± 0.04
Soil solution NH_4 (mg N l^{-1})***	0.58 ± 0.17	0.08 ± 0.01	0.23 ± 0.03	0.17 ± 0.03	0.14 ± 0.04
Soil solution DOC (mg C l^{-1}) **	33.0 ± 5.67	17.0 ± 0.92	23.8 ± 2.09	22.6 ± 2.84	17.3 ± 1.38
Soil solution DIC (mg C l^{-1})	2.24 ± 0.20	2.59 ± 0.51	2.76 ± 0.28	2.70 ± 0.31	3.88 ± 1.06
Soil CH_4 (ppmv)***	9.35 ± 5.27	5.52 ± 1.13	2.73 ± 0.29	3.13 ± 0.41	48.2 ± 31.7
Soil CO_2 (ppmv)**	4488 ± 894	3852 ± 802	2678 ± 411	3149 ± 535	2891 ± 538
Soil N_2O (ppmv)	0.35 ± 0.01	0.36 ± 0.02	0.44 ± 0.05	0.44 ± 0.03	0.37 ± 0.04

Spatial variability

– *Influence of microtopographic/vegetative group*

The mean CH_4 flux from all chambers was 89.8 μg m^{-2} hr^{-1}; the median, maximum and minimum were 0.72, 990 and -25.6 μg m^{-2} hr^{-1}, respectively. The coefficient of variation in integrated means across the 21 individual chambers was 300%. However, the distribution of the CH_4 flux data was heavily skewed towards 2 chambers in the riparian zone with means an order of magnitude higher than the rest of the chambers. As well as containing the 2 highest integrated means, the 3 chambers situated within the riparian zone also contained the minimum integrated mean value. Excluding the 3 chambers in the riparian zone (site 3), the new mean, median, maximum and minimum were 7.13, -0.98, 69.19 and -12.71 μg m^{-2} hr^{-1}, respectively. However, by excluding the riparian zone chambers, the coefficient of variation was only reduced to 284%. The N_2O fluxes were much smaller and more variable than the CH_4 fluxes, and followed a more normal distribution. The mean,

median, maximum and minimum N_2O fluxes across all chambers were 0.99, -0.36, 9.91 and -4.25 μg m^{-2} hr^{-1}, respectively. The coefficient of variation in integrated means was 410%.

Variables which showed significant ($p < 0.05$) or near-significant ($p < 0.10$) differences across microtopographic/vegetative groups included pH, water table depth, soil extractable NH_4 and DOC, soil solution DOC, NO_3 and NH_4 and soil atmosphere CH_4, CO_2 and N_2O concentrations (Table 2). The Riparian chambers in particular showed characteristics distinct from the other groups (Table 3), of which the greatest difference was in pH; the mean pH across Riparian chambers was 5.83 as opposed to a mean of 4.18 for all other groups combined.

Table 3 Results from ANOVA tests describing variables which make Riparian chambers distinct from all other groups combined. Arrows indicate whether variable is higher or lower in Riparian chambers.

Variable		F	P
CH_4 flux	↑	18.55	< 0.01
Soil respiration	↑	3.94	< 0.01
pH	↑	52	< 0.01
Soil extracted DOC	↓	3.51	0.08
Soil solution DIC	↑	5.33	0.03
Soil CH_4 concentration	↑	13.30	< 0.01

Over the full study period, only the Riparian chambers showed CH_4 fluxes significantly different ($p < 0.01$) from the other groups. CH_4 fluxes from the riparian zone were consistently higher, with a mean more than an order of magnitude greater than the other groups (Table 2). A similar pattern was observed in below ground CH_4 concentrations, with concentrations increasing in the order Sedge/Hummock < Juncus/Hummock < Hollow < Calluna < Riparian (Table 2). When the full dataset was considered collectively, the Spearman's rank correlation between emissions and below-ground concentrations was not significant at the 95% confidence limit ($t = 2.54$, $p = 0.08$). However, when separated by season the results were significant in all cases (growing season 2006: $t = 3.29$, $p < 0.01$; winter season: $t = 2.20$, $p < 0.05$; growing season 2007: $t = 2.45$, $p < 0.05$). During growing season 2006, only the Riparian group had a net CH_4 emission, however, due to high within group variability the difference from the other groups was not statistically significant. Net uptake was greatest in the Juncus/Hummock group followed by the

Sedge/Hummock, Hollow and finally the Calluna chambers (Figure 2a). During the winter season, both the Hollow and Riparian chambers were statistically similar, showing much greater fluxes than the other groups (Figure 2b). In contrast to growing season 2006, when all but the Riparian chambers displayed a net uptake, net emissions were measured from all chambers during growing season 2007; again Riparian fluxes were significantly higher than fluxes from the other chamber types.

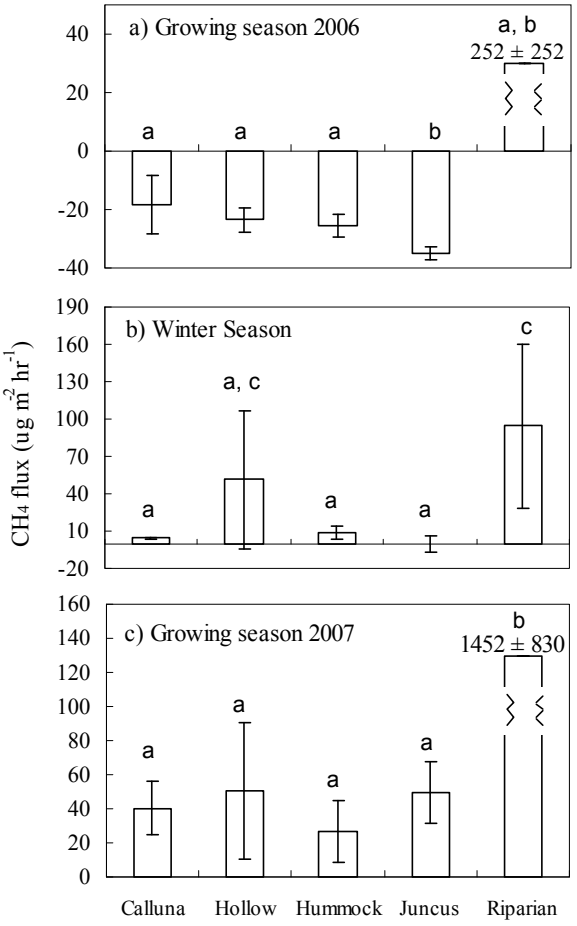

Figure 2 Mean integrated CH_4 flux during a) growing season 2006, b) the winter period and c) growing season 2007, separated by microtopographic/vegetative group. Error bars represent the standard error of the mean. Common letters indicate statistically similar fluxes ($p < 0.05$)

A series of ANOVA tests were carried out comparing the conditions in the Riparian group (site 3) with all other chambers (Table 3). Aside from CH_4 concentrations and emissions, the riparian zone was characterized by having a high soil respiration, pH and soil solution DIC concentration relative to the rest of the sites. The Riparian soil also contained significantly less extractable DOC than the rest of the groups combined, though a similar level to the Juncus/Hummock chambers (Table 2).

The N_2O fluxes were more variable and approximately one order of magnitude lower than CH_4 fluxes. No significant differences were observed between groups when the full dataset was used. Again, no significant group effect was evident during the 2006 growing season (Figure 3a), with standard error bars crossing the x-axis in all but the Hollow and Juncus/Hummock groups, which both showed net N_2O uptake. During the winter season (Figure 3b) a net uptake was measured in the Hollow chambers, in contrast to the net emissions measured in both the Sedge/Hummock and Juncus/Hummock groups. All groups displayed a net emission during growing season 2007 (Figure 3c) with emissions from the Riparian chambers significantly greater than any other group.

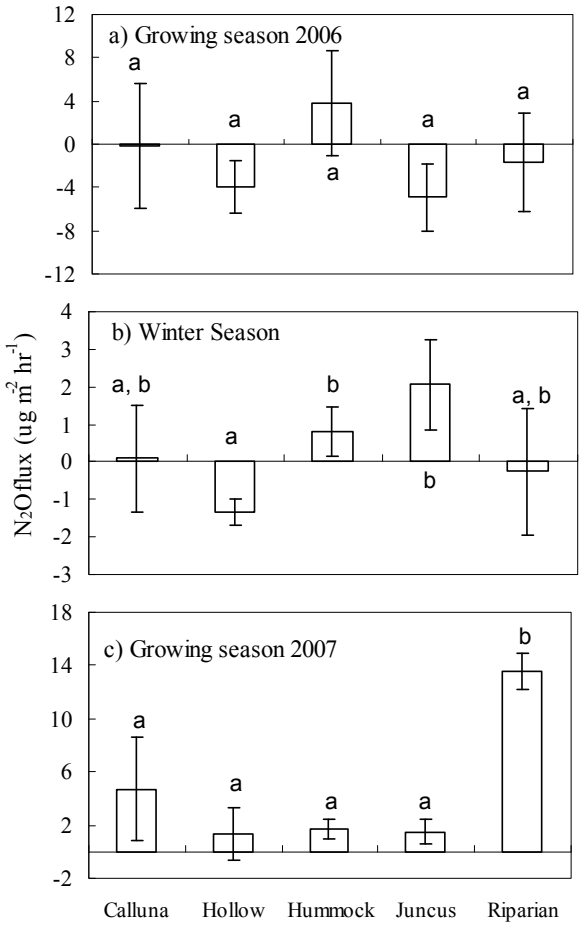

Figure 3 Mean integrated N_2O flux during a) growing season 2006, b) the winter period and c) growing season 2007, separated by microtopographic/vegetative group. Error bars represent the standard error of the mean. Common letters indicate statistically similar fluxes ($p < 0.10$)

– *Modelling spatial variability*

Using best subset multiple regression on the full dataset (n = 21), spatial variability in CH_4 fluxes could be modelled with an r^2 of 0.81 ($p < 0.01$) using the variables soil moisture and soil CH_4 concentration. When separated by season, soil CH_4 concentration was the major variable evident in all models (data not shown). However, the model was highly influenced by the chambers situated in the riparian zone and therefore not applicable to the rest of the catchment. Model fitting was repeated after excluding the 3 chambers in the riparian zone (Table 4). Over the full study period an r^2 of 0.46 was achieved using the variables percent sedge cover, pH, water extractable DOC, soil solution DIC and soil moisture. The variability in CH_4 flux during growing season 2006 was well modelled ($r^2 = 0.80$), with emissions increasing in response to a lower proportion of rushes, a decrease in the depth of the water table and concentration of soil NO_3, and an increase in soil moisture, soil solution DOC and below-ground CH_4 concentration (Table 4b). Variability in CH_4 emissions during the winter season was modelled ($r^2 = 0.36$, $p = 0.05$), with negative correlations between CH_4 emission and soil respiration and soil solution DIC, and positive correlations with percent moss cover and below-ground CH_4 concentration (Table 4c). Lastly, the best model for emissions during growing season 2007 ($r^2 = 0.45$, $p = 0.02$) included percent sedge cover (negative) and soil pH (positive) (Table 4d).

Variables that were significantly correlated with below-ground CH_4 concentrations were assessed using a series of Spearman's rank correlation tests (Figure 4); again chambers in the riparian zone were omitted from the analyses. Water table depth was only significantly related to below ground CH_4 concentrations during growing season 2006 when the water table was drawn down to ~50 cm for most of the summer (Figure 1); no significant correlations with soil moisture were found. Significant negative correlations were found in all seasons with either percent sedge and percent rush cover. Negative correlations were also found with soil extractable NO_3, soil solution NO_3 and soil N_2O concentrations.

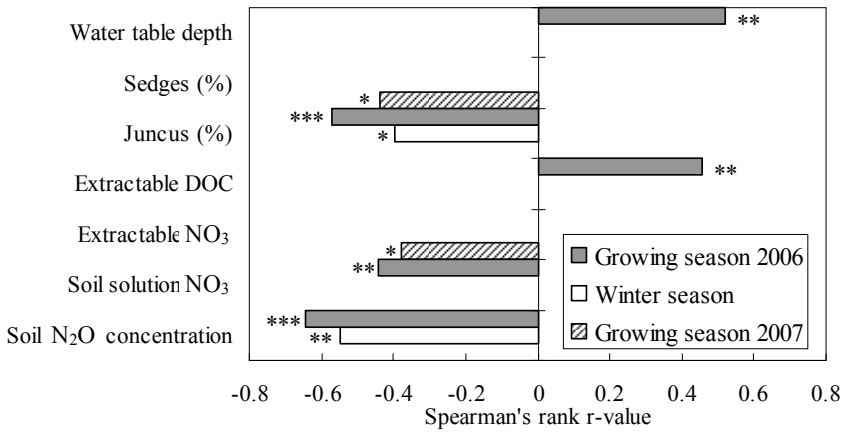

Figure 4 Results from Spearman's rank correlations on soil CH_4 concentration using chambers from sites 1 and 2 only (i.e. excluding riparian zone). P-values represent: $p < 0.01$***, $p < 0.05$**, $p < 0.1$*

Although water table position appeared only in the 2006 growing season model (Table 4b), the maximum CH_4 emissions recorded on each sampling occasion often occurred where the water table was closest to the surface. Within all 21 chambers, 3 chambers repeatedly ranked in the top 3 CH_4 emitters, with the same 3 chambers repeatedly ranked among the 3 highest water tables and 3 highest soil moisture contents. The highest CH_4 emitters included 2 chambers within the riparian zone and 1 chamber located on a hollow in site 2. The 2 chambers in the riparian zone ranked within the top 3 highest CH_4 emitters on 94% and 63% of all sampling occasions, respectively; on 89% and 14% of occasions their water table positions were in the top 3 highest and on 47% and 56% of occasions their soil moisture contents were in the top 3 highest, respectively. The Hollow chamber in site 2 ranked within the top 3 highest CH_4 emitters, highest water table and highest soil moisture content on 61%, 83% and 41% of occasions, respectively.

Table 4 Results from best subset multiple regression model describing the spatial variation in CH_4 and N_2O fluxes across a) the full dataset, b) growing season 2006, c) the winter season 2006-07 and d) growing season 2007 with the riparian chambers excluded.

CH_4 flux			N_2O flux		
Variable	T	P	Variable	T	P
a) Full study period					
($r^2 = 0.46$; $p = 0.03$)			($r^2 = 0.25$; $p = 0.05$)		
Intercept	---	---	Intercept	---	---
Sedges (%)	-1.37	0.10	pH	-1.94	0.07
pH	2.39	0.03	Soil N_2O concentration	1.81	0.09
Extractable DOC	2.22	0.05			
Soil solution DIC	-2.50	0.03			
Soil moisture	1.92	0.08			
b) Growing season 2006					
($r^2 = 0.80$; $p < 0.01$)			($r^2 = 0.14$; $p = 0.07$)		
Intercept	---	---	Intercept	---	---
Rushes (%)	-4.04	< 0.01	pH	-1.93	0.07
Water table depth	-2.52	0.03			
Soil moisture	6.04	< 0.01			
Extractable NO_3	-3.54	< 0.01			
Soil solution DOC	2.65	0.02			
Soil CH_4 concentration	2.48	0.03			
c) Winter season 2006-07					
($r^2 = 0.36$; $p = 0.05$)			($r^2 = 0.44$; $p < 0.01$)		
Intercept	---	---	Intercept	---	---
Soil respiration	-2.28	0.04	Soil CO_2 concentration	-3.66	< 0.01
Soil solution DIC	-2.65	0.02			
Soil CH_4 concentration	2.70	0.02			
Mosses (%)	2.36	0.04			
d) Growing season 2007					
($r^2 = 0.45$; $p = 0.02$)			($r^2 = 0.65$; $p < 0.01$)		
Intercept	---	---	Intercept	---	---
Sedges (%)	-2.07	0.06	pH	2.58	0.02
pH	2.07	0.02	Soil solution DOC	2.27	0.04
			Soil N_2O concentration	1.69	0.12

Spatial variability in N_2O emissions amongst all chambers over the full study period, was best modelled using only soil respiration ($r^2 = 0.28$, $p < 0.01$). Excluding the riparian chambers from the analysis, soil respiration was no longer significant and the best model ($r^2 = 0.25$, $p = 0.05$) was achieved by including a negative correlation

with pH and a positive correlation with below-ground N_2O concentrations (Table 4a). Other variables which appeared in the seasonal models included soil CO_2 concentration (winter season: $t = -3.66$, $p < 0.01$) and soil solution DOC (growing season 2007: $t = 2.27$, $p < 0.05$).

Temporal variability (Site 2)

Temporal variability in CH_4 emissions from all 9 chambers at site 2 was best modelled ($r^2 = 0.55$, $p < 0.01$) using the variables soil moisture and soil temperature at 40 cm (Table 5a). The mean (± SE) Q_{10} across all 9 chambers was 4.16 ± 0.96. Having separated the chambers by group, both the Hollows ($r^2 = 0.68$, $p < 0.01$) and Juncus/Hummocks ($r^2 = 0.41$, $p < 0.01$) responded negatively to soil respiration (Table 5b and d). However, in the Hollow group water table depth and soil temperature where also important. The primary drivers of emissions in the Sedge/Hummock plots appeared to be soil moisture and again soil temperature (Table 5c). Neither the Sedge/Hummock nor the Juncus/Hummock plots appeared to be affected by changes in water table depth.

The temporal variability in N_2O emissions across all plots (Table 5a) was poorly captured by even the best available model ($r^2= 0.18$, $p < 0.05$). Again both soil respiration, to which emissions were negatively correlated, and soil temperature at 40 cm appeared as primary variables using both the full 9 chambers and the Juncus/Hummock group alone. The mean (± SE) Q_{10} across the 9 chambers was 7.12 ± 1.25. Variability in emissions was best captured in the Hollow chambers where water table depth and soil moisture, in addition to soil respiration, were significant factors (Table 5b); N_2O emissions increased in response to near-surface water tables and increasing soil moisture contents. Soil moisture was again significant in the Sedge/Hummock plots (Table 5c); although soil temperature alone was not significant, its exclusion from the model increased the overall model p-value above 0.05 and was therefore left in.

Table 5 Results from best subset multiple regression model describing the temporal variation in CH_4 and N_2O fluxes across in a) all chambers within site 2 (n = 9), b) Hollow chamber within site 2 (n = 3), c) Sedge/Hummock chambers within site 2 (n = 3) and d) Juncus/Hummock chambers within site 2 (n = 3)

CH_4 flux			N_2O flux		
Variable	T	P	Variable	T	P
a) All chambers					
($r^2 = 0.55$; $p < 0.01$)			($r^2 = 0.18$; $p = 0.03$)		
Intercept	---	---	Intercept	---	---
Soil moisture	5.85	< 0.01	Soil respiration	-2.67	0.01
Soil temperature (40 cm)	3.45	< 0.01	Soil temperature (40 cm)	1.76	0.09
b) Hollow					
($r^2 = 0.68$; $p < 0.01$)			($r^2 = 0.45$; $p < 0.01$)		
Intercept	---	---	Intercept	---	---
Soil respiration	-2.09	0.05	Soil respiration	-1.98	0.06
Water table depth	-6.13	< 0.01	Soil moisture	2.00	0.06
Soil temperature (5 cm)	4.59	< 0.01	Water table depth	-4.43	< 0.01
c) Sedge/Hummock					
($r^2 = 0.50$; $p < 0.01$)			($r^2 = 0.25$; $p = 0.01$)		
Intercept	---	---	Intercept	---	---
Soil moisture	5.13	< 0.01	Soil moisture	3.28	< 0.01
Soil temperature (40 cm)	3.85	< 0.01	Soil temperature (40 cm)	1.55	0.13
d) Juncus/Hummock					
($r^2 = 0.41$; $p < 0.01$)			($r^2 = 0.16$; $p = 0.04$)		
Intercept	---	---	Intercept	---	---
Soil respiration	-4.40	< 0.01	Soil respiration	-2.24	0.03
			Soil temperature (40 cm)	2.07	0.05

Discussion

Flux magnitude – comparison with other studies

Using an unsupervised, ground-truthed, classification of a Quickbird satellite image taken in May 2006 (Dinsmore, data not shown, 2008), and assuming a riparian zone spanning approximately 3 m either side of the Black Burn stream, the percent cover within the catchment of Calluna, Hollow, Sedge/Hummock, Juncus/Hummock and Riparian zone were estimated as 10%, 29%, 29%, 28% and 0.6%, respectively.

Weighting the above means accordingly, and assuming values are representative of the mean daily emission, the mean catchment fluxes of CH_4 and N_2O from April 2006 until October 2007 were 291 and 5.12 μg m^{-2} d^{-1}, or 1.06 and 0.019 kg ha^{-1} y^{-1}, respectively. Ignoring the different groups and treating the chambers as replicates gave mean fluxes for CH_4 and N_2O of 2156 and 23.6 μg m^{-2} d^{-1}, respectively, or 171 and 12.1 μg m^{-2} d^{-1} if the riparian chambers were excluded. With the riparian chambers included, treating the chambers as replicates significantly overestimated CH_4 emissions whilst excluding them led to an underestimation of emissions; N_2O emissions were overestimated with or without the riparian chambers included.

The riparian zone alone contributed approximately 12% of the total catchment CH_4 emission (although uncertainty in this estimate is very high), highlighting the importance of identifying and including emission hotspots in catchment budgets even if they cover only a small proportion of the overall area, a result also found by McNamara *et al.* (2008). Even after separating the chambers into groups to minimize spatial variability, the uncertainty within each group was still large. Furthermore, the exact weight given to each group in the final catchment calculation has significant uncertainties. By sequentially changing the percent cover estimates by plus or minus 10% and evenly distributing the difference among the remaining groups, the total catchment CH_4 and N_2O means varied by up to 36% and up to 38% (± 10% Juncus/Hummock cover), respectively. Despite the large measured fluxes, due to the relatively small area of the riparian zone, a 10% error in its relative size altered the final catchment mean by the least amount (CH_4 2.86%, N_2O 0.97%).

Flux measurements using a similar method to that described here were made from 3 chambers at Auchencorth Moss in May 1995 (unpublished observations, MacDonald, 1997). The mean calculated flux extrapolated to the annual catchment scale gave a CH_4 emission of 1.23 kg ha^{-1} y^{-1}. Despite the level of upscaling, this figure is very similar to the 1.06 kg ha^{-1} y^{-1} calculated in this study. Our calculated CH_4 emission rates were however low in comparison to other literature reported values for peatland systems. Emissions from Caithness (Scotland), Glencar (Ireland) and Moor House (England) were calculated as 69, 62 and 173 kg ha^{-1} y^{-1}, respectively (Hargreaves and Fowler, 1998; Laine *et al.*, 2007; McNamara *et al.*, 2008); the Moor House estimate

was up-scaled from summer measurements only. Estimates from non-UK peatlands were also higher than those measured here, e.g. 49 kg ha^{-1} y^{-1} from Mer Bleue, Canada (Roulet *et al.*, 2007) and 21 – 131 kg ha^{-1} y^{-1} from Lakkasuo mire, Finland (Minkkinen and Laine, 2006). The low emissions measured at Auchencorth Moss were most likely a result of the relatively shallow peat layer (~0.5 m) at the study sites, even though there are significant areas of deep peat within the catchment. During periods of water table drawdown, in particular during the 2006 growing season, the water table in some chambers dropped below the peat layer into the underlying mineral soil layer; therefore no true permanently saturated catotelm exists over much of the site.

N_2O emissions from other peatland sites reported in the literature vary considerably, which is unsurprising given the large within-site variation. Growing season N_2O fluxes from Dunslair Heights moorland (peaty podzol), Scotland, averaged 519 ± 842 (SD) μg m^{-1} d^{-1} in 1994 (MacDonald *et al.*, 1997), two orders of magnitude greater than the 5.12 μg m^{-1} d^{-1} measured in this study. However, fluxes from the same site measured in 1995 averaged only 2.72 ± 130 (SD) μg m^{-1} d^{-1}, well within the range measured here (MacDonald *et al.*, 1997). Regina *et al.* (1996) measured fluxes from Finnish ombrotrophic bogs ranging from an uptake of -30 ± 15 (SD) μg m^{-1} d^{-1} to emissions of 24 ± 14 (SD) μg m^{-1} d^{-1}, again our mean lies well within these limits and the large variability measured here is not uncommon.

Controls on spatial variation

Clear differences in CH_4 emissions were observed both between the growing seasons and the winter season, and between the growing seasons in 2006 and 2007, respectively (Figure 2). The differences were less pronounced for N_2O fluxes, primarily due to the very large variation seen across all chamber types within seasons (Figure 3). The most striking difference between groups was the consistently large CH_4 emissions and below-ground CH_4 concentrations measured in the riparian chambers. Although DOC, often quoted as the primary substrate for methanogenic bacteria (Segers, 1998), was low in the riparian zone (247 μg C g^{-1}) compared to the rest of the catchment (386 μg C g^{-1}), the pH was significantly higher (Riparian 5.83,

Catchment 4.81), hence closer to the methanogenic optima of ~7 (Segers, 1998). Studies have repeatedly reported an increase in potential CH_4 production in response to increased pH (Dunfield *et al.*, 1993; Valentine *et al.*, 1994; Yavitt *et al.*, 1987). The depth of the water table at the riparian site was not significantly higher than the rest of the catchment due to extremely high variability among the 3 riparian chambers. However, in 2 of the 3 riparian chambers water table was repeatedly in the top 3 highest. In particular, one of the chambers, which was also in the top 3 highest CH_4 emitters on 94% of sampling occasions, had the highest water table on 89% of occasions. Even during the relatively dry summer of 2006 when catchment water tables were drawn down to an average of almost 50 cm below the soil surface, the water table at this one chamber remained within 18 cm of the surface.

Among the variables included in the CH_4 flux spatial variation models (Table 4) were pH, DOC, water table depth and soil moisture. Water table depth and DOC also correlated well with below ground CH_4 concentrations (Figure 4). The correlation with water table depth has been well documented in previous studies (Aerts and Ludwig, 1997; Dinsmore *et al.*, 2008; Hargreaves and Fowler, 1998; MacDonald *et al.*, 1998; Moore and Dalva, 1993); water table depth determines the depth of the oxic/anoxic boundary and the redox level within the soil. Soil moisture is strongly linked to water table depth and may act as an indication of not only current but also antecedent water levels. Therefore in some cases soil moisture represents a better indicator of CH_4 emission than an instantaneous water table measurement. The effect of water table depth on CH_4 emissions was only significant during growing season 2006 when it ranged from approximately 5 to 50 cm below the peat surface. Similarly Shannon and White (1994) found that water table was only important in one of 3 annual cycles, corresponding to the year with the greatest range of water table depths (15cm – 50 cm). Soil respiration represents a measure of aerobic microbial activity and thus is likely to correlate strongly with rates of CH_4 oxidation, hence the negative correlation with emissions during the winter season.

During the growing seasons CH_4 emissions were negatively correlated with the frequency of either rushes or sedges inside the chambers (Table 4b and d); the same was seen in below-ground concentrations across all seasons (Figure 4). Although

contrary to much of the current literature which suggests the presence of aerenchyma containing vegetation (i.e. rushes and sedges) increases emissions (Greenup *et al.*, 2000; Shannon *et al.*, 1996; Yu *et al.*, 1997), a similar result to that observed here was found in an earlier study with mesocosms collected from Auchencorth Moss (Dinsmore *et al.*, in press for Plant and Soil). As well as providing a source of readily available organic substrate, plants containing aerenchymous tissue can provide a direct pathway for many greenhouse gases to the atmosphere, bypassing the aerobic surface horizon and therefore reducing the potential for oxidation (Bartlett and Harriss, 1993; Minkkinen and Laine, 2006). However, studies have also shown that aerenchyma can transport O_2 into the rhizosphere and can significantly alter the redox state of the surrounding peat (Watson *et al.*, 1997; Visser *et al.*, 2000; Wiebner *et al.*, 2002). Similarly, Arah and Stephen (1998) found that increasing root-mediated transport in a CH_4 flux model led to a decrease in simulated CH_4 emissions, due to the increase in oxidation outweighing the positive influence of increased CH_4 transport.

For emissions to increase via plant-mediated transport, roots must penetrate areas of high CH_4 production, thought to occur ~15-20 cm below the water table (Daulat and Clymo, 1998; Kettunen *et al.*, 1999), and bypass the surface oxidizing peat layer. As the water table was drawn down to almost 50 cm during much of the 2006 growing season, and repeatedly to similar low levels during 2007, it is likely that no significant reservoir of CH_4 was present in the shallow peat for the plant roots to tap into. Roura-Carol and Freeman (1999) suggest that the radial loss of O_2 from plant roots is likely to be dependent on photosynthetic activity. Rhizospheric oxidation is likely to be minimal during the winter when plants are relatively inactive, and this may explain the lack of an aerenchymous vegetation variable in our winter season model (Table 4c). In the riparian zone where water table levels remained high throughout the growing season and high below-ground CH_4 concentrations were evident, the effect of plant-mediated transport may outweigh rhizospheric oxidation. However, this could not be tested as all our riparian chambers included *J. effusus*.

The optimum pH for denitrifiers is often thought to be between approximately 6.5-8.0 (Knowles, 1981; Šimek and Cooper, 2002), therefore any increase above the

mean catchment pH of 4.18 should theoretically increase N_2O production. However the partitioning of N_2O and N_2 is also influenced by pH with a higher proportion of N_2O in more acid conditions (Šimek *et al.*, 2002). In this study, pH was negatively correlated with N_2O in both the full study period and the growing season 2006 models (Table 4a and b). Soil pH was also strongly negatively correlated with both soil extractable NO_3 ($r = -0.61$, $p < 0.001$) and soil extractable NH_4 ($r = -0.75$, $p < 0.01$) concentrations over the same period. Therefore the reduction of N_2O emissions at higher pH values could also have occurred as an indirect response to low soil nitrogen availability.

Controls on temporal variation (site 2)

Considering all of the 9 plots within site 2 where measurements were made fortnightly, the main drivers of temporal variability in CH_4 emissions appeared to be soil moisture and soil temperature (Table 5a). The temporal response in CH_4 emissions to variations in temperature is consistent with previous studies (Frolking and Crill, 1994; Laine *et al.*, 2007; Shannon and White, 1994) and the mean Q_{10} of 4.16 is similar to values previously reported for a different Scottish peatland (MacDonald *et al.*, 1998). Although significant changes in water table depth (e.g. drainage or drain blocking) have repeatedly been shown to strongly influence CH_4 emissions (Alm *et al.*, 1999; Strack *et al.*, 2004), a much weaker relationship is often observed with temporal water table variability in the field (Frolking and Crill, 1994; Shannon and White, 1994). In this study water table was a significant correlate only in the Hollow chambers, although soil moisture, which may provide a better measure of both current and antecedent soil water conditions, was also apparent in the Sedge/Hummock model. The presence of aerenchyma containing vegetation in the Sedge/Hummock and Juncus/Hummock chambers might have partially off-set any increase in CH_4 emissions associated with a rise in water table by increasing oxidation in the rhizosphere. Hence differences between studies in the strength of water table as a driver of variability may be caused in part by differences in site-specific vegetation cover.

Net CH_4 flux is dependent on the balance between oxidation and production processes. As the temperature response in methanogens is generally greater than that of methanotrophs (Segers, 1998), the overall effect on net emissions was positive. Where temperature is a significant driver of variability, as in both Hollow and Sedge/Hummock chambers, it suggests that variability is due primarily to changes in methanogen activity rather than oxidation. However the primary driver of net emissions in the Juncus/Hummock plots was soil respiration, itself likely to be an indicator of aerobic microbial activity, and as such correlate with potential oxidation. The dominance of oxidation in controlling emission variability in the Juncus/Hummock plots may be due to potential methanogenesis being limited by lower substrate availability, possibly reflected in the lower concentrations of extractable DOC in the Juncus/Hummock chambers (Table 2).

Soil temperature was again an important driver of temporal N_2O dynamics with a very high Q_{10} of 7.12, and an apparent switch from consumption to production at approximately 8ºC (data not shown). A very similar result was observed by Dinsmore *et al.* (in press for Plant and Soil) in mesocosms collected from Auchencorth Moss, where a switch from consumption to production was recorded between approximately 7.5 and 8.5ºC. However, as was also the case in Dinsmore *et al.* (in press for Plant and Soil) N_2O fluxes are low and variability high, so further work is required to assess the validity of this switch.

A number of peaks in CH_4, and to a lesser extent N_2O emissions were recorded during growing season 2007 (Figure 1), often following shortly after significant rises in water table. Similar pulses following a rise in water table level were observed in Dinsmore *et al.* (in press for Plant and Soil) and were attributed to an increase in methanogenic substrate due to increased biomass recycling and mineralization during the preceding dry period. Previous studies have also indicated a pulse in emissions following a drop in water table (Dinsmore *et al.*, in press for Plant and Soil; Moore *et al.*, 1990; Shurpali *et al.*, 1993) associated with degassing due to a reduction in hydrostatic pressure. This was not observed during this field study although peaks may have been missed due to the low sampling frequency.

Conclusions

CH_4 emissions varied considerably across the catchment, with the riparian zone representing a significant hotspot. Spatial variability was influenced by water table only during growing season 2006 when drawdown was at its most extreme. Contrary to many previous studies, the presence of either sedges or rushes containing aerenchymous tissue decreased net CH_4 emissions during the 2 growing seasons. Temporal variability in CH_4 emission was driven primarily by soil moisture content and temperature. Water table was a significant driver only in the Hollow plots; we suggest that oxidation in the rhizosphere of aerenchymous plants may partially negate increases in methanogenesis caused by a near-surface water-table. Temporal variability in CH_4 fluxes from the Juncus/Hummock plots was best explained using only soil respiration. This indicated that oxidation rather than methanogenesis drove the variability in net emissions in these chambers. Drivers of spatial variability in N_2O emissions included pH and below-ground CO_2 concentration; the data also suggests an indirect link to soil nitrogen availability. Temporal N_2O variability was explained using the variables temperature, soil moisture and water table.

Upscaling the calculated fluxes using vegetation cover estimates from a satellite image gave mean catchment CH_4 and N_2O emissions of 291 μg CH_4 m^{-2} d^{-1} and 5.12 μg N_2O m^{-2} d^{-1}. High variability among the chambers even within designated microtopographic/vegetation classes led to significant uncertainty in these final estimates; furthermore the values were extremely sensitive to error in the cover estimates. A change of up to 36% for CH_4 and up to 38% for N_2O in the emission estimate occurred in response to a 10% error in the estimate of coverage for individual groups. When planning future studies we suggest preliminary work should include identifying the potential emission hotspots, such as the riparian zone, and other potential sources of spatial variability across the site. Depending on the heterogeneity of the site, a number of spatially distinct integrated models may provide a better representation of the longer-term temporal changes in the full catchment budget, rather than a single model based on averaged values.

Acknowledgements

The work was funded by the UK Natural Environment Research Council (NERC) through an algorithm PhD studentship grant

References

Aerts, R., Ludwig, F., 1997. Water-table changes and nutritional status affect trace gas emissions from laboratory columns of peatland soils. Soil Biology and Biochemistry 29, 1691-1698.

Alm, J., Saarnio, S., Nykänen, H., Silvola, J., Martikainen, P. J., 1999. Winter CO_2, CH_4 and N_2O fluxes on some natural and drained boreal peatlands, Biogeochemistry 44, 163-186.

Arah, J. R. M., Stephen, K. D., 1998. A model of the processes leading to methane emissions from peatland. Atmospheric Environment 32, 3257-3264.

Bartlett, K. B., Harriss R. C., 1993.Review and Assessment of Methane Emissions from Wetlands, Chemosphere 26, 261-320.

Billett, M. F., Palmer, S. M., Hope, D., Deacon, C., Storeton-West, R., Hargreaves, K. J., Flechard, C., Fowler D., 2004. Linking land-atmosphere-stream carbon fluxes in a lowland peatland system. Global Biogeochemical Cycles 18, GB1024.

Bubier, J. L., Moore, T. R., Roulet, N. T., 1993. Methane emissions from wetlands in the midboreal region of northern Ontario, Canada. Ecology 74, 2240-2254.

Daulat, W. E., Clymo, R. S., 1998. Effects of temperature and watertable on the efflux of methane from peatland surface cores. Atmospheric Environment 32, 3207-3218.

Dinsmore, K. J., Skiba, U. M., Billett, M. F., Rees, R. M., in press. Effect of water table on greenhouse gas emissions from peatland mesocosms. Plant and Soil.

Dunfield, P., Knowles, R., Dumont, R., Moore, T. R., 1993. Methane production and consumption in temperate and subarctic peat soils: Response to temperature and pH. Soil Biology and Biochemistry 25, 321-326.

Frolking, S., Crill, P., 1994. Climate Controls on Temporal Variability of Methane Flux from a Poor Fen in Southeastern New-Hampshire - Measurement and Modeling. Global Biogeochemical Cycles 8, 385-397.

Gorham, E., 1991. Northern Peatlands: Role in the Carbon-Cycle and Probable Responses to Climatic Warming. Ecological Applications 1, 182-195.

Greenup, A. L., Bradford, M., McNamara, N., Ineson, P., Lee, J., 2000. The role of Eriophorum vaginatum in CH_4 flux from an ombrotrophic peatland. Plant and Soil 227, 265-272.

Griffis, T. J., Rouse, W. R., 2001. Modelling the interannual variability of net ecosystem CO_2 exchange at a subarctic sedge fen. Global Change Biology 7, 511-530.

Gut, A., Blatter, A., Fahrni, M., Lehmann, B. E., Neftel, A., Staffelbach, T., 1998. A new membrane tube technique (METT) for continuous gas measurements in soils. Plant and Soil 198, 79-88.

Hargreaves, K. J., Fowler, D., 1998. Quantifying the effects of water table and soil temperature on the emission of methane from peat wetland at the field scale. Atmospheric Environment 32, 3275-3282.

Hutchinson, G. L., 1995. Biosphere-atmosphere exchange of gaseous N oxides. In: Lal, R., Kimble, J., Levine, E., Stewart, B. A. (Eds.), Soils and Global Change. Lewis Publishers, Boca Raton, pp. 219-236.

Huttunen, J. T., Nykänen, H., Turunen, J., Nenonen, O., Martikainen, P. J., 2002. Fluxes of nitrous oxide on natural peatlands in Vuotos, an area projected for a hydroelectric reservoir in northern Finland. Suo (Helsinki), 53, 87-96.

Huttunen, J. T., Nykänen, H., Turunen, J., Martikainen, P. J., 2003. Methane emissions from natural peatlands in the northern boreal zone in Finland, Fennoscandia. Atmospheric Environment 37, 147-151.

Kettunen, A., Kaitala, V., Lehtinen, A., Lohila, A., Alm, J., Silvola, J., Martikainen, P. J., 1999. Methane production and oxidation potentials in relation to water table fluctuations in two boreal mires. Soil Biology and Biochemistry 31, 1741-1749.

Knowles, R., 1981. Denitrification. Marcel Dekker, New York, pp. 323-369.

Lafleur, P. M.,. Roulet, N. T, Bubier, J. L., Frolking, S., Moore, T. R., 2003. Interannual variability in the peatland-atmosphere carbon dioxide exchange at an ombrotrophic bog. Global Biogeochemical Cycles 17, 1036.

Laine, A., Wilson, D., Kiely, G., Byrne, K. A., 2007. Methane flux dynamics in an Irish lowland blanket bog. Plant soil 299, 181-193.

Livingston, G. P., Hutchinson, G. L., 1995. Enclosure-based measurement of trace gas exchange: applications and sources of error. In: Matson, P. A., Harriss, R. C. (Eds.), Biogenic trace gases: measuring emissions from soil and water. Marston Lindsey Ross International Ltd., Oxford.

Lund, M., Lindroth, A., Christensen, T. R., Ström, L., 2007. Annual CO_2 balance of a temperate bog. Tellus Series B 59, 804-811.

MacDonald, J. A., Skiba, U., Sheppard, L. J., Hargreaves, K. J., Smith, K. A., Fowler, D., 1996. Soil environmental variables affecting the flux of methane from a range of forest, moorland and agricultural soils. Biogeochemistry 34, 113-132.

MacDonald, J. A., Skiba, U., Sheppard, L. J., Ball, B., Roberts, J. D., Smith, K. A., Fowler, D., 1997. The effect of nitrogen deposition and seasonal variability on methane oxidation and nitrous oxide emission rates in an upland spruce plantation and moorland. Atmospheric Environment 31, 3693-3706.

MacDonald, J. A., Fowler, D., Hargreaves, K. J., Skiba, U., Leith, I. D., Murray, M. B., 1998. Methane emission rates from a northern wetland; response to temperature, water table and transport. Atmospheric Environment 32, 3219-3227.

McNamara, N. P., Plant, T., Oakley, S., Ward, S., Wood, C., Ostle, N., 2008. Gully hotspot contribution to landscape methane (CH_4) and carbon dioxide (CO_2) fluxes in a northern peatland. Science of the Total Environment doi: 10.1016/j.scitotenv.2008.03.015.

Minkkinen, K., Laine, J., 2006. Vegetation heterogeneity and ditches create spatial variability in methane fluxes from peatlands drained for forestry. Plant and Soil 285, 289-304.

Moore, T., Roulet, N., Knowles, R., 1990. Spatial and temporal variations of methane flux from subarctic/northern boreal fens. Global Biogeochemical Cycles 4, 29-46.

Moore, T. R., Dalva, M., 1993. The influence of temperature and water table on carbon dioxide and methane emissions from laboratory columns of peatland soils. European Journal of Soil Science 44, 651-664.

Nungesser, M. K., 2003. Modelling microtopography in boreal peatlands: hummocks and hollows. Ecological Modelling 165, 175-207.

Regina, K., Nykänen, H., Silvola, J., Martikainen, P. J., 1996. Fluxes of nitrous oxide from boreal peatlands as affected by peatland type, water table level and nitrification capacity. Biogeochemistry 35, 401-418.

Roulet, N., Lafleur, P. M., Richard, P. J. H., Moore, T. R., Humphreys, E. R., Bubier, J., 2007. Contemporary carbon balance and late Holocene carbon accumulation in a northern peatland. Global Change Biology 13, 397-411.

Roura-Carol, M., Freeman, C., 1999. Methane release from peat soils: effects of Spagnum and Juncus. Soil Biology and Biochemistry 31, 323-325.

Segers, R., 1998. Methane production and methane consumption: a review of processes underlying wetland methane fluxes. Biogeochemistry 41, 23-51.

Shannon, R. D., White, J. R., 1994. A three-year Study of Controls on Methane Emissions from 2 Michigan Peatlands. Biogeochemistry 27, 35-60.

Shannon, R. D., White, J. R., Lawson, J. E., Gilmour, B. S., 1996. Methane efflux from emergent vegetation in peatlands. Journal of Ecology 84, 239-246.

Shurpali, N., Verma, S. B., Clement, R. J., Billesbach, D. P., 1993. Seasonal distribution of methane flux in a Minnesota peatland measured by eddy correlation. Journal of Geophysical Research 98, 20649-20655.

Šimek, M., Cooper, J. E., 2002. The influence off soil pH on denitrification: preogress towards the understanding of this interaction over the last 50 years. European Journal of Soil Science 53, 345-354.

Šimek, M., Jisova, L., Hopkins, D. W., 2002. What is the so-called optimum pH for denitrification in soil? Soil Biology and Biochemistry 34, 1227-1234.

Strack, M., Waddington, J. M., Tuittila, E. –S., 2004. Effect of water table drawdown on northern peatland methane dynamics: implications for climate change. Global Biogeochemical. Cycles 18, GB4003.

Ström, L., Ekberg, A., Mastepanov, M., Christensen, T. R., 2003. The effect of vascular plants on carbon turnover and methane emissions from a tundra wetland. Global Change Biology 9, 1185-1192.

Townend, J., 2002. Practical statistics for environmental and biological scientists. John Wiley & Sons Ltd, Chicester.

Updegraff, K., Bridgham, S. D., Pastor, J., Weishampel, P., Harth, C., 2001. Response of CO_2 and CH_4 emissions from peatlands to warming and water table manipulation. Ecological Applications 11, 311-326.

Valentine, D. W., Holland, E. A., Schimel, D. S., 1994. Ecosystem and physiological controls over methane production in northern wetlands. Journal of Geophysical Research 99, 1563-1571.

Visser, E. J., Colmer, T. D., Blom, C. W. P. M., Voesenek L. A. C. J., 2000. Changes in growth, porosity, and radial oxygen loss from adventitious roots of selected mono- and dicotyledonous wetland species with contrasting types of aerenchyma. Plant, Cell and Environment 23, 1237-1245.

Waddington, J. M., Roulet, N. T., 1996. Atmosphere-wetland carbon exchange: Scale dependency of CO2 and CH4 exchange on the developmental topography of a peatland. Global Biogeochemical Cycles 10, 233-245.

Watson, A., Stephen, K. D., Nedwell, D. B., Arah, J. R. M., 1997. Oxidation of methane in peat: kinetics of CH_4 and O_2 removal and the role of plant roots. Soil Biology & Biochemistry 29, 1257-1267.

Whalen, S. C., Reeburgh, W. S., 2000. Methane oxidation, production, and emission at contrasting sites in a boreal bog. Geomicrobiology Journal 17, 237-251.

Whiting, G. J., Chanton, J. P., 1996. Control of diurnal pattern of methane emission from aquatic macrophytes by gas transport mechanisms. Aquatic Botany 54, 237-253.

Wiebner, A., Kuschk, P., Stottmeister, U., 2002. Oxygen release by roots of Typha latifolia and Juncus effusus in laboratory hydroponic systems. Acta Biotechnologica 22, 209-216.

Yavitt, J. B., Lang, G. E., Wieder, R. K., 1987. Control of carbon mineralization to CH_4 and CO_2 in anaerobic, Sphagnum derived peat from Big run Bog, West Virginia. Biogeochemistry 4, 141-157.

Yu, K. W., Wang, Z. P., Chen, G. X., 1997. Nitrous oxide and methane transport through rice plants. Biology and Fertility of Soils 24, 341-343.

6. Paper II

Effect of water table on greenhouse gas emissions from peatland mesocosms

Kerry J. Dinsmore, Ute M. Skiba, Michael F. Billett, Robert M. Rees

Accepted for publication in 'Plant and Soil'
(doi:10.1007/s11104-008-9832-9)

Effect of water table on greenhouse gas emissions from peatland mesocosms

Kerry J. Dinsmore, Ute M. Skiba, Michael F. Billett, Robert M. Rees

Greenhouse gases, Water table, Vegetation, Microtopography, Peatland, Mesocosm

Abstract:

Peatland landscapes typically exhibit large variations in greenhouse gas (GHG) emissions due to microtopographic and vegetation heterogeneity. As many peatland budgets are extrapolated from small-scale chamber measurements it is important to both quantify and understand the processes underlying this spatial variability. Here we carried out a mesocosm study which allowed a comparison to be made between different microtopographic features and vegetation communities, in response to conditions of both static and changing water table. Three mesocosm types (hummocks + *Juncus effusus*, hummocks + *Eriophorum vaginatum*, and depressions dominated by moss) were subjected to 2 water table treatments (0-5 cm and 30-35 cm depth). Measurements were made of soil-atmosphere GHG exchange, GHG concentration within the peat profile and soil water solute concentrations. After 14 weeks the high water table group was drained and the low water table group flooded. Measurement intensity was then increased to examine the immediate response to change in water table position.

Mean CO_2, CH_4 and N_2O exchange across all chambers was 39.8 μg m^{-2} s^{-1}, 54.7 μg m^{-2} h^{-1} and -2.9 μg m^{-2} h^{-1}, respectively. Hence the GHG budget was dominated in this case by CO_2 exchange. CO_2 and N_2O emissions were highest in the low water table treatment group; CH_4 emissions were highest in the saturated mesocosms. We observed a strong interaction between mesocosm type and water table for CH_4 emissions. In contrast to many previous studies, we found that the presence of aerenchyma-containing vegetation reduced CH_4 emissions. A significant pulse in both CH_4 and N_2O emissions occurred within 1-2 days of switching the water table treatments. This pulsing could potentially lead to significant underestimation of landscape annual GHG budgets when widely spaced chamber measurements are upscaled.

Introduction:

Northern peatlands are estimated to contain 455 Gt of carbon (Gorham 1991), representing approximately a third of the estimated total global soil carbon pool. They are considered to be net sinks of CO_2 and net sources of CH_4 (Bartlett and Harriss 1993; Gorham 1991; Huttunen *et al.* 2003), though annual and inter-annual variation can be extremely high. Peatlands also represent an important source of dissolved organic carbon to drainage waters (Urban *et al.* 1989; Billett *et al.* 2004; Dawson *et al.* 2004). As soluble nitrogen is often limited, soil-atmosphere fluxes of N_2O tend to be small, although with a global warming potential of 298 (IPCC 2007) they can still contribute significantly to the total GHG budget. Some of the primary consequences of climate change, including increased temperatures, increased drought and increased frequency and intensity of rainfall events, are likely to directly influence peatland ecosystems. This in addition to management practices such as peatland drainage, means that it is becoming increasingly important to accurately predict the biospheric feedbacks of peatlands to climate.

The main controls on soil carbon and nitrogen cycling in peatlands are a) temperature, as it controls the rate of microbial activity; b) water table depth as it determines the depth of the oxic/anoxic boundary and redox level within the soil; and c) plant community composition and structure which influences the quantity and quality of organic substrate available, and can alter the aerobic capacity of the peat by transporting O_2 to the rhizosphere (Bartlett and Harriss 1993; Dise *et al.* 1993; Ström *et al.* 2003; Whiting and Chanton 1996; Yavitt *et al.* 1997). In the same way that certain plant species have the ability to transport O_2 from the atmosphere to the rhizosphere, they can provide a direct pathway for many GHGs to the atmosphere, bypassing the aerobic peat horizon (Bartlett and Harriss 1993; Minkkinen and Laine 2006). Such plant mediated transport has been demonstrated to account for >80% of CH_4 emissions from rice paddies (Butterbach-Bahl *et al.* 1997; Yu *et al.* 1997).

The microtopographic pattern of elevated hummocks, wetter depressions and submerged pools, typical of many peatlands, can cause significant variation in soil environmental conditions (Nungesser 2003). Such differences are further reinforced

by the colonisation of distinct plant communities. As a result GHG production, emission and consumption within peatlands can vary considerably at scales <1 m^2. Problems arise when gas exchange measurements, made using chambers of usually <0.5 m^2, require up-scaling to catchment level.

The influence of water table depth on CO_2 and CH_4 soil-atmosphere exchange has been studied repeatedly using flask experiments on disturbed peat (Blodau and Moore 2003a; Öquist and Sundh 1998), measurements on relatively undisturbed peat cores (Aerts and Ludwig 1997; Moore and Dalva 1993), and field studies (Hargreaves and Fowler 1998; MacDonald *et al.* 1998). Only a small number of controlled experiments have been carried out with the vegetation structure intact (Blodau *et al.* 2004; Blodau and Moore 2003a). Fewer still have compared different vegetation/microtopography types (though examples include: Updegraff *et al.* 2001), despite studies showing that the influence of vegetation is species-specific (Butterbach-Bahl *et al.* 1997; Ström *et al.* 2005). Such comparisons are important as the relative coverage of each community type may be altered following ecological succession resulting from long-term environmental change (Strack *et al.* 2006; Weltzin *et al.* 2003). The general consensus from these studies is that lowering the water table increases C mineralization and decreases CH_4 emissions. Studies into the effects of water table depth on peatland N_2O emissions include those by Aerts and Ludwig (1997) and Regina *et al.* (1999); they conclude that lowering the water table depth leads to a net increase in N_2O emissions.

The aims of this study are: a) to compare the greenhouse gas budget (with emphasis on CH_4 and N_2O) and temperature response of peatland mesocosms under high and low water table conditions; b) to quantify the immediate CH_4 and N_2O exchange response to a sudden change in water table depth; and c) to assess the influence of vegetation/microtopography on these responses.

Materials and Methods

Site description

Cores were collected from Auchencorth Moss peatland (55º47'34N; 3º14'35W), approximately 17 km south of Edinburgh (Scotland). Mean annual precipitation at the site (1995-2006) is 1016 mm (Coyle, unpublished data, 2008) with maximum and minimum monthly mean temperatures (1971-2000) of 19ºC in July and 0.7ºC in January respectively (www.metoffice.gov.uk).

The catchment is a 335 ha grass dominated, lowland ombrotrophic peatland with an elevation range of 249 to 300 m (Billett *et al.* 2004). The land-use is primarily low intensity sheep grazing, though overgrown grips are evidence of past drainage. The vegetation is a patchy mix of coarse grasses and soft rush covering a *Sphagnum* base layer. *Calluna vulgaris* is present in the south-west of the catchment where drainage is better. The microtopography consists of a series of hummocks and depressions. Hummocks are typically small (~40 cm diameter, ~30 cm height) and dominated by either a mix of *Deschamsia flexuosa* and *Eriophorum vaginatum*, or *Juncus effusus*. Depressions refer to the areas between hummocks and are dominated by mosses (*Sphagnum papillosa* and *Polytrichum commune*) and a thinner layer of grasses; depressions often become submerged after periods of intense or sustained rainfall. Water table at the site generally fluctuates between the peat surface and ~20 cm depth, although during dry periods it is often drawn down to >35 cm (Coyle, unpublished data, 2008). The mean water extractable DOC is 312 ± 15.9 (SE) µg C g^{-1} dry soil and KCL extractable NO_3^- and NH_4^+ are 4.45 ± 0.48 (SE) and 21.8 ± 1.85 (SE) µg N g^{-1} dry soil, respectively (Dinsmore, unpublished data, 2008). Total N and S deposition at the site are 16.5 kg N ha^{-1} a^{-1} and 6.9 kg S ha^{-1} a^{-1} respectively (Smith, personal communication, 2008).

To minimise variation in factors other than microtopography, the cores were all collected within an area of approximately 10 m^2. Peat depth at the sample site was approximately 0.5 m, overlaying a mineral subsoil. Peat core pH ranged from 3.8-4.3, typical of the catchment as a whole which ranges from 3.6-4.6 (Dinsmore, unpublished data). Mean bulk density was 0.12 g cm^{-3}.

Experimental Design

Three distinct peatland topographic/vegetation features were identified as comprising the majority of the field heterogeneity; depressions, hummocks dominated by the rush *Juncus effusus*, and hummocks dominated by a mixture of grass and sedge. Eight cores were collected from each ecotope in December 2006; 24 cores in total. A 30 cm diameter, 50 cm long, stainless-steel, cylindrical corer was used to cut into the peat. The core was then dug out, cut to size and immediately transferred to near-parallel sided buckets (30 cm diameter, 41 cm height) with as little disturbance to the soil as possible. The following terminology will be used henceforth in reference to the 3 different mesocosm types: hummock + *J. effusus* (Juncus/Hummock), hummock + grass and sedge (Sedge/Hummock), depression (Depression).

Dip wells, consisting of perforated pipes inserted into the soil and sealed at the top with rubber bungs, were placed into each mesocosm. Deep and shallow soil atmosphere wells were created by inserting water tight, gas permeable tubing (Accurel©, Gut *et al.* 1998) horizontally into the mesocosms at depths of 10 cm and 30 cm below the soil surface. The Accurel© was sealed to gas tight tubing (using Plasti Dip©) which was then extended to the mesocosm surface for sample collection (Fig. 1); the surface sampling port was closed to the atmosphere using a 3-way tap. Mesocosms were individually placed within larger buckets and the space between filled with polystyrene chips to insulate and mimic field conditions (Fig. 1).

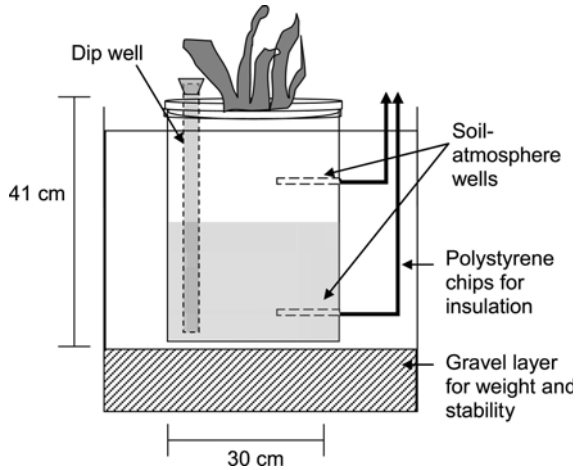

Fig. 1 Illustration of mesocosm design. Note diagram is not to scale

Each mesocosm was assigned to either a high or low water table group, leading to a repeated measures factorial design. The mesocosms were arranged using a randomised block design into 6 rows of 4 under a rain shelter, located outside the Centre for Ecology and Hydrology Edinburgh, approximately 10 km from the Auchencorth Moss field site. Mesocosms were allowed to acclimatise *in-situ* for 4 weeks before measurements began.

Static water table treatment

From core collection until the end of May 2007, water table depth was held constant by daily inspection and manually refilling with rain water collected on-site. The mean ion concentrations in rainwater (mmol m^{-2} $week^{-1}$), measured from June to October 2006, were as follows: Sodium 0.56; Ammonium 0.26; Potassium 0.05; Calcium 0.37; Magnesium 0.13; Chloride 0.85; Nitrate 0.36; Sulphate 0.34 (Cape *et al.*, pre-publication, 2008). Water table depth in the high and low water table groups was held at 0-5 cm and 30-35 cm below the soil surface, respectively. Weekly measurements of CH_4 and N_2O were made using static chambers. A clear plastic lid was sealed to each mesocosm and air samples collected at time zero, after 20 minutes and after 40 minutes. Soil air samples were collected weekly from the gas permeable tubing, and water samples collected fortnightly from the dip wells. Soil temperature at ~5 cm was measured at the same time as flux measurements and soil atmosphere sampling. Total mesocosm net ecosystem exchange (NEE) was measured using a static chamber connected to a PP-Systems EGM-4 infrared gas analyser, which measures CO_2 concentrations every 4 seconds. Measurements were made under 4 different light conditions produced using full sunlight, 1 shade cloth, 2 shade cloths and a black out cloth and combined to produce light response curves. Photosynthetically active radiation (PAR) and temperature were measured inside the NEE chamber alongside CO_2 concentration. Photosynthesis was calculated as total NEE minus the combined plant and soil respiration (NEE under dark conditions).

Rewetting/Draining

At the end of May (after approximately 14 weeks of measurements), the water table treatments were reversed. Drainage of the saturated mesocosms was achieved using a

siphon placed in the dip well; re-wetting of the drier mesocosms was carried out by periodic watering over a 2 day period. Thereafter, CH_4 and N_2O fluxes were measured and solute samples collected daily for one week and then every 2 days for a second week.

Analytical methods

Both chamber and soil atmosphere samples were analysed using a HP5890 Series II gas chromatograph (detection limits: CO_2 < 199 ppmv, CH_4 < 1.26 ppmv, N_2O < 0.2 ppmv). Water samples were analysed for DOC and DIC on a Rosemount-Dohrmann DC-80 total organic carbon analyser (detection range 0.1 to 4000 ppmv), using ultraviolet oxidation and sparging with N_2 to remove acidified inorganic carbon. NO_3^- and NH_4^+ were analysed on a dual channel CHEMLAB continuous flow colorimetric analyser (detection range NH_4^+-N: 0.25 to 3.0 ppmv; NO_3^-N: 0.25 to 5.0 ppmv).

Statistical Analysis

Repeated measures MANOVA was used when testing the significance of mesocosm type and water table treatment on measured variables; an interaction term was also included in the model specification. ANOVA was used when considering mesocosm respiration, photosynthesis and NEE, with temperature as a covariate where appropriate. Quoted test results refer to Pillai's test statistic (Townend 2002) unless stated otherwise. Normality was assessed using the Kolmogorov-Smirnov test (Townend 2002) and datasets adjusted, where appropriate, using log transformations. Temperature responses were tested using regression; trend lines are compared using multiple regression with temperature, group identifier (e.g. water table treatment 1 or 2 referring to high and low respectively), and temperature*group as independent variables. Depending on the normality of the data, correlations were carried out using either Pearson's product-moment or Spearman's rank correlation (Townend 2002). Where mean values are quoted, the ± value that follows refers to the standard error of the mean unless otherwise stated. Analyses were carried out in 'Minitab15'.

Results:

Comparison of mesocosm types/peatland features

The observed differences in species composition (Fig. 2) within the mesocosms was shown to be highly statistically significant using MANOVA ($F = 6.36$, $p < 0.01$). All 3 mesocosm types had an average coverage of more than 60% moss. The 'Sedge/Hummock' group was dominated by grass and moss, and also contained a significant amount of the sedge *E. vaginatum*. The 'Depression' group was dominated primarily by mosses and the 'Juncus/Hummock' group, whilst still being dominated by moss and grass, also contained an average of 40% *J. effusus* coverage. Small but significant differences were apparent in soil pH across mesocosm types; 'Juncus/Hummock' 4.2 ± 0.1 (SD), 'Sedge/Hummock' 3.9 ± 0.1 (SD), 'Depression' 4.0 ± 0.1 (SD).

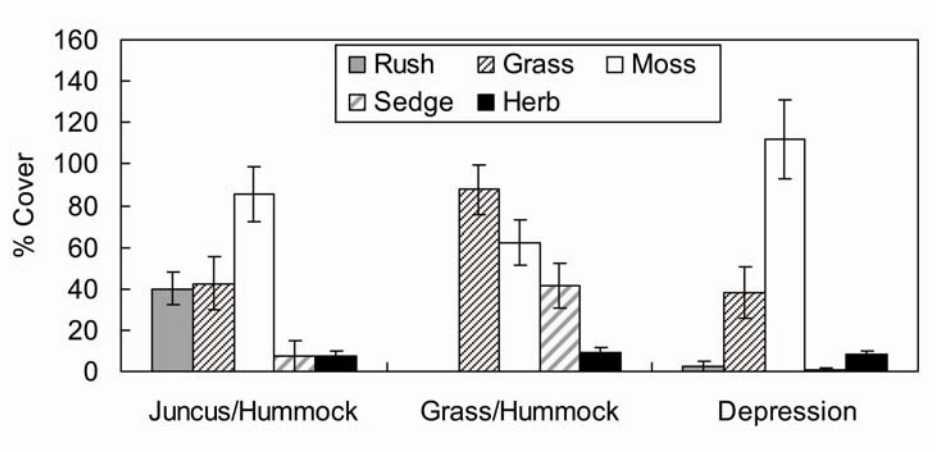

Fig. 2 Vegetation composition within different mesocosm types. Error bars represent standard deviations. Rush refers only to *J. effusus* and sedge to *Eriophorum vaginatum*. The grass was predominantly *Deschampsia flexuosa*; *Agrostis stolonifera, Anthoxanthum odoratum*, *Festuca ovina*, and *Molinia caerulea* are also present in some mesocosms. The dominant mosses are *Sphagnum papillosa* and *Polytrichum commune*. The herb species present were *Potentilla erecta* and *Galium saxatile*

Static water table treatment

Uptake/Emissions

Mean combined plant and soil respiration across replicates during the static water table portion of the study ranged from 92 to 167 µg CO_2 m^{-2} s^{-1} (Table 1). Respiration was highest in the 'Sedge/Hummock' group. In both the

'Sedge/Hummock' and 'Depression' mesocosms, respiration was higher in the low water table group; no difference was observed in the 'Juncus/Hummock' group. Although the observed patterns were not statistically significant, this was expected due to the low level of replication. Light response curves were used to predict photosynthesis at a PAR of 210 μmol m^{-2} s^{-1}, the mean PAR at the Auchencorth Moss field site over the measurement period (Coyle, unpublished data). Photosynthesis (Table 1) was highest in the 'Juncus/Hummock' mesocosms, followed by the 'Sedge/Hummock' and finally the 'Depression' mesocosms ($F = 5.25$, $p < 0.05$). The effect of water table depth on photosynthesis was insignificant ($F = 3.68$, $p < 0.10$); however, lower water tables indicated a 44%, 36% and 21% decrease in photosynthesis in the 'Juncus/Hummock', 'Sedge/Hummock' and 'Depression' mesocosms, respectively. The resulting NEE calculated from the respiration and photosynthesis data showed no significant effect of either mesocosm type or water table position. However, in general the lower water table treatment increased the flux of CO_2 to the atmosphere (Table 1). The 'Juncus/Hummock' mesocosms in the high water table treatment were the only group to show a net CO_2 uptake.

Table 1 Mean (± SE) fluxes of CO_2, CH_4 and N_2O separated by water table depth and mesocosm type. Values of CO_2 are based on 2 sampling occasions; values for CH_4 and N_2O represent weekly fluxes the full 14 week static water table treatment. Note different units for CO_2

	Juncus/Hummock		Sedge/Hummock		Depression	
	High	Low	High	Low	High	Low
CO_2 (μg m^{-2} s^{-1})						
Respiration	101± 12	102 ± 7.6	124 ± 10	167 ± 26	92 ± 7.1	105 ± 5.8
Photosynthesis*	165 ± 75	92 ± 25	69 ± 24	44 ± 10	45 ± 13	36 ± 3.8
NEE	-65 ± 53	9.1 ± 11	55 ± 22	123 ± 19	58 ± 12	70 ± 3.8
CH_4 (μg m^{-2} h^{-1})	11 ± 5.2	0.19 ± 5.2	117 ± 28	3.2 ± 3.4	191 ± 27	5.8 ± 4.9
N_2O (μg m^{-2} h^{-1})	-3.2 ± 2.2	-0.82 ± 2.1	-3.4 ± 2.1	-1.8 ± 1.7	-0.55 ± 1.5	-0.85 ± 2.0

Mean CH_4 fluxes from individual chambers over the 14 week period of static water table treatment ranged from -30.7 to 358 μg CH_4 m^{-2} h^{-1}; mean N_2O fluxes over the same period ranged from -17.3 to 12.5 μg N_2O m^{-2} h^{-1}. Averages across chamber types and water table levels for both CH_4 and N_2O are presented in Table 1. Variation in mean CH_4 flux was high within all groups, and neither water table level nor mesocosm type alone had a significant effect on CH_4 efflux; the effect of water

table was almost significant ($F = 3.41$, $p < 0.10$). However, there was a significant interaction effect ($F = 1.65$, $p < 0.05$). Only in the high water table group did mesocosm type have a significant effect on CH_4 flux (Depression > Sedge/Hummock > Juncus/Hummock). A highly significant increasing trend in mean CH_4 flux ($r^2 = 0.59$, $p < 0.01$) was observed in the 'Sedge/Hummock' time series plot (Fig. 3). When the experiment began mean CH_4 emissions from the 'Sedge/Hummock' mesocosms were similar in magnitude to the 'Juncus/Hummock' mesocosms; however, from early April onwards the 'Sedge/Hummock' mesocosms were more similar to the 'Depression' mesocosms. Mean CH_4 flux in all groups was positive, representing a net emission; however, uptake was measured at least once throughout the experiment in all but 2 of the mesocosms.

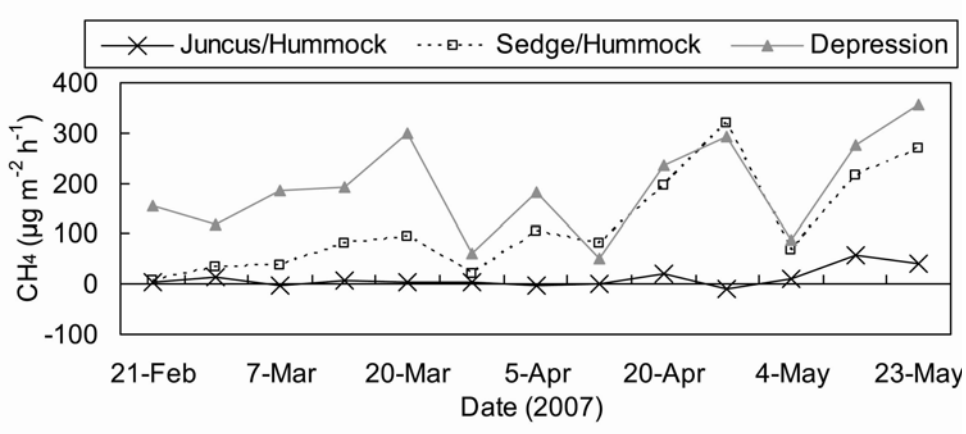

Fig. 3 Time series of mean CH_4 emissions in high water table group during static water table treatment

There was a net uptake of N_2O in 21 of the 24 mesocosms over the 14 week period reflected in a net uptake across all chamber types irrespective of water table (Table 1); however, variation was extremely high. No significant effect of either water table depth or mesocosm type on N_2O flux was observed using Pillai's MANOVA test. However, using the Lawley-Hotelling (Townend 2002) MANOVA post-hoc, the interaction effect was statistically significant ($F = 1.72$, $p < 0.05$); again mesocosm type was only important in the high water table treatment.

Below ground concentrations

Mean CO_2 concentrations in the deep and shallow soil atmosphere wells were 764 ± 52 and 680 ± 25 ppmv respectively; mean CH_4 concentrations 127 ± 52 and 111 ± 37

ppmv and mean N_2O concentrations 0.38 ± 0.01 and 0.37 ± 0.01 ppmv (Table 2). Strong positive correlations were found between the deep and shallow well concentrations for CO_2 ($r = 0.90$, $p < 0.01$) and N_2O ($r = 0.93$, $p<0.01$). However, no correlation was observed between CH_4 concentrations in the deep and shallow wells ($r = -0.10$, $p = 0.80$). Variability in the measured CH_4 concentrations was large, ranging from below the detection limit to 5755 ppmv, suggesting the presence of pockets of high CH_4 concentrations within the peat profile. No water table or mesocosm type effects were observed for CO_2 or N_2O concentrations (Table 2). Although not statistically significant, CH_4 concentrations appeared to be higher in the high water table treatment. The highest concentrations were observed in the 'Sedge/Hummock' mesocosms, where the water table effect was also most pronounced, followed by the 'Depressions', and lastly the 'Juncus/Hummock' group, where no visible difference was apparent between high and low water table.

Table 2 Mean (± SE) concentrations of CO_2, CH_4 and N_2O in soil atmosphere wells during static water table treatment. Units are ppmv

	Juncus/Hummock		Sedge/Hummock		Depression	
	High	Low	High	Low	High	Low
CO_2						
Shallow	694 ± 88	722 ± 63	711 ± 71	687 ± 80	574 ± 63	695 ± 74
Deep	739 ± 89	924 ± 203	726 ± 105	756 ± 102	801 ± 160	639 ± 60
CH_4						
Shallow	19 ± 8.2	7.1 ± 2.6	484 ± 173	88 ± 77	39 ± 14	29 ± 13
Deep	19 ± 4.1	28 ± 8.2	222 ± 148	42 ± 24	433 ± 148	17 ± 9.3
N_2O						
Shallow	0.39 ± 0.02	0.42 ± 0.03	0.37 ± 0.02	0.38 ± 0.01	0.31 ± 0.01	0.37 ± 0.01
Deep	0.44 ± 0.04	0.41 ± 0.04	0.37 ± 0.01	0.38 ± 0.01	0.31 ± 0.01	0.39 ± 0.01

Soil solution DOC concentrations ranged from 8.0-124 mg l^{-1} with a mean of 43 ± 2.1 mg l^{-1}. Concentrations of DIC, NO_3^- and NH_4^+ covered a much smaller range with mean values of 3.61 ± 0.26, 0.03 ± 0.01 and 1.16 ± 0.09 mg l^{-1} respectively. No consistent patterns were observed across mesocosm type or water table treatment in soil water solute concentrations.

Temperature sensitivity

Both high and low water table groups showed a highly significant CH_4 response ($p < 0.01$) to natural variations in soil temperature (Fig. 4a) during the static water table period. In the high water table group CH_4 emissions increased with increasing temperature (Q_{10} [5-15°C] = 6.7; $r^2 = 0.50$); in the low water table group increasing temperature led to a decrease in emissions (Q_{10} [5-15°C] = -2.3; $r^2 = 0.26$). The slopes of the 2 different trend lines were significantly different ($t = -4.51$, $p < 0.001$), with a much stronger response to temperature in the high water table group. The N_2O flux responded positively to increased soil temperature (Q_{10} [5-15°C] = 2.6; $r^2 = 0.28$) with no significant difference in the trend lines between water table treatments (Fig. 4b). The N_2O flux showed a switch from uptake to emissions between approximately 7.5 and 8.5ºC.

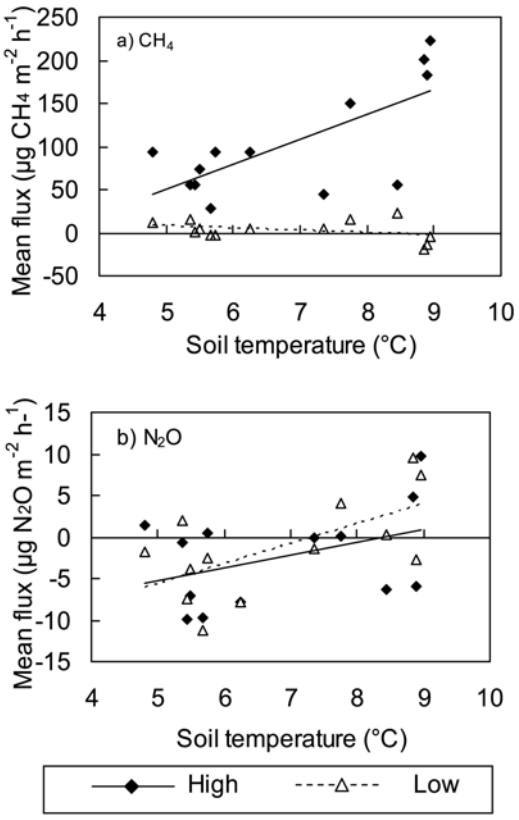

Fig. 4 (a) CH_4 and (b) N_2O flux response to temperature in high and low water table treatment groups

The temperature response of CH_4 in the high water table treatment group, separated by mesocosm type is shown in Fig. 5. The trend lines for the 'Sedge/Hummock' ($r^2 =$

0.62, $p < 0.01$) and 'Depression' ($r^2 = 0.43$, $p < 0.05$) mesocosms were offset (i.e. the 'Depression' mesocosms had higher CH_4 emissions) though the slope of the lines (i.e. the response to increasing temperature) were similar. The slope of the 'Juncus/Hummock' trend line was negligible and not significant at $p < 0.05$. Mesocosm type had no significant effect on CH_4 response in the low water table treatment group.

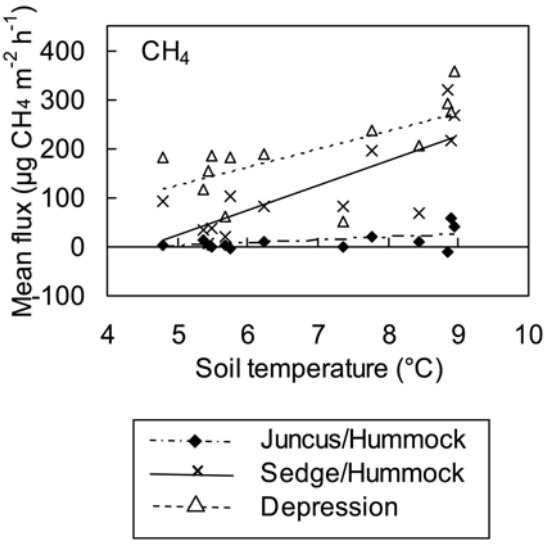

Fig. 5 CH_4 flux response to temperature in high water table treatment separated by mesocosm type

Response to draining/rewetting

After the initial 14 week static water table treatment, the water table levels in the 2 treatments were switched. Over a 2 day period the high water table group was drained to a new water table depth of 30-35 cm, and the low water table group was wetted up until water table depth reached 0-5 cm.

A significant and immediate pulse, raising the CH_4 flux rate to over 160 µg m^{-2} h^{-1} above what it was prior to rewetting, was observed in both the 'Depression' and the 'Sedge/Hummock' mesocosms; a similar, though slightly lower pulse was observed a day later in the 'Juncus/Hummock' mesocosms (Fig. 6a). The CH_4 flux returned to a rate similar to its pre-change mean before rising more slowly again after approximately 8-10 days. The rate of increase in the latter stage of the response was greatest in the 'Sedge/Hummock' mesocosms, followed by the 'Depression' mesocosms; very little increase was observed in the 'Juncus/Hummock' mesocosms.

To test the significance of differences between mesocosm types, the post-change period was split into 3 separate time intervals; days 0-5, 5-10 and 10-15. Each section was analyzed independently using a repeated measures MANOVA test. The test confirmed the statistical significance of the differences in mesocosm types between days 10-15 after rewetting ($F = 4.00$, $p < 0.01$).

A pulse of CH_4, similar to that caused by rewetting was also seen in response to drainage (Fig. 6c). However, the magnitude of this pulse was approximately 700 µg m^{-2} h^{-1} above the pre-change mean in both the 'Sedge/Hummock' and the 'Depression' mesocosms, and more than 200 µg m^{-2} h^{-1} above the pre-change mean in the 'Juncus/Hummock' mesocosms; in all cases significantly higher than after rewetting. After ~8 days the fluxes appeared to level off at approximately -10, -70 and -120 µg m^{-2} h^{-1} below the pre-change mean in the 'Juncus/Hummock', 'Sedge/Hummock' and 'Depression' mesocosms, respectively. The effect of mesocosm type on response to drainage was only significant between days 5-10 ($F = 2.95$, $p < 0.05$)

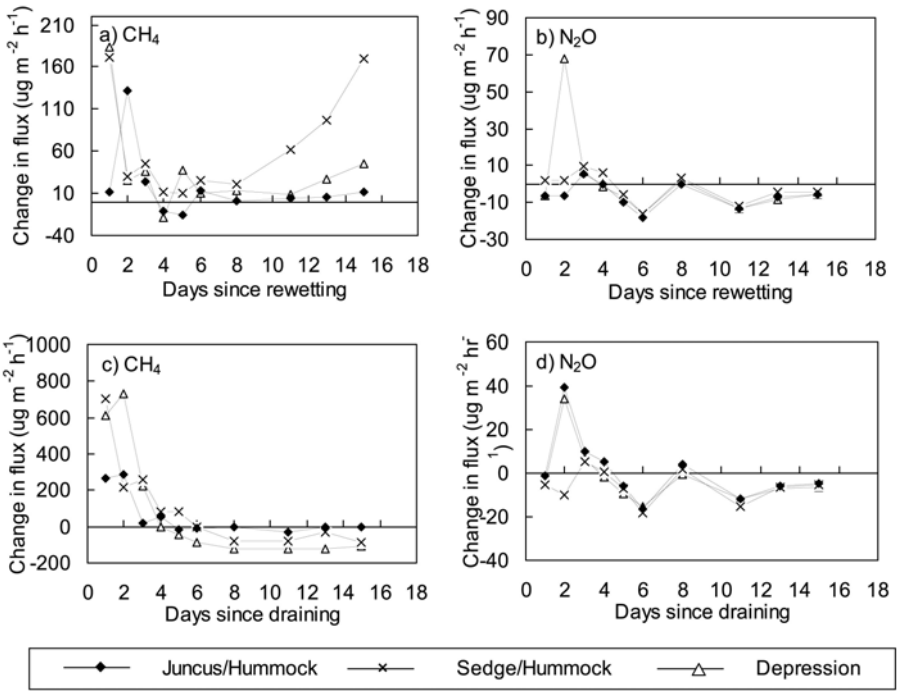

Fig. 6 Change in flux relative to mean prior to water table switch; a) and b) illustrate response to rewetting, c) and d) illustrate response to draining. Positive values represent an increase from pre-change mean; negative values indicate a decrease in flux rate from the pre-change mean

In both the rewetting and the draining treatments, peaks in the N_2O response occurred after 2 days (Fig. 6b and d). The pulse effect occurred only in the 'Depression' mesocosms after rewetting, and in both the 'Depression' and 'Juncus/Hummock' mesocosms after draining. After the initial pulse, all mesocosms, both in the rewetting and drainage treatments followed a very similar pattern in terms of N_2O response. This response showed no correlation with temperature.

Solute concentrations were also collected and analysed for DOC, DIC, NH_4^+ and NO_3^- during both the rewetting and draining experiments. However, no significant response to draining/rewetting was observed.

Discussion:

Comparison between mesocosms and field conditions

Variability in mesocosm fluxes was extremely high for all gases. Mean NEE across the different water table treatments and mesocosm types ranged from -65 to 123 µg CO_2 m^{-2} s^{-1} (Table 1). During the same study period, mean NEE measured at the Auchencorth Moss field site using eddy covariance was -8.4 µg CO_2 m^{-2} s^{-1} (Coyle, unpublished data). Despite the low replication, different conditions, and different measurement technique, the field site NEE was still within the range measured here. Mean CH_4 and N_2O fluxes ranged from 0.19 to 191 µg CH_4 m^{-2} h^{-1} and from -3.4 to -0.55 µg N_2O m^{-2} h^{-1} (Table 1). Fortnightly field measurements over comparable vegetation types during the same period gave a mean CH_4 and N_2O flux of 9.9 ± 4.1 µg CH_4 m^{-2} h^{-1} and -3.3 ± 1.5 µg N_2O m^{-2} h^{-1} (Dinsmore, unpublished data); again the field mean is within the range measured in this study. Mean mesocosm DOC and NH_4^+ concentrations were approximately double the mean concentrations measured in the field. The higher DOC and NH_4^+ concentrations in the mesocosms may indicate an increase in mineralization caused by the death of plant roots cut during mesocosm collection; this may also explain why our mesocosms had a net CO_2 emission whilst field measurements over the same period showed a net uptake. DIC and NO_3^- concentrations were similar between field and mesocosms. For a number of GHGs and solutes, our mesocosms therefore appear to represent field conditions relatively well.

Effect of water table depth and mesocosm type

Although not statistically significant our results demonstrated that under lower water table conditions respiration increased and photosynthesis decreased. This is consistent with similar studies (e.g. Blodau *et al.* 2004; Moore and Roulet 1993), as water table controls the depth of the oxic peat layer, and hence the volume of peat where aerobic decomposition can occur (Moore and Dalva 1993; Silvola *et al.* 1996). However, the relationship between water table depth and respiration is not linear throughout the profile with several authors reporting a breakdown in the relationship below ~30 cm (e.g. Silvola 1996; Lafleur *et al.* 2005). Blodau *et al.* (2004) demonstrated a drop in photosynthesis of 24% and 42% in two different Canadian peatlands, associated with a 30 cm drop in water level; similarly, in this study we measured a drop of between 21-44% with a similar water level change. In mesocosms dominated by *J. effusus* and *E. vaginatum*, Ström *et al.* (2005) measured mean respiration rates of 78 μg m^{-2} s^{-1} and 121 μg m^{-2} s^{-1} respectively, similar to the 100 μg m^{-2} s^{-1} and 123 μg m^{-2} s^{-1} for *J. effusus* and *E. vaginatum* in this study. The response of ecosystems to water table manipulations has previously been shown to be dominated primarily by processes associated with respiration rather than photosynthesis (Funk *et al.* 1994). As such, in both this study and others (for example Blodau and Moore 2003a; Chimner and Cooper 2003; Moore and Dalva 1993), the net effect of lowered water tables is an increase in CO_2 flux to the atmosphere. However, despite the agreement with similar studies, these results should not be directly extrapolated to predict the ecosystem response to longer-term water table draw-down. Laiho (2006) highlights the importance of differentiating between 'wet' and 'dry' sites. If deeper soil layers are continuously exposed to aerobic decomposition, the carbon at depth becomes highly recalcitrant. The associated decrease in decomposition potential is likely to negate the effect of an increased aerobic zone. Several other studies have also argued that in 'dry' peats, large relative changes in respiration at depth have little effect on surface fluxes due to the low contribution of deeper peat to total respiration (Blodau *et al.* 2007; Knorr *et al.* 2007; Lafleur *et al.* 2005). As the natural water table regime at Auchencorth Moss often exposes deeper layers to aerobic conditions it is unsurprising that the relationship found here was small and not statistically significant.

In accordance with previous studies (Aerts and Ludwig 1997; Moore and Dalva 1993), we measured higher CH_4 emissions in our high water table treatment. In the high water table group, the effect of mesocosm type on CH_4 emissions was highly significant. Based on both current literature and our photosynthesis data (Table 1), we expected the order 'Juncus/Hummock' > 'Sedge/Hummock' > 'Depression' due to the potential for plant-mediated transport and substrate release (Greenup *et al.* 2000; Shannon *et al.* 1996; Yu *et al.* 1997). In this study we found the opposite to be true. Emissions were lower in the 'Juncus/Hummock' and the 'Sedge/Hummock' mesocosms, both of which contained a large proportion of aerenchyma containing plants (*J. effusus*, *D. flexuosa* and *E. vaginatum*).

As well as providing a transport route for CH_4, aerenchyma also transports O_2 into the rhizosphere and can significantly alter the redox state of saturated peat, resulting in decreased methanogenesis and increased oxidation (Visser *et al.* 2000; Wiebner *et al.* 2002). Lombardi *et al.* (1997) measured CH_4 oxidation potentials of 44-318 mg m^{-2} d^{-1} in the rhizosphere of common aerenchymous wetland species. The amount of radial oxygen loss through the plant roots is likely to be dependent on photosynthetic activity (Roura-Carol and Freeman 1999). In the low water table treatment group, due to the limited depth of our mesocosms, only a very shallow anoxic layer for methanogenesis is likely to have existed. The absence of a significant CH_4 reservoir for plant roots to tap into may have restricted the potential for plant-mediated transport. Although the majority of studies have found a positive effect of vascular plants on CH_4 emissions, a few have reported results similar to this study, where emission inhibition by rhizospheric oxidation appears to be greater than the increase in emissions via plant-mediated transport and enhanced substrate release (Grünfeld and Brix 1999; Kutzbach *et al.* 2004). Similarly Arah and Stephen (1998) found that increasing the root-mediated transport potential in a CH_4 flux model resulted in decreased net emissions due to the increase in oxidation outweighing increased CH_4 transport.

The increase in CH_4 emissions from the 'Sedge/Hummock' mesocosms throughout the study period (Fig. 3) may indicate a seasonal shift in the balance of positive and negative effects of vascular plants on CH_4 emissions. The conduit potential of

aerenchyma containing plants is likely to increase seasonally due to the relationship between root biomass and stem cross-sectional area (Arenovski and Howes 1992; Waddington *et al.* 1996). The production of deep roots reaching the anoxic peat layer (Wein 1973), or increased substrate release early in the growing season (Saarnio *et al.* 2004), may also cause seasonal changes in plant-related emissions. The earlier initiation of *E. vaginatum* growth than *Juncus effusus* (Wein 1973) may explain why a similar increasing trend is not observed in the 'Juncus/Hummock' mesocosms. Longer-term measurements are needed to test this hypothesis.

The pattern of below ground CH_4 concentrations ('Sedge/Hummock' > 'Depression') was opposite to that seen in surface emissions ('Depression' > 'Sedge/Hummock'). This suggests that although more CH_4 is produced in the 'Sedge/Hummock' mesocosms, there is a barrier preventing soil-atmosphere transfer. This could be either oxidation in the rhizosphere (assuming soil atmosphere wells did not sample the rhizosphere), or a physical barrier such as the thick layer of hummock biomass preventing diffusion across the soil-atmosphere boundary. As bubble formation does not occur until partial pressures of >0.21 atm (Fechner-Levy and Hemond 1996), this is unlikely to be important in our mesocosms. The extremely high variability in soil-atmosphere CH_4 concentrations and the lack of correlation between shallow and deep wells may indicate spatial heterogeneity in rates of production and oxidation within the soil profile caused by plant roots. High concentrations in the Sedge/Hummock mesocosms may also be due to substrate availability. *E. vaginatum* has previously been shown to release much higher quantities of acetate, a substrate of major importance to CH_4 production, than *J. effusus* (Ström *et al.* 2005).

Relatively few conclusions can be drawn from the pattern of N_2O fluxes and concentrations due to the very high temporal variability. Low NO_3^- concentrations in soil water may indicate low nitrification rates and/or high denitrification rates. An increased rate of nitrification has been observed after water-table drawdown in several studies (Neill 1995; Regina *et al.* 1996). Similarly in this study, although not significant, concentrations of NO_3^- were higher in the low water table treatment in both 'Sedge/Hummock' and 'Depression' mesocosms. Alternatively, the low NO_3^- pool may be a consequence of high turnover rates. N_2O consumption from complete

denitrification may be the dominant process controlling N_2O fluxes to and from this system.

Temperature response

The clear difference in the temperature response of CH_4 emissions between the high and low water table groups (Fig. 4) was likely a result of different processes contributing to the net flux. In anoxic (high water table) conditions the dominant process was methanogenesis which increases emissions as microbial activity increases in response to increasing temperature. This is in agreement with previous studies which show a stronger temperature response in methanogenesis than methanotrophy (Dunfield *et al.* 1993). In oxic (low water table) conditions methanotrophy as well as methanogenesis contributed to the net flux, dampening the overall response. The responses of both the 'Depression' and the 'Sedge/Hummock' mesocosms were similar, suggesting a common dominant process (methanogenesis). The 'Juncus/Hummock' however, more closely resembled the response of the low water table group, indicating that methanotrophy was also important. This supports the assertion that rhizospheric oxidation was important in the 'Juncus/Hummock' mesocosms. The temperature responses here appeared to be linear compared to the exponential responses observed in other studies (Dise *et al.* 1993; MacDonald *et al.* 1998). However, this may simply be a consequence of the limited range of temperatures our mesocosms were exposed to.

We found a positive linear response of N_2O emissions to temperature with a switch from consumption to production between approximately 7.5 and 8.5ºC. This suggests that N_2O producing processes are more responsive to temperature than N_2O consumption processes. Water table position had no effect on the magnitude of the N_2O temperature response. Further work is required to assess the validity of the observed switch from consumption to production as N_2O fluxes in this study are low and variability high.

Pulsing effect

After switching water table positions, both drainage and rewetting produced evidence of a significant pulse in CH_4 and N_2O emissions within 1 or 2 days. This pulse may

be the direct result of the physical disturbance (water table shift) causing a release of CH_4 and N_2O from below ground reservoirs. Episodic pulsing after water table drawdown was seen by both Moore *et al.* (1990) and Shurpali *et al.* (1993) and was attributed to degassing due to reduced hydrostatic pressure. Alternatively, pulses may be a biological response to increased substrate availability from enhanced biomass recycling or redox-induced chemical breakdown (Blodau and Moore 2003b). Similar pulses in mineralization rates have been observed in response to water level fluctuations (Aerts and Ludwig 1997). After the initial pulse, the CH_4 response to drainage occurred faster than the response to rewetting. This is consistent with previous studies (Whalen and Reeburgh 2000). N_2O fluxes were similar across all mesocosm types and water table positions.

Implications

From continuous water table measurements made at the Auchencorth Moss peatland in 2007 (Coyle, unpublished data), a rise in water table by more than 20 cm in less than 48 hours occurred 9 times in 8 months. Assuming emissions peak each time this occurs and the peak lasts approximately 24 hours, fortnightly field measurements may fail to capture these peaks. The results from the mesocosm study suggest that CH_4 pulsing after rewetting could potentially contribute an additional 16% to the average annual flux. Using the same assumptions, net N_2O flux could switch from a net sink of 0.008 to a net source of 0.02 $\mu g\ m^{-2}\ h^{-1}$ (Dinsmore *et al.*, unpublished data, 2008). Although this is only a rough calculation and the assumptions are large, it illustrates the potential importance of these emission pulses after a sudden rise in field water table levels. No such calculation was carried out on the pulses observed after drainage as it is extremely unlikely that a water table drop of this magnitude would occur over only 2 days in the field. Further work is required to assess the actual implications of this pulsing under natural field conditions.

Using the 100 year global warming potentials published by the IPCC (2007), the GHG fluxes in CO_2 equivalents for each group of mesocosms were calculated (Table 3). In this system, CO_2 fluxes dominated the budget entirely. CH_4 fluxes were an order of magnitude smaller than in many studies (e.g. Dowrick *et al.* 2006; Hargreaves and Fowler 1998; Minkkinen *et al.* 2002; Minkkinen and Laine 2006;

Roulet *et al.* 2007), though studies such as MacDonald et al (1998) found similar values in Scottish blanket peats. Fluxes of CO_2-equivalents from N_2O were in the same order of magnitude as CO_2-equivalents from CH_4. Lowering the water table by 30 cm greatly increased the net flux of CO_2-equivalents to the atmosphere, which was dominated by NEE. Of the different mesocosm types, only the *J. effusus* dominated hummocks showed a net uptake of CO_2-equivalents. Hence it is important to accurately account for the relative proportions of each community type when up-scaling chamber measurements made in the field.

Table 3 GHG fluxes from mesocosms using 100 yr global warming potentials of 298 for N_2O and 25 for CH_4 (IPCC 2007). Flux units are mg CO_2-eq m^{-2} d^{-1} ± SE; positive and negative values represent emissions and uptake respectively

	Water table	CO_2	CH_4	N_2O	Net CO_2-eq
Juncus/Hummock	High	-5592 ± 3264	6.7 ± 5.5	-23 ± 29	-5608
	Low	792 ± 936	6.2 ± 5.8	-6.0 ± 27	792
Sedge/Hummock	High	4776 ± 1656	70 ± 30	-25 ± 26	4822
	Low	10608 ± 1176	1.9 ± 3.6	-13 ± 22	10597
Depression	High	4008 ± 912	115 ± 29	-4.1 ± 19	4119
	Low	6024 ± 288	3.4 ± 5.3	-6.0 ± 25	6021

Conclusions:

Our results agree with previous studies on the flux response to low water table conditions. We have also demonstrated a strong interaction between water table depth and vegetation. The effect of vegetation within the mesocosms was counter to what we had originally hypothesised based on the available literature. What determines the ratio between flux enhancing and flux inhibiting mechanisms in plant communities is still largely unclear and may be related to both site-specific and species-specific variables, which may change seasonally with plant growth stage. Despite the uncertainty in the mechanisms involved, it is clear that species composition has a dramatic effect on ecosystem functioning, and as such it is important that community type is considered when up-scaling chamber measurements. It also highlights the need to include some form of vegetation succession in models used to predict the long-term effects of landscape management and environmental change on GHG budgets.

We observed a pulse in both CH_4 and N_2O emissions occurring between 1-2 days after manually changing the depth of the water table by ± 30 cm. Though further work is required to quantify the importance of this pulse under field conditions, it can be concluded that widely spaced chamber measurements may significantly underestimate mean annual emissions.

Acknowledgements

We thank Frank Harvey and the staff at CEH Edinburgh for their help and advice throughout the study, and John Parker (Scottish Agricultural College) for his help with laboratory work. The work was funded by the UK Natural Environment Research Council (NERC) through an algorithm PhD studentship grant.

References

Arah J R M and Stephen K D (1998) A model of the processes leading to methane emission from peatland. Atmos Environ 32:3257-3264

Aerts R and Ludwig F (1997) Water-table changes and nutritional status affect trace gas emissions from laboratory columns of peatland soils. Soil Biol Biochem 29:1691-1698

Arenovski A L and Howes B L (1992) Lacunal allocation and gas transport capacity in the salt marsh grass *Spartina alterniflora*. Oecologia 90:316-322

Bartlett K B and Harriss R C (1993) Review and Assessment of Methane Emissions from Wetlands. Chemosphere 26:261-320

Billett M F, Palmer SM, Hope D, Deacon C, Storeton-West R, Hargreaves KJ, Flechard C and Fowler D (2004) Linking land-atmosphere-stream carbon fluxes in a lowland peatland system, Global Biogeochem Cycles 18: GB1024, doi:10.1029/2003GB002058.

Blodau C, Basiliko N and Moore T R (2004) Carbon turnover in peatland mesocosms exposed to different water table levels. Biogeochemistry 67:331-351

Blodau C and Moore T R (2003a) Experimental response of peatland carbon dynamics to a water table fluctuation. Aquat Sci 65:47-62

Blodau C and Moore T R (2003b) Micro-scale CO_2 and CH_4 dynamics in a peat soil during a water table fluctuation and sulphate pulse. Soil Biol Biochem 35:535-547

Blodau C, Roulet N T, Heitmann, T, Stewart H, Beer J, Lafleur P and Moore T R (2007) Belowground carbon turnover in a temperate ombrotrophic bog. Global Biogeochem Cycles 21:GB1021

Butterbach-Bahl K, Papen H and Rennenberg H (1997) Impact of gas transport through rice cultivars on methane emission from rice paddy fields. Plant Cell Environ 20:1175-1183

Chimner R A and Cooper D J (2003) Influence of water table levels on CO_2 emissions in a Colorado subalpine fen: an in situ microcosm study. Soil Biol Biochem 35:345-351

Dawson J J C, Billett M F, Hope D, Palmer S M and Deacon C M (2004), Sources and sinks of aquatic carbon in a peatland stream continuum, Biogeochemistry 70: 71-92

Dise N B, Gorham E and Verry E S (1993) Environmental-Factors Controlling Methane Emissions from Peatlands in Northern Minnesota. J Geophys Res [Atmos] 98:10583-10594

Dowrick D J, Freeman C, Lock M A and Reynolds B (2006) Sulphate reduction and the suppression of peatland methane emissions following summer drought. Geoderma 132:384-390

Dunfield P, Knowles R, Dumont R and Moore T R (1993) Methane production and consumption in temperate and subarctic peat soils: Response to temperature and pH. Soil Biochemistry 25:321-326

Fechner-Levy E J and Hemond H F (1996) Trapped methane volume and potential effects on methane ebullition in a northern peatland. Limnol Oceanogr 41:1375-1383

Funk D W, Pullman E R, Peterson K M, Crill P M and Billings W D (1994) Influence of Water-Table on Carbon-Dioxide, Carbon-Monoxide, and Methane Fluxes from Taiga Bog Microcosms. Global Biogeochem Cy 8:271-278

Gorham E (1991) Northern Peatlands: Role in the Carbon-Cycle and Probable Responses to Climatic Warming. Ecol Appl 1:182-195

Greenup A L, Bradford M A, McNamara N P, Ineson P and Lee J A (2000) The role of Eriophorum vaginatum in CH_4 flux from an ombrotrophic peatland. Plant Soil 227:265-272

Grünfeld S and Brix H (1999) Methanogenesis and methane emissions: effects of water table, substrate and presence of *Phragmites australis*. Aquat Bot 64:63-75

Gut A, Blatter A, Fahrni M, Lehmann B E, Neftel A and Staffelbach T (1998) A new membrane tube technique (METT) for continuous gas measurements in soils. Plant Soil 198:79-88

Hargreaves K J and Fowler D (1998) Quantifying the effects of water table and soil temperature on the emission of methane from peat wetland at the field scale. Atmos Environ 32:3275-3282

Huttunen J T, Nykanen H, Turunen J and Martikainen P J (2003) Methane emissions from natural peatlands in the northern boreal zone in Finland, Fennoscandia. Atmos Environ 37:147-151

IPCC (2007) Technical Summary. In Climate Change (2007): The Physical Science Basis. Contribution of Working Group 1 to the Forth Assessment Report of the Intergovernmental Panel on Climate Change. Eds. S Solomon, D Qin, M Manning, Z Chen, M Marquis, K B Averyt, M Tignor and H L Miller. Cambridge University Press, Cambridge, United Kingdom and New York, NY, USA

Knorr K –H, Osterwoud M and Blodau C (2007) Experimental drought changes rates of soil respiration and methanogenesis but not carbon exchange in fen soils. Soil Biol Biochem 40:1781-1791

Kutzbach L, Wagner D and Pfeiffer E M (2004) Effect of microrelief and vegetation on methane emission from wet polygonal tundra, Lena Delta, Northern Siberia. Biogeochemistry 69:341-362

Lafleur P M, Moore T R, Roulet N T and Frolking S (2005) Ecosystem respiration in a cool temperate bog depends on peat temperature but not water table. Ecosystems 8:619-629

Laiho (2006) Decomposition in peatlands: reconciling seemingly contrasting results on the impacts of lowered water levels. Soil Biol Biochem 38:2011-2024

Lombardi J E, Epp M A and Chanton J P (1997) Investigation of the methyl fluoride technique for determining rhizospheric methane oxidation. Biogeochemistry 36:153-172

MacDonald J A, Fowler D, Hargreaves K J, Skiba U, Leith I D and Murray M B (1998) Methane emission rates from a northern wetland; response to temperature, water table and transport. Atmos Environ 32:3219-3227

Minkkinen K, Korhonen R, Savolainen I and Laine J (2002) Carbon balance and radiative forcing of Finnish peatlands 1900-2100 - the impact of forestry drainage. Glob Change Biol 8:785-799

Minkkinen K and Laine J (2006) Vegetation heterogeneity and ditches create spatial variability in methane fluxes from peatlands drained for forestry. Plant Soil 285:289-304

Moore T R and Dalva M (1993) The influence of temperature and water table on carbon dioxide and methane emissions from laboratory columns of peatland soils. J Soil Sci 44:651-664

Moore T R and Roulet N T (1993) Methane Flux - Water-Table Relations in Northern Wetlands. Geophys Res Lett 20:587-590

Moore T R, Roulet N T and Knowles R (1990) Spatial and temporal variations of methane flux from subarctic/northern boreal fens. Glob Biogeochem Cycles 4:29-46

Neill C (1995) Seasonal flooding, nitrogen mineralization and nitrogen utilization in a prairie marsh. Biogeochemistry 30:171-189

Nungesser M K (2003) Modelling microtopography in boreal peatlands: hummocks and hollows. Ecol Model 165:175-207

Öquist M and Sundh I (1998) Effects of a transient oxic period on mineralization of organic matter to CH_4 and CO_2 in anoxic incubations. Geomicrobiol J 15:325-333

Regina K, Nykanen H, Silvola J and Martikainen P J (1996) Fluxes of nitrous oxide from boreal peatlands as affected by peatland type, water table level and nitrification capacity. Biogeochemistry 35:401-418

Regina K, Silvola J and Martikainen P J (1999) Short-term effects of changing water table on N_2O fluxes from peat monoliths from natural and drained boreal peatlands. Glob Change Biol 5:183-189

Roulet N, Lafleur P M, Richard P J H, Moore T R, Humphreys E R and Bubier J (2007) Contemporary carbon balance and late Holocene carbon accumulation in a northern peatland. Glob Change Biol 13:397-411

Roura-Carol M and Freeman C (1999) Methane release from peat soils: effects of *Spagnum* and *Juncus*. Soil Biol Biochem 31:323-325

Saarnio S, Wittenmayer L and Merbach W (2004) Rhizospheric exudation of *Eriophorum vaginatum* L. - Potential link to methanogenesis. Plant Soil 267:343-355

Shannon R D, White J R, Lawson J E and Gilmour B S (1996) Methane efflux from emergent vegetation in peatlands. J Ecol 84:239-246

Shurpali N J, Verma S B, Clement R J and Billesbach D P (1993) Seasonal distribution of methane flux in a Minnesota peatland measured by eddy-correlation. J Geophys Res [Atmos] 98:20649-20655

Silvola J, Alm J, Ahlholm U, Nykänen H and Martikainen P J (1996) CO2 fluxes from peat in boreal mires under varying temperature and moisture conditions. J Ecol 84:219-228

Strack M, Waller M F and Waddington J M (2006) Sedge succession and peatland methane dynamics: a potential feedback to climate change. Ecosystems 9:278-287

Ström L, Ekberg A, Mastepanov M and Christensen T R (2003) The effect of vascular plants on carbon turnover and methane emissions from a tundra wetland. Glob Change Biol 9:1185-1192

Ström L, Mastepanov M and Christensen T R (2005) Species-specific Effects of Vascular Plants on Carbon Turnover and Methane Emissions from Wetlands. Biogeochemistry 75:65-82

Townend J (2002) Practical statistics for environmental and biological scientists. John Wiley & Sons Ltd, Chicester

Updegraff K, Bridgham S D, Pastor J, Weishampel P and Harth C (2001) Response of CO_2 and CH_4 emissions from peatlands to warming and water table manipulation. Ecol Appl 11:311-326

Urban N R, Bayley S E and Eisenreich S J (1989) Export of dissolved organic carbon and acidity from peatlands. Water Resour Res 25:1619-1628

Visser E J, Colmer T D, Blom C W P M and Voesenek L A C J (2000) Changes in growth, porosity, and radial oxygen loss from adventitious roots of selected mono- and dicotyledonous wetland species with contrasting types of aerenchyma. Plant Cell Environ 23:1237-1245

Waddington J M, Roulet N T and Swanson R V (1996) Water table control of CH4 emission enhancement by vascular plants in boreal peatlands. J Geophys Res [Atmos] 101:22775-22785

Wein R W (1973) Eriophorum Vaginatum L. J Ecol 61:601-615

Weltzin J F, Bridgham S D, Pastor J, Chen J and Harth C (2003) Potential effects of warming and drying on peatland plant communty composition. Glob Change Biol 9:141-151

Whalen S C and Reeburgh W S (2000) Methane oxidation, production, and emission at contrasting sites in a boreal bog. Geomicrobiol J 17:237-251

Whiting G J and Chanton J P (1996) Control of Diurnal pattern of methane emission from aquatic macrophytes by gas transport mechanisms. Aquat Bot 54:237-253

Wiebner A, Kuschk P and Stottmeister U (2002) Oxygen release by roots of *Typha latifolia* and *Juncus effusus* in laboratory hydroponic systems. Acta Biotechnol 22:209-216

Yavitt J B, Williams C J and Wieder R K (1997) Production of methane and carbon dioxide in peatland ecosystems across North America: Effects of temperature, aeration, and organic chemistry of the peat. Geomicrobiol J 14:299-316

Yu K W, Wang Z P and Chen G X (1997) Nitrous oxide and methane transport through rice plants. Biol Fert Soils 24:341-343

7. Paper III

Continuous measurement and modelling of CO_2 losses from a peatland stream during stormflow

Kerry J. Dinsmore and Michael F. Billett

Published in 'Water Resources Research', 44: W12417 (2008)
(doi:10.1029/2007WR007284)

Continuous measurement and modeling of CO_2 losses from a peatland stream during stormflow events

Kerry J. Dinsmore and Michael F. Billett

Carbon Dioxide, Storm Events, Peatland, Drainage Water, Hysteresis

Abstract

Whilst streams draining peatland and wetland systems are known to be supersaturated in CO_2 with respect to the atmosphere, relatively little is known about short-term temporal variability in response to extreme hydrological events. Here we use submerged, non-dispersive infra-red (NDIR) sensors to make continuous measurements of CO_2 concentrations during 18 storm events in a Scottish peatland stream. Individual storms exhibited 3 distinct types of hysteresis loop. We suggest that differences in loop form may be due to differences in the relative contributions of soil water or differences in contributing catchment source area. We found a negative concentration-discharge relationship over the full study period, suggesting that CO_2 rich deep peat/ground water was the major source of aquatic CO_2 under low flow conditions. By removing the effect of dilution and estimating additions and losses of CO_2, we also show the importance of both surface peat CO_2 inputs into the stream and evasion loss during stormflow. The best model of temporal variability in CO_2 was achieved by separating the dataset into 'storm flow' and 'dry periods'. Downstream CO_2 export during the study period was dominated by stormflow events (71%), highlighting the importance of accurately accounting for high flow CO_2 sources.

Introduction

Surface waters associated with peatlands have repeatedly been shown to be highly and consistently supersaturated in CO_2 and CH_4 with respect to the atmosphere [*Billett and Moore*, 2008; *Dawson et al.*, 1995; *Hope et al.*, 2001; *Jones and Mulholland*, 1998; *Kling et al.*, 1991; 1992; *Raymond et al.*, 1997]. Through degassing at the water surface (evasion), streams have the potential to act as an important pathway directly linking the peatland carbon pool to the atmosphere. The limitations of previous measurement techniques have meant that our understanding of stream water CO_2 dynamics has, until now, been patchy and of poor temporal resolution. Furthermore, manual techniques employed in low frequency, periodic sampling regimes are unlikely to fully capture the importance of storm-flow extremes, possibly leading to error in estimating aquatic catchment carbon losses. In order to gain a more complete understanding of soil-stream biogeochemical interactions and hydrological connectivity, it is important to understand the dynamics of concentration and flow during extreme discharge events. With respect to both CO_2 and total dissolved inorganic carbon (DIC), relatively few high-frequency direct measurements have been made during high flow events [*Dawson et al.*, 2001; *Elsenbeer et al.,* 1994; *Johnson et al.*, 2007]. What measurements there are suggest that DIC concentrations decrease with increasing discharge [*Billett et al.,* 2004; *Edwards,* 1973; *Edwards et al.,* 1984].

Concentrations of dissolved CO_2 in aquatic systems can be measured directly using 'headspace analysis' [*Billett et al.*, 2004; *Billett and Moore*, 2008; *Hope et al.*, 2001; *Kling et al.*, 1991] or inferred by calculating the inorganic carbon speciation in samples of known DIC concentration [*Maberly,* 1996; *Waldron et al.,* 2007]. However, due to the need for manual sample collection, these methods are of limited use when describing temporal variability. Quasi-continuous CO_2 concentrations can be calculated using pH, temperature and alkalinity as in *Neal et al.*, [1998], or inferred using inorganic speciation of a modelled DIC dataset, such as that constructed by *Waldron et al.* [2007] using pH and discharge. However assumptions about the carbonate equilibrium system and inaccuracies in pH measurements (especially in organic rich peatland waters) add significant uncertainty to final

estimates [*Hope et al.,* 1995; *Neal et al.*, 1998; *Herczeg and Hesslein,* 1984]. Furthermore as alkalinity, required in both methods, is itself often extrapolated from calculations based on spot samples (frequently biased towards low flows), the issue of increased uncertainty in CO_2 concentrations at high flow is not overcome [*Jarvie et al.*, 2001]. An automated, high-frequency (5 minute) system for the direct measurement of dissolved CO_2 and O_2 concentrations is described by *Carignan* [1998], though to our knowledge the system has not yet been employed in flowing water in the field.

In many northern peatlands, where low temperatures and low water pH restrict in-stream processing, aquatic CO_2 is derived primarily from the terrestrial system through the input of CO_2-rich drainage water [*Hope et al.,* 1997; *Kling et al.,* 1991; *Palmer et al.,* 2001]. The input of CO_2 to surface drainage waters is likely to be highly dependent on the dominant hydrological flow path and water residence time within the catchment. As well as controlling the timing and the shape of the storm hydrograph, the different biogeochemical processes associated with the various paths of subsurface flow can significantly alter the chemistry of stream runoff [*Jarvie et al.*, 2001; *Vogt and Muniz*, 1997]. Peatland flow-paths include saturation- and infiltration-excess overland flow, near-surface throughflow, throughflow from deeper peat layers and groundwater flow through the underlying mineral and bedrock layers [*Holden and Burt*, 2003a, and references therein]. Networks of soil pipes and macropores have also been shown to be important pathways for rapid water transport [*Holden and Burt*, 2003b], though their contribution to the transfer of solutes and dissolved gases is still largely unclear.

Concentration-discharge hysteresis during storm events has been demonstrated for many stream water solutes [*House and Warwick*, 1998; *Rose*, 2003; *Stutter et al.*, 2008]. Assuming constant concentrations in the various input components (end members), it is often possible to use the shape and direction of the hysteresis loop to identify the major hydrological flow-paths [*Evans and Davies*, 1998] and hence solute sources within the catchment. In many cases the assumption of a constant input concentration is not met and the hysteresis loop may indicate the flushing and depletion of a finite soil pool throughout the storm event. To our knowledge, no

previous study has demonstrated the presence of hysteresis in dissolved CO_2 concentrations.

Here we use submerged, non-dispersive infra-red sensors (NDIR) to make high-resolution measurements of dissolved CO_2 in a Scottish peatland stream during the winter period when storm-flow dominates the hydrological regime. The study aims to a) model the primary drivers of variability in aquatic CO_2 concentrations, b) examine the concentration-discharge relationship during storm events for evidence of hysteresis and c) quantify the potential importance of storm-flow events to the overall long-term export of aquatic CO_2.

Catchment Characteristics

Auchencorth Moss is a relatively flat, low lying, 335 ha, ombrotrophic peatland, located approximately 17 km south of Edinburgh, Scotland (55º47'34 N; 3º14'35 W). The land-use is primarily low-intensity sheep grazing with an area of peat extraction at the western edge of the catchment. A consistent pattern of overgrown, parallel grips are evidence of past drainage. The catchment drains in a northeast direction via the Black Burn into the North Esk. Mean annual precipitation (1995-2006) is 1016 mm (*Coyle*, unpublished data, 2008). The stream hydrograph is characterized by a rapid ("flashy") response to storm or snowmelt events producing high-flow events with high DOC concentrations [*Billett et al.,* 2004].

Histosols (peats) cover approximately 85% of the catchment with areas of Gleysol (9%), Humic Gleysol (3%) and Cambisol (3%) occurring at the catchment margins [*Billett et al.*, 2004, Figure 1]. Peat depth ranges from <0.5 m to >5 m, underlain by a layer of Upper Carboniferous/Lower Devonian sandstones and shaly sandstones containing occasional bands of limestone, mudstone, coal and clay; thicker units of limestone are also apparent in some areas of the catchment [*Billett et al.*, 2004]. The vegetation is a patchy mix of coarse grasses and soft rush covering a *Sphagnum* base layer. *Calluna vulgaris* dominates the south western edge of the catchment where drainage is better. The microtopography consists of a series of hummocks (~40 cm diameter, ~30 cm height) dominated by *Juncus effuses* or *Eriophorum vaginatum*, and hollows dominated by mosses.

Methods and Materials

Field measurements

Measurements of dissolved aquatic CO_2 in the Black Burn were made continuously, alongside auxiliary measurements, from November 2007 until mid-February 2008. Measurements of dissolved CO_2 in both the stream channel and the adjacent peat (~20 cm depth; ~5 m from stream), were made using Vaisala CARBOCAP® (transmitter series GMT220), single-beam dual-wavelength, non-dispersive infra-red absorption (NDIR) sensors. The accuracy of the sensors is given as 1.5% of the calibrated range (0-1% in water; 0-5% in soil) + 2% of the reading. Each sensor was enclosed by a polytetrafluoroethylene (PTFE) membrane (International Polymer Engineering, Tempe, AZ) which is highly permeable to CO_2 but impermeable to water. The PTFE tubing was sealed at both the cable-end and the non-cable end of the sensor using Plasti Dip (Plasti Dip International, Blaine, MN USA) rendering the sensor completely water-tight. The sensor was then secured underwater and connected to a Campbell Scientific CR1000 datalogger. The sensor is therefore measuring the concentration of CO_2 in the air retained within the headspace of the PTFE membrane, which is assumed to be in equilibrium with the concentration of CO_2 dissolved in the surrounding water. Equilibration time of the headspace to changes in the external water concentrations were less than the measurement frequency of 10-minutes [*Johnson et al.,* 2006]. The sensors were originally adapted for use in soils by *Tang et al.* [2003] and *Jassal et al.* [2004] though have since been deployed in the aquatic environment by *Johnson et al.* [2006] and *Dinsmore et al.* [2009]. Comparisons with concentrations measured using the traditional headspace technique in a range of aquatic environments, is given by *Johnson et al.* [in preparation for Limnology and Oceanography Methods, 2008]. Additional sensors were used to measure stage height (PDCR 1830 series pressure transducer), soil temperature (CS108), water conductivity/temperature (CS547A), and water pH (CSIM11). Measurements were made every minute with 10 minute averages recorded. Half-hourly point precipitation and water table data was obtained from the Auchencorth Moss EMEP (European Monitoring and Evaluation Programme) monitoring site located ~350 m from the Black Burn sensor site (Coyle, personal

communication, 2008). Although periods of snowfall did occur, precipitation was dominated by rainfall. Where the term rainfall is used in the following text, it is therefore acknowledged that in some cases this may also include precipitation in the form of snow.

Data analysis

To avoid systematic error in sensor readings, the volume fraction output of the stream water NDIR sensor was corrected for variations in temperature and pressure. The reference temperature and pressure for the sensor was 22.5°C ± 1% and 100.7 kPa ± 1%, respectively. Concentrations were corrected using the method described in *Tang et al.* [2003]. As the NDIR sensor was fixed at a particular height above the stream bed, its depth relative to the water surface fluctuated with stage height. Hence to avoid confusion due to variations in pressure, volume fraction units were converted to mg C L^{-1} before subsequent analysis. Concentrations are expressed in either mg L^{-1} or units of excess partial pressure (*ep*CO_2), the latter defined as the partial pressure of CO_2 in solution divided by the partial pressure of the CO_2 in equilibrium with the atmosphere. CO_2 concentrations are assumed to be uniform throughout the channel profile, an assumption considered reasonable due to the turbulent nature of the stream. Although periodic inundation of the soil sensor is likely to have occurred during periods of high water table, it is assumed that the soil sensor is primarily measuring concentrations in the soil atmosphere. Soil concentrations are therefore expressed in units of ppmv.

Continuous discharge data was calculated from a curvilinear stage-discharge rating curve (r^2 = 0.85, n = 11) built from a series of dilution-gauging measurements. A simple dilution model was used to calculate the change in dissolved CO_2 concentration between each time step attributable solely to an increase/decrease in water volume. The increase/decrease in water volume between each time step was calculated from the change in discharge; the dilution related change in CO_2 concentration could then be calculated by adjusting the volume fraction CO_2 concentration, assuming no change in the volume of CO_2. The observed minus the dilution-modelled value is referred to hereafter as 'excess CO_2'; positive values

indicate an addition of CO_2 to the stream, negative values indicate an overall loss from the stream. Excess CO_2 is therefore defined as the change in CO_2 concentration not explained by dilution.

The measurement period was separated into either 'storm events' or 'dry periods'. Storm events were classified as events which raised the discharge by >50 L s^{-1} above the pre-event level. Events were considered distinct if the time between discharge peaks was >15 hours. These limits were based upon visual examination of the discharge and rainfall time series. The event start was identified by the onset of precipitation; the event end was the point where both discharge and CO_2 stabilized. The following parameters were used to describe stream and catchment conditions for individual storm events in the subsequent analysis: peak rainfall, total rainfall, rainfall duration, antecedent water table, antecedent soil CO_2, change in soil CO_2, peak discharge, background discharge, discharge lag, slope of rising discharge limb, time since previous storm event, peak excess CO_2, total excess CO_2, lag in excess CO_2, background stream CO_2 and change in stream CO_2. Peak is the difference between maximum and pre-event discharge or concentration. Change in CO_2, in reference to both soil and water concentrations, refers to the difference between pre-event concentrations and the point at which concentrations stabilize; positive values indicate an increase from background concentrations, negative values indicate a decrease. Lag refers to the time (in hours) between peak rainfall and the peak of the measured variable.

Statistical analysis

Analyses were carried out both on individual storm events and using the complete time series. Trends in soil and water CO_2 concentrations were compared using Pearson's correlation analysis on 12-hour averages adjusted for first order autocorrelation. For individual storm events, best subsets multiple regression was used to identify variables controlling excess CO_2. The time series data were adjusted for autoregression, and maximum correlation lag times examined using cross-correlation analysis. The datasets were then adjusted for lag where appropriate and excess CO_2 modelled using best subsets multiple regression. Stepwise regressions

were carried out both individually for 'storm event' and 'dry period' data, and for the full dataset without event separation.

Where an average value is quoted, the ± value refers to the standard error of the mean unless stated otherwise. In datasets which display significant autocorrelation and hence the assumption of independence is not met, standard errors are calculated using the effective rather than the real sample size. This estimates the actual number of independent observations using the first order autocorrelation coefficient rather than including all non-independent measurements.

Results

Underlying stream characteristics

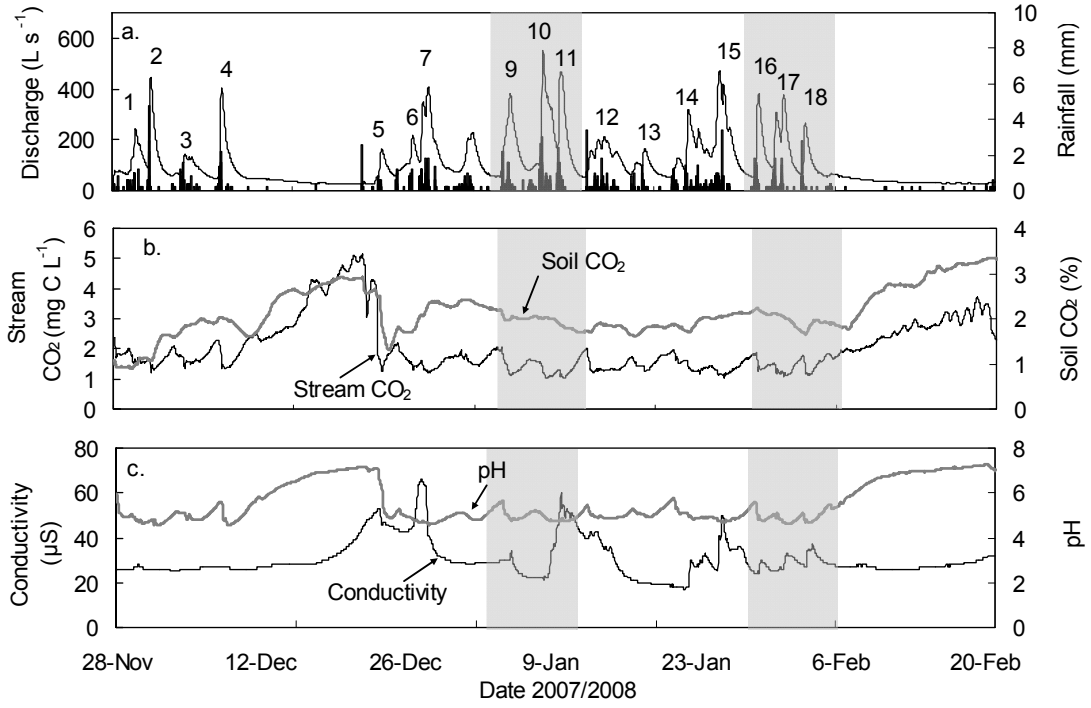

Figure 1 Stream hydrochemical characteristics over the measurement period; a) discharge and rainfall (bars), b) soil and stream water dissolved CO_2-C concentrations and c) stream water conductivity and pH. Shaded areas represent periods of snow cover in the catchment. Rainfall bars represent mm per 30-minutes.

In total 18 distinct storm events were identified during the study period (Figure 1a), accounting for 56% of the collected data. Mean discharge during dry periods was 44 ± 4.1 L s^{-1}, corresponding to a mean water depth of 0.27 ± 0.01 m. The maximum discharge over the study period was 555 L s^{-1}, recorded on the 8th of January (storm

10, Figure 1a). The mean discharge lag was 7.5 ± 0.9 hours. Mean water pH was 5.7 ± 0.1 reaching a maximum of 7.3 during an extended period of base flow and a minimum of 4.6 during storm 2 (Figure 1a). Mean pH during storm events was 4.9 ± 0.05 (Figure 1c). Mean conductivity and stream temperature over the study period were 41.1 ± 2.5 µS and 4.4 ± 0.3°C, respectively.

Mean water CO_2 concentration over the whole study period was 2.04 ± 0.11 mg C L^{-1}, equivalent to an *ep*CO_2 value of 6.98 ± 0.38, similar to the values reported in *Billett et al.* [2004] who measured concentrations in the Black Burn during 1996 and 1997. A clear diurnal cycle during dry periods was evident in the plot of mean concentration per time step, with maximum concentrations occurring between 13:00 to 14:00 hr (Figure 2); this was approximately 8 hours after the daily minimum water temperature. The cycle was still evident with the inclusion of storm event data, although the amplitude of the signal was muted.

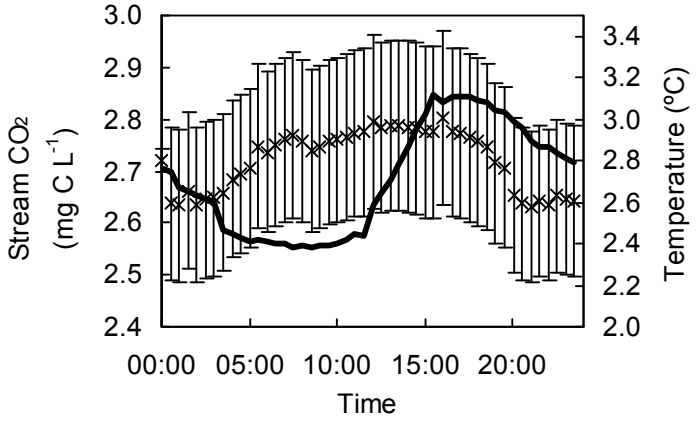

Figure 2 Diurnal variability in stream CO_2 concentrations ('×' ± 1 standard error) and stream temperature (solid line) during dry periods. For display purposes data was only plotted every 30 minutes.

The relationship between stream water CO_2 concentration (C) and discharge (Q) over the full study period was negative curvilinear, following a power function of the form shown in equation 1 where 'a' and 'b' refer to constants 12.70 and 0.43 respectively (Figure 3).

$C = aQ^{-b}$ (Equation 1)

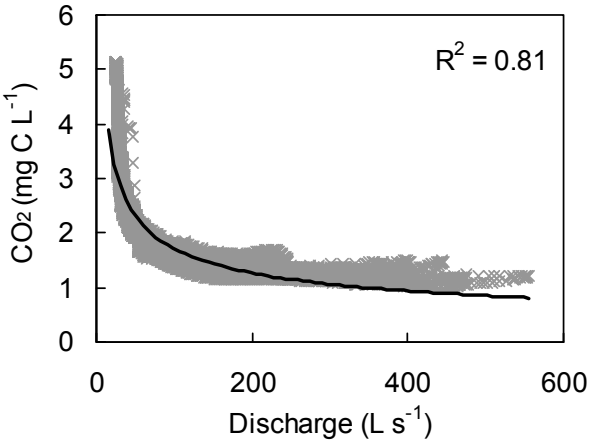

Figure 3 Concentration – Discharge relationship for Dissolved CO_2 – C over the measurement period

Closer examination of the storm-flow periods revealed the presence of significant hysteresis loops, discussed in more detail below. Soil CO_2 concentrations followed a similar overall pattern to water concentrations though the signal appeared muted with less small scale temporal variability (Figure 1b). Considering 12-hour averages, the correlation between soil and water concentrations was highly significant ($r = 0.22$, $p < 0.01$). CO_2 concentrations in both stream water and soil, alongside water pH (Figure 1c), increased to reach a maximum value during extended periods of base flow, dropping suddenly in response to significant increases in discharge.

A more detailed examination of storm 4 shows a typical hydrochemical sequence of events following rainfall (Figure 4). Shortly after rainfall, excess CO_2 within the stream channel rose to a peak, it then dropped to negative values, indicating a loss from the stream, before returning to its original value. Figure 4b shows a clear response in excess CO_2 to the double rainfall peak. Shortly after excess CO_2 peaked, the minimum CO_2 concentrations were reached (Figure 4c). Discharge reached its peak as CO_2 concentration and excess CO_2 returned to pre-rainfall values.

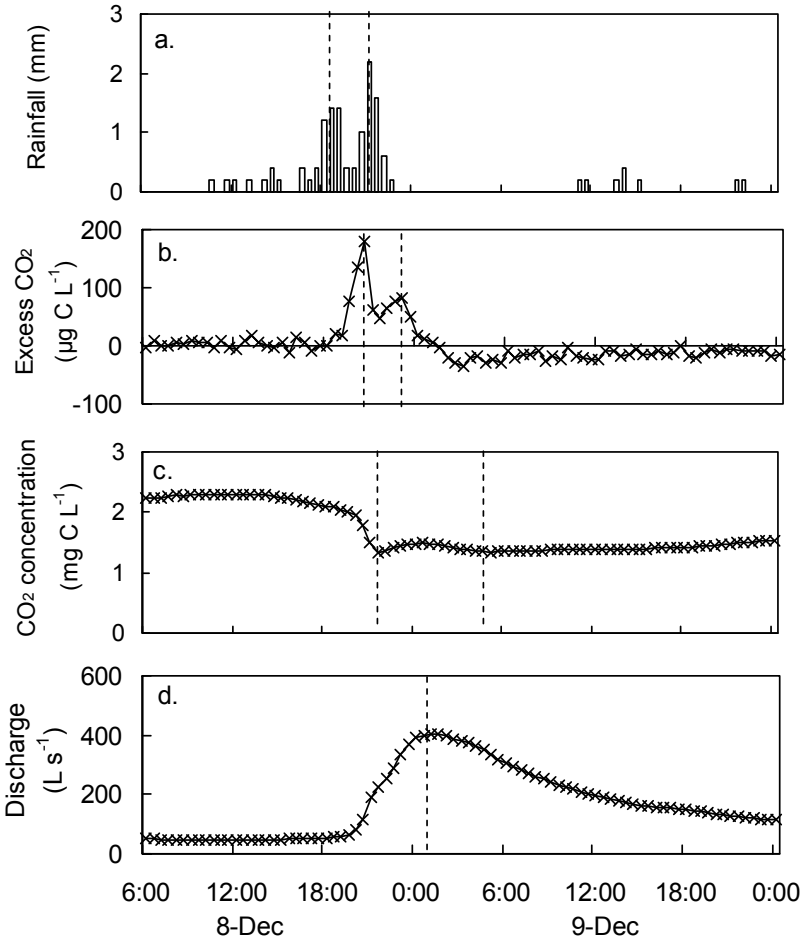

Figure 4 Temporal variability in a) rainfall, b) excess CO_2, c) CO_2 concentration and d) discharge during a storm event (data interval = 30 min). Dashed lines indicate corresponding peaks/troughs to illustrate differences in response times.

Storm event characteristics

After using the dataset to define 18 individual storms (Figure 1a), each storm was described using the parameters listed above. Discharge peaks ranged from 141 to 553 L s^{-1} with a mean of 324 L s^{-1}. The total amount of rainfall per storm event ranged from 5.2 to 27.7 mm with a mean of 14.7 mm; mean rainfall duration was 23 hours. Excess CO_2 reached a peak of mean 80.9 ± 11.6 µg C L^{-1} at a mean time lag of 3.3 ± 0.3 hours after peak rainfall. Peak excess CO_2 was modelled from the full set of storm event parameters using best subsets multiple regression. The best model contained only peak discharge with $r^2 = 0.59$ (Figure 5b). Stream CO_2 concentrations dropped over the course of individual storms. Although not statistically significant, Figure 5a indicates a greater decrease in concentration during storms with the

greatest peak discharge. In contrast, total excess CO_2 is significantly and positively correlated to peak discharge (Figure 5b).

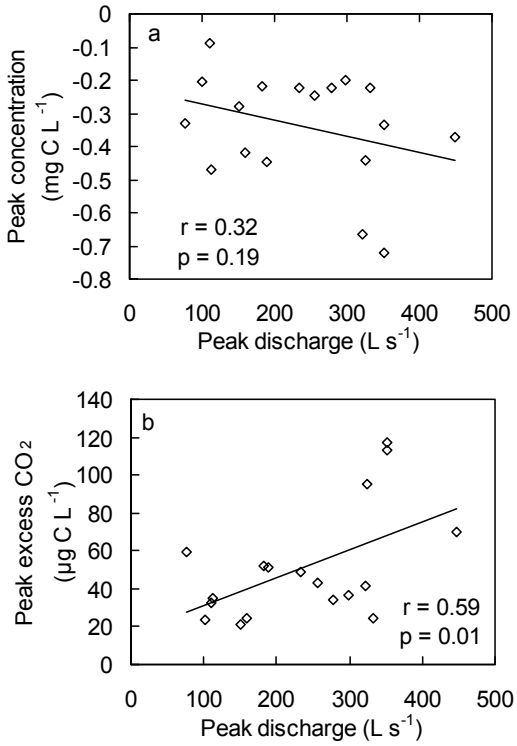

Figure 5 Relationship between peak discharge and a) actual CO_2 – C concentration and b) Excess CO_2 – C for 18 individual storms events

Model of excess CO_2

Autoregression and crosscorrelation analyses were carried out on the full time series dataset to adjust for autocorrelation and lag (Table 1a). Residuals were then separated into 'storm event' and 'dry period' according to the classification described earlier. Best subset multiple regression was used to model excess CO_2 using the parameters: rainfall, antecedent rainfall (6 hours, 12 hours, 48 hours), water table, soil CO_2, soil temperature, discharge, stream pH, conductivity, stream temperature, and various interaction terms combining variables.

The 'storm event' data could be modelled ($r^2 = 0.41$) using the variables antecedent rainfall (6 hours), discharge, and an interaction term combining soil CO_2 and rainfall (Table 1b). The dry period model, combining conductivity, pH, discharge, water table and soil CO_2, produced an r^2 of only 0.08 (Table 1b), therefore explaining very little of the observed variability. Modeling excess CO_2 without prior separation into

'storm event' and 'dry period', produced a model with an r^2 of 0.27, and contained a mixture of the variables included in the above 2 separated models (Table 1c).

Table 1 Model parameters and test statistics for controls on excess CO_2 from stream water. In models (b) and (c) autocorrelation in both dependent and independent variables was removed prior to analysis using autoregression; model (a) describes the autoregression parameters for excess CO_2.

		Lag (h)	Coefficient	T	P
a)	Autoregression model				
	Order 1	---	0.74	47.5	<0.01
	Order 2	---	-0.073	-4.71	<0.01
b)	Storm and dry period model				
	Model of storm-flow residuals (r^2 = 0.41)				
	Intercept	---	3.84	---	---
	Antecedent rainfall (6 h)	-2	3.51	3.45	<0.01
	Discharge	0	1.70	16.4	<0.01
	Interaction [Soil CO_2*Rainfall]	0	-0.05	-1.51	0.07
	Model of dry period residuals (r^2 = 0.08)				
	Intercept		---	-0.41	---
	Conductivity	-1	36049	2.94	<0.01
	pH	0	-197	-2.2	<0.05
	Discharge	0	1.83	1.79	0.07
	Interaction [Soil CO_2*water table]	-1	0.52	2.26	<0.05
	Interaction [Discharge*pH]	0	-572	-3.98	<0.01
c)	Full dataset model				
	Model of residuals (r^2 = 0.27)				
	Intercept		---	-0.08	---
	Antecedent rainfall (12 h)	-4	2.80	4.59	<0.01
	Water temperature	0	97.4	13.5	<0.01
	Discharge	0	1.98	25.6	<0.01
	Interaction [Soil CO_2*rainfall]	-12	-0.23	-23.6	<0.01
	Interaction [Discharge*pH]	0	-13.5	-5.39	<0.01

The 'storm event' and 'dry period' models were combined, creating a single, continuous, modelled dataset for the full study period. This new dataset was compared to the excess CO_2 calculated from measured values (Figure 6a). Excess CO_2 is captured well during storm events though the model consistently underestimates CO_2 output during dry periods (Figure 6a). In particular it fails to capture the CO_2 deficit which repeatedly occurs after the peak in excess CO_2 has subsided. The mean overestimation of excess CO_2 during dry periods was 0.50 ± 0.13 μg C L^{-1}. Similarly, the model created from the dataset that was not separated

prior to regression (Table 1c), also underestimated CO_2 output during dry periods. However, this full dataset model also underestimated the excess CO_2 during storm events (Figure 6b).

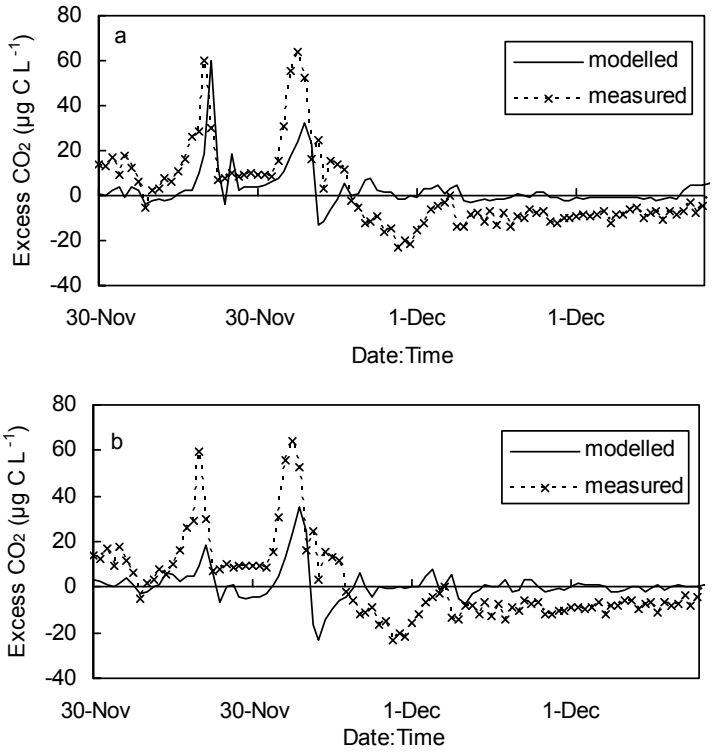

Figure 6 Illustration of modelled vs. measured excess CO_2 over a 2 day period using a) the model built by combining separate storm and dry period models and b) the model built using the full non-separated dataset

Hysteresis

The CO_2 concentration-discharge plots from all 18 of the identified storm events could be classified into 1 of 3 distinct hysteresis loop types (Figure 7a, c and e). The figure-of-8 loop was the most complex in form. Although the exact shape varied, the rotational direction was common among all storms in the group with the concentration in the rising limb greater at the onset, before dropping below the falling limb, and then rising again at approximately peak discharge. In almost all cases there was a negative correlation between concentration and discharge. The anticlockwise and clockwise loops differ in their rotational directions, though both display the same negative trend as seen in the figure-of-8 loops. Of the 18 storm events, 7 displayed figure-of-8 loops, 2 (storm 5 and 6) displayed the anticlockwise

loop form, and the remaining 9 displayed clockwise loops. The relationships between excess CO_2 and discharge for all 18 storms showed very similar, clockwise rotational hysteresis loops, which were independent of differences in concentration/discharge loop type (Figure 7b, d, f).

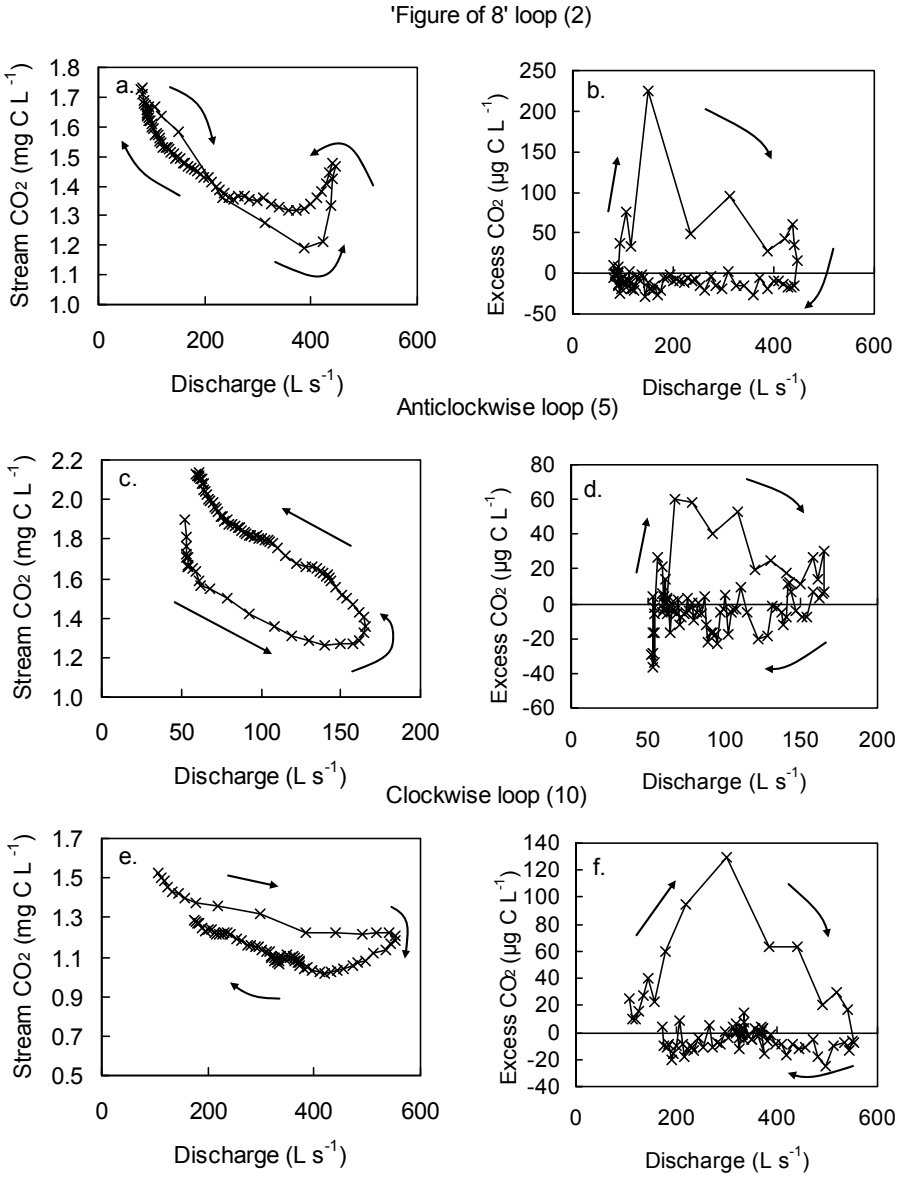

Figure 7 Illustration of 3 distinct hysteresis loops observed in dissolved CO_2 (a, c, e) and excess CO_2 (b, d, f) during individual storm events. The number in brackets following the loop type relates to individual storm events (Figure 1).

The variables mentioned above, which describe individual storms, were used in a 'principal components analysis' (PCA) [*Townend,* 2002] to group storms by common characteristics (Figure 8). The PCA produced a relatively good separation of the

figure-of-8 and clockwise hysteresis loops, though the 2 anticlockwise loops are widely spaced.

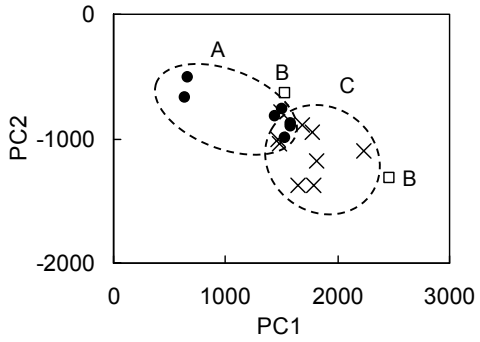

Figure 8 Separation plot of 18 individual storm events grouped by hysteresis type, based on PCA analysis where 'A', 'B' and 'C' refer to figure-of-8, anticlockwise and clockwise loop forms, respectively. Both PC1 and PC2 were dominated primarily by rainfall parameters.

The results from a series of ANOVA tests, carried out on the variables most heavily weighted in the PCA analysis, are displayed in Table 2. As only 2 storm events were found to display anticlockwise loops, statistical analysis was not appropriate. Considering all the 18 storm-flow events, event 5 was the only event to follow on from an extended dry period (Figure 1). As such the water tables prior to the both events 5 and 6 (-9.6 cm and -6.5 cm, respectively), were much lower than the mean water table level prior to events displaying either the much commoner figure-of-8 or clockwise hysteresis loops (-1.73 cm and -2.05 cm, respectively). Soil CO_2 was also much higher prior to storm 5 and showed a large decrease during the storm event. Storms displaying figure-of-8 loops had significantly shorter precipitation-discharge lags than storms showing clockwise loops, and had significantly lower pre-event soil CO_2 concentrations. Soil concentrations decreased over the course of the storm for figure-of-8 loops; during anticlockwise loops, soil concentrations increased over the course of the storm. Clockwise loops coincided with storms with significantly higher peak discharges and rates of increase during the rising limb. Although no direct measurement of snow melt was made, all 6 of the storm events occurring during periods of light snow cover in the catchment (Figure 1), displayed clockwise hysteresis loops.

Table 2 Table summarising results from ANOVA tests; different letters represent differences based on p-values of * < 0.1, ** < 0.05, *** < 0.01. Upward pointing arrows indicate a result significantly higher than other groups; downward pointing arrows indicate a variable lower than other groups. Only variables showing significant results are displayed. P-values refer only to differences between the 'figure of 8' and 'clockwise' loops; arrows in the 'anticlockwise' group are observations as n=2

Variable	Hysteresis Type		
	Figure-of-8	Clockwise	Anticlockwise
Time since previous event	a	b ↑	a
Peak discharge *	a	a	b ↑
Slope of rising limb	a	b ↓	a
Discharge lag **	a ↓	ab	b
Soil CO_2 before event ***	a ↓	b ↑	c
Change in soil CO_2 ***	a ↓	b ↑	c
Water table before event	a	b ↓	a

To aid interpretation of the hysteresis loops, both pH and conductivity for the individual storms were plotted against discharge (data not shown). Hysteresis was evident in all plots. A complex series of patterns was seen for pH with loops often very similar to CO_2 concentration plots. Storms 5 and 6 are the only events to show a significant difference between CO_2 concentration and pH hysteresis loops; in these cases the rotational direction of the loops are reversed. The conductivity loops displayed a variety of complex loop shapes with both positive and negative relationships with discharge. However, no consistent link to CO_2 loop types could be found.

Discussion

To identify the origin of streamwater CO_2, three different approaches were taken, which indicate the presence of distinct CO_2 sources that vary in relative importance depending on the primary flow path of water through the catchment. Firstly the temporal variability in dissolved CO_2 concentrations is discussed in terms of both diurnal cycling and correlations with discharge and various storm parameters. Secondly the results from the time series regression analysis on excess CO_2 are considered, and thirdly the discharge hysteresis behavior of CO_2 is discussed in detail.

Drivers of variability in dissolved CO_2 concentrations

Diurnal cycles in aquatic CO_2 concentrations (Figure 2) similar to those seen here were also recorded in Mer Bleue peatland, Canada [*Dinsmore et al.,* 2009], and in

both CO_2 [*Dawson et al.,* 2001] and total DIC [*Waldron et al.*, 2007] in waters draining the Glen Dye catchment (NE Scotland). The off-set between cycles of CO_2 and temperature in this study (Figure 2), indicate that temperature dependent changes in gas solubility cannot fully explain the diurnal variation in CO_2. Furthermore, no significant temperature effect was observed in the best subset model (Table 1), suggesting that the effect of temperature is masked or complicated by other factors, such as inputs from the surrounding soils.

No clear diurnal signal in soil CO_2 concentration was observed in this study due primarily to the periodic inundation of the sensor following fluctuations in water table. However, previous studies have found diurnal cycling in soil CO_2 similar to that shown by soil temperature which, once adjusted for time lags to account for the transport of soil water, may help explain the signal in aquatic CO_2 [*Dawson et al*, 2001; *Osozawa and Hasegawa*, 1995]. Although CO_2 concentration and pH both decrease with increasing discharge, the dry period model indicated a significant negative correlation between the two variables (Table 1). Diurnal variation in stream water pH is likely to result in diurnal changes in the relative proportion of different forms of DIC, hence influencing CO_2 concentrations. However, since CO_2 inputs may also influence water pH, the causality of the relationship is unclear.

The negative curvilinear relationship between CO_2 concentration and discharge (Figure 3) is typical of the behavior of a range of groundwater-derived solutes (including DIC) diluted during stormflow [e.g. *Gregory and Walling*, 1973; *Edwards,* 1973]. The fact that coefficient b, the slope of the logarithmic plot, is less than 1, indicates that whereas concentrations decrease with increasing discharge, total load actually increases. This is confirmed when the simple dilution model was applied and a peak in excess CO_2 was observed after rainfall events (Figure 4).

The fast response time of excess CO_2 after rainfall suggests an initial flush of soil-derived CO_2. This is most likely via near-surface throughflow transporting CO_2-rich soil water from the surface peat to the stream. The mean soil CO_2 concentration measured over the study period was 21350 ± 3646 ppmv, approximately 15 times atmospheric concentrations. Despite the significant positive relationship between

excess CO_2 and discharge peak (Figure 5b), the smaller secondary peak in excess CO_2 (e.g. in Figure 4), suggests either a depletion in the CO_2 source or a change in flow path due to previously wet conditions (i.e. a switch to saturation-excess overland flow). Whilst CO_2 is being flushed into the stream, the concentration in the input water is clearly less than at base flow, suggesting that deep peat/groundwater inputs are a major source of CO_2 in the Black Burn. Similarly, *Waldron et al.* [2007] observed a significant negative linear relationship between inverse discharge and DIC concentration, concluding that groundwater represented a higher concentration source of DIC than shallow surface runoff.

The presence of 2 distinct sources of aquatic CO_2 supports isotopic measurements made previously on the Black Burn. *Billett et al.* [2007] found that evaded CO_2 was most likely derived from a mixture of recently fixed organic matter, and aged CO_2 (up to 1449 years B.P.) from either deep peat or carbonate-enriched groundwater. In terms of hydrological connectivity these equate to a shallow and a deep pool of CO_2. Data from isotopic analyses also revealed the presence of two distinct DIC sources in the Glen Dye catchment, NE Scotland [*Waldron et al.,* 2007]; although DIC does not exclusively refer to CO_2, even in these low pH waters.

Model of excess CO_2

The results from the time series regression analyses (Table 1b) suggest that different mechanisms control CO_2 concentrations during storm-flow and dry periods. The overriding control exerted by dilution masked variations in CO_2 input/output which could be seen when excess CO_2 was calculated. Variations in storm-flow excess CO_2 were explained using data on rainfall, discharge and soil CO_2, suggesting that the major source was terrestrial inputs. Similar conclusions about the importance of terrestrial CO_2 inputs were reached by *Hope et al.* [2004]. Only a very weak model (r^2 = 0.08) could be produced for dry period CO_2 with the primary variables including conductivity and pH, indicating a greater relative contribution from in-stream processing. When no prior distinction was made between storm-flow and dry periods, the model underestimated excess CO_2 during storm-flow. The degree of soil-water connectivity has previously been shown to vary spatially along the length of

river systems [*Hope et al.,* 2004]; the results from our study suggest that connectivity also varies temporally. This highlights the need to understand storm-flow CO_2 dynamics separately from periods of base flow; studies biased towards low flow conditions could potentially underestimate CO_2 inputs and lead to misconceptions about the primary sources of aquatic CO_2.

The important process of water surface CO_2 evasion is not accounted for in either the storm-flow or dry period model and may represent an important source of error in the above models. Since our measurements were made in a low pH, organic-rich system during winter, the decrease in excess CO_2 to negative values after the peak has subsided (Figure 4b) is most likely a reflection of losses through evasion, rather than within stream processing. Estimates of CO_2 evasion from the Black Burn range from 3.8 to 25.9 g C m^{-2} d^{-1} [*Billett et al.*, 2004]. From these values, the deficit due to evasion over each 10-minute time step can be estimated as 0.10 to 0.67 μg C L^{-1}; the difference between modelled and measured excess CO_2 during dry periods (0.50 ± 0.13 μg C L^{-1}) falls within this range of evasion losses; however caution is needed when interpreting the excess CO_2 concentrations during dry periods as these mainly fall within the range of sensor error. Though evasion is also important during storm-flow, the magnitude of allochthonous inputs is likely to mask evasion losses. Therefore accurate estimates of catchment aquatic CO_2 losses need to account for both inputs of excess CO_2 as well as evasion losses from the stream channel.

Hysteresis

The excess CO_2 hysteresis plots (Figure 7b, d, f) all display patterns corresponding to C1 type loops using the classification system devised by *Evans and Davies* [1998], described as having clockwise rotation and convex curvature. The anticlockwise and clockwise loops (Figure 7b and c) are classified as ‘A3’ and ‘C3’ loops, respectively. The figure-of-8 concentration hysteresis loops (Figure 7a) were similar in shape to what *Chanat et al.* [2002] describe as ‘indeterminate’ loops. However, *Chanat et al.* [2002] do not differentiate between loops such as our figure-of-8 form and those with the opposite rotational direction.

The interpretations of the loop forms by *Evans and Davies* [1998] are based on raw concentration data and are therefore inappropriate for the dilution corrected (excess CO_2) values in this study. Furthermore, interpretation of the data is complicated by a combination of flushing and exhaustion of the CO_2 sources, as well as losses from the stream channel through evasion. The initial increase in excess CO_2 (Figure 7b, d, f) indicates an increase in input from the terrestrial system. Although turbulence-driven evasion is likely to be high throughout the course of the storm it is initially masked by high inputs of soil derived CO_2, hence values of excess CO_2 become negative as a result of evasion only on the falling limb of the storm hydrograph (Figure 7b, d, f).

Using a 3-component model based on surface event water, soil water and ground water, where peak event water precedes peak soil water, and ground water is closely correlated with peak discharge, *Evans and Davies* [1998] interpreted the hysteresis forms in terms of component concentrations. In terms of the concentration hysteresis plots (Figure 7a, c, e), forms similar to our clockwise loops (Figure 7e) were produced when component input concentrations were ordered: ground water > event water > soil water. Forms similar to our anticlockwise plots (Figure 7c) were produced with component concentrations: ground water > soil water > event water. In the case of dissolved CO_2, deep peat/ground water is likely to contain the greatest concentrations; hence the prominence of dilution at higher flows (Figure 3). If we classify event water as a combination of 3 components (direct channel precipitation, overland flow and near-surface flow), it is reasonable to assume that soil water concentrations are intermediate and event water concentrations lowest. Therefore our anticlockwise plots of storm events 5 and 6 appear to be consistent with the idealized hydrograph separation used by *Evans and Davies* [1998].

Storm events 5 and 6 were the only events to show a reversal in loop direction between concentration (anticlockwise) and pH (clockwise) hysteresis plots. The negative correlation between pH and discharge, suggests that pH was highest in deep peat/groundwater (pH < 7.3). Furthermore, since the mean soil pH (10-30 cm) measured at several sites at Auchencorth Moss (n = 21) was 4.4 ± 0.1 [*Dinsmore et al.,* 2008], we can assume that the pH of soil water is lower than event water.

Therefore the reversal of rotational direction can be attributed to the change in relative component concentrations, and plots for storms 5 and 6 again appear to be consistent with the hydrograph separation of *Evans and Davies* [1998].

Hysteresis loop form can be further interpreted by allowing the component volumes to vary relative to each other [*Chanat et al.,* 2002]. With component concentrations remaining in the order soil water > event water, clockwise loops can theoretically be produced by increasing the relative volume of the soil water component. Hence a possible explanation for the different rotational directions between our anticlockwise and clockwise loops is a difference in soil water contribution. The lower water table preceding storms 5 and 6 suggests that little resident soil water may have been available to contribute to runoff, hence a greater prominence of event water leading to anticlockwise loop rotation.

Our figure-of-8 plots were similar in form to the clockwise plots except for a delayed increase in CO_2 concentration roughly coinciding with peak discharge. Peat depth adjacent to the measurement station is relatively shallow with deeper peats dominating in the south west area of the catchment [*Billett et al.*, 2004]. Soil water originating from this area is likely to contain high concentrations of dissolved CO_2. The mean CO_2 concentration at the stream source (approximately 2 km upstream) was measured as 9.8 ± 0.9 mg C L^{-1} (n = 8) in 2005 and 2006 (M. F. Billett, unpublished data, 2008), well above the maximum of 5.1 mg L^{-1} measured during base flow at the downstream site used in this study. The delayed arrival of this source/near-source water containing high concentrations of CO_2 may explain the sudden increase in stream water concentrations. Hence it is likely that the more complex figure-of-8 loops are a result of variable source area contributions within the catchment.

Conclusions and implications

Billett et al. [2004] estimated a flux of CO_2 through the Black Burn, including both downstream export and evasion from the water surface, of 55 kg C ha^{-1} a^{-1}, compared to a catchment net ecosystem exchange (NEE) uptake of 278 kg C ha^{-1} a^{-1}. Hence aquatic CO_2 losses equate to ~20% of NEE uptake and therefore represent an

important part of the catchment carbon budget. By combining the concentration and discharge data, the total CO_2 load transported by the stream during the study period was calculated as 1.25 tonnes of carbon, 71% of which occurred during storm events (56% of the study time period). A similar result was found by *Billett et al.* [2004] who found that the greatest downstream C losses were associated with periods of high precipitation or snow melt. From continuous stage height data and using the same criteria as for the winter study period, storm-flow comprised 45% and 53% of flow conditions during 2006 and 2007 respectively [*Dinsmore,* unpublished data], highlighting the importance of accurately measuring the storm-flow component for annual estimates.

Concentration-discharge plots during individual storm events revealed the presence of 3 distinct hysteresis loop types, suggesting stream water CO_2 is influenced by changes in the relative dominance of different flow paths and variable source areas within the catchment. The strong dilutional effect indicates that deep peat/groundwater, which sustains base flow during the dry periods, is a major source of dissolved CO_2. By removing the effect of dilution and deriving "excess CO_2", we show the importance of terrestrial CO_2 inputs during storm events. The presence of 2 distinct sources of CO_2 is in agreement with isotopic data from the same catchment [*Billett et al.*, 2007].

Excess CO_2 during storm-flow was underestimated when the full time series dataset was used. However, when the dataset was separated into storm events and dry periods prior to modeling, a much better fit during storm-flow was achieved (r^2 = 0.41), showing the importance of temporal variability in soil-stream connectivity. It is therefore likely that previous up-scaled annual estimates, where manual measurements have been biased towards low flows, underestimate the importance of aquatic CO_2 as a pathway for terrestrial carbon loss.

Despite an overall decrease in stream water CO_2 concentration with increasing discharge, excess stream water CO_2 was correlated with the height of peak discharge (Figure 5). Excess CO_2 during storm events was more closely correlated with catchment and rainfall characteristics than in-stream variables, suggesting excess

CO_2 was primarily the result of terrestrial inputs. Discharge peak rather than total rainfall or total storm-related discharge correlated with excess stream CO_2. As peak discharge is a function of catchment hydrology and geomorphology, changes due to land management (e.g. drainage and drain-blocking) have the potential to significantly alter catchment CO_2 export. The correlation between soil and water CO_2 concentrations (Figure 1) illustrates the close connectivity between the soil-stream system. This suggests that changes in the terrestrial carbon cycle will not only have a significant effect on DOC and POC [e.g. *Dawson and Smith*, 2007; *Grieve,* 2006], but also on CO_2 concentrations and fluxes in drainage systems.

Acknowledgements:

The work was funded by the UK Natural Environment Research Council (NERC) through an algorithm PhD studentship grant.

References

Billett, M. F., S. M. Palmer, D. Hope, C. Deacon, R. Storeton-West, K. J. Hargreaves, C. Flechard, and D. Fowler (2004), Linking land-atmosphere-stream carbon fluxes in a lowland peatland system, *Global Biogeochem. Cycles*, *18*, GB1024, doi:10.1029/2003GB002058.

Billett, M. F., and T. R. Moore (2008), Supersaturation and evasion of CO_2 and CH_4 in surface waters at Mer Bleue peatland, Canada, *Hydrol. Processes, 22*(12), 2044-2054, doi:10.1002/hyp.6805.

Billett, M. F., M. H. Garnett and F. Harvey (2007), UK peatland streams release old carbon dioxide to the atmosphere and young dissolved organic carbon to rivers, *Geophys. Res. Lett., 34*, doi:10.1029/2007GL031797.

Carignan, R. (1998), Automated determination of carbon dioxide, oxygen, and nitrogen partial pressures in surface waters, *Limnol. Oceanogr.*, *43*, 969-975.

Chanat, J. G., K. C. Rice, and G. M. Hornberger (2002), Consistency of patterns in concentration-discharge plots, *Water Resour. Res.*, *38*(8), 1147, doi:10.1029/2001WR000971.

Dawson, J. J. C., D. Hope, M. S. Cresser and M. F. Billett (1995), Downstream Changes in Free Carbon-Dioxide in an Upland Catchment from Northeastern Scotland, *J. Environ. Qual.*, *24*, 699-706.

Dawson, J. J. C., M. F. Billett and D. Hope (2001), Diurnal variations in the carbon chemistry of two acidic peatland streams in north-east Scotland, *Freshwat. Biol.*, *46*(10), 1309-1322, doi:10.1046/j.1365-2427.2001.00751.

Dawson, J. J. C., P. Smith (2007), Carbon losses from soil and its consequences for land-use management, *Sci. Tot. Environ.*, *382*(2-3), 165-190, doi:10.1016/j.scitotenv.2007.03.023.

Dinsmore, K. J., M. F. Billett and T. R. Moore (in press), Transfer of carbon dioxide and methane through the soil-water-atmosphere system at Mer Bleue peatland, Canada, *Hydrol. Process.*

Edwards, A. C., J. Creasey and M. S. Cresser (1984), The conditions and frequency of smapling for elucidation of transport mechanisms and element budgets in upland drainage basins, *IAHS Publ.,* No. 150, Wallingford, UK.

Edwards, A. M. C. (1973), The variation of dissolved constituents with discharge in some Norfol rivers, *J. Hydrol., 18*, 219-242.

Elsenbeer, H., A. West, M. Bonell (1994), Hydrologic pathways and stormflow hydrochemistry at South Creek, northeast Queensland, *J. Hydrol., 162*, 1-21.

Evans, C., and T. D. Davies (1998), Causes of concentration/discharge hysteresis and its potential as a tool for analysis of episode hydrochemistry, *Water Resour. Res.*, *34*(1), 129-138, doi:10.1029/97WR01881.

Gregory, K. J., and D. E. Walling (1973), *Drainage basin form and process: a geomorphological approach*, Edward Arnold Ltd, London.

Grieve, I. C. (2006), Seasonal, hydrological, and land management factors controlling dissolved organic carbon concentrations in the loch fleet catchments, Southwest Scotland, *Hydrol. Process.*, *4*(3), 231-239, doi:10.1002/hyp.3360040304.

Herczeg, A. L. and R. H. Hesslein (1984), Determination of hydrogen ion concentration in softwater lakes using carbon dioxide equilibria, *Geochim. Cosmochim. Acta, 48,* 837-845, doi:10.1016/0016-7037(84)90105-4.

Holden, J., and T. P. Burt (2003a), Runoff production in blanket peat covered catchments, *Water Resour. Res., 39*(7), doi:10.1029/2002WR001956.

Holden, J., and T. P. Burt (2003b), Hydrological studies on blanket peat: the significance of the acrotelm-catotelm model, *J. Ecol.*, *91*, 86-102, doi:10.1046/j.1365-2745.2003.00748.x.

Hope, D., J. J. C. Dawson, M. S. Cresser and M. F. Billett (1995) A method for measuring free CO_2 in upland streamwater using headspace analysis, *J. Hydrol., 166*, 1-14, doi: 10.1016/0022-1694(94)02628-O.

Hope, D., M. F. Billett and M. S. Cresser (1997) Exports of organic carbon in two river systems in NE Scotland, *J. Hydrol., 193*, 61-82, doi: 10.1016/S0022-1694(96)03150-2.

Hope, D., S. M. Palmer, M. F. Billett and J. J. C. Dawson (2001), Carbon dioxide and methane evasion from a temperate peatland stream, *Limnol. Oceanogr.*, *46*, 847-857.

Hope, D., S. M. Palmer, M. F. Billett, and J. J. C. Dawson (2004), Variations in dissolved CO2 and CH4 in a first order stream and catchment: An investigation of soil-stream linkages, *Hydrol. Process.*, *18*, 3255– 3275.

House, W. A., and M. S. Warwick (1998), Hysteresis of the solute concentration/discharge relationship on rivers during storms, *Wat. Res.*, *32*(8), 2279-2290, doi:10.1016/S0043-1354(97)00473-9.

Jarvie, H. E. P., C. Neal, R. Smart, R. Owen, D. Fraser, I. Forbes and A. Wade (2001), Use of continuous water quality records for hydrograph separation and to assess short-term variability and extremes in acidity and dissolved carbon dioxide for the River Dee, Scotland, *Sci. Tot. Environ.*, *265*(1-3), 85-97, doi:10.1016/S0048-9697(00)00651-3.

Jassal, R. S., T. A. Black, G. B. Drewitt, M. D. Novak, D. Gaumont-Guay and Z. Nesic (2004), A model of the production and transport of CO_2 in soil: predicting soil CO_2 concentrations and CO_2 efflux from a forest floor, *Agric. For. Meteorol.*, *124*, 219-236.

Johnson, M. S., J. Lehmann, E. G. Couto, J. P. N. Filho and S. J. Riha (2006), DOC and DIC in flowpaths of Amazonian headwater catchments with hydrologically contrasting soils, *Biogeochemistry*, *81*(1), 45-57, doi:10.1007/s10533-006-9029-3.

Johnson, M. S., M. Weiler, E. G. Couto, S. J. Riha, J. Lehmann (2007), Storm pulses of dissolved CO_2 in a forested headwater Amazonian stream explored using hydrograph separation, *Water. Resour. Res., 43*, doi:10.1029/2007WR006359.

Jones, J. B., and P. J. Mulholland (1998), Methane input and evasion in a hardwood forest stream: effects of subsurface flow from shallow and deep pathways, *Limnol. Oceanogr.*, *43*, 1243-1250.

Kling, G. W., G. W. Kipphut and M. C. Miller (1991), Arctic lakes and streams and gas conduits to the atmosphere: implications for tundra carbon budgets, *Science*, *251*, 298-301, doi:10.1126/science.251.4991.298.

Kling, G. W., G. W. Kipphut and M. C. Miller (1992), The Flux of CO_2 and CH_4 from Lakes and Rivers in Arctic Alaska, *Hydrobiologia*, *240*(1-3), 23-36, doi:10.1007/BF00013449.

Maberly. S. C. (1996), Diel, episodic and seasonal changes in pH and concentrations of inorganic carbon in a productive lake, *Freshwat. Biol., 35*, 579-598.

Neal, C., M. Harrow and R. J. Williams (1998), Dissolved carbon dioxide and oxygen in the River Thames: Spring-summer 1997, *Sci. Tot. Environ.*, *210-211*, 205-217, doi:10.1016/S0048-9697(98)00013-8.

Osozawa, S. and S. Hasegawa (1995), Diel and seasonal changes in carbon dioxide concentration and flux in an andosol, *Soil Sci., 160*, 117-124.

Palmer, S. M., D. Hope, M. F. Billett, J. J. C. Dawson and C. L. Bryant (2001), Sources of organic and inorganic carbon in a headwater stream: evidence from carbon isotope studies, *Biogeochemistry, 52,* 321-338, doi:10.1023/A:1006447706565.

Raymond, P. A., N. F. Caraco and J. J. Cole (1997), Carbon dioxide concentration and atmospheric flux in the Hudson river, *Estuaries*, *20*(2), 381-390, doi:10.1007/BF02690380.

Rose, S. (2003), Comparative solute-discharge hysteresis analysis for an urbanized and a control basin in the Georgia (USA) Piedmont, *J. Hydrol.*, *284*(1-4), 45-56, doi:10.1016/j.jhydrol.2003.07.001.

Stutter, M. I., S. J. Langan and R. J. Cooper (2008), Spatial contributions of diffuse inputs and within-channel processes to the form of stream water phosphorous over storm events, *J. Hydrol.*, *350*(3-4), 203-214, doi:10.1016/j.jhydrol.2007.10.045.

Tang, J., D. D. Baldocchi, Y. Qi and L. Xu (2003), Assessing soil CO_2 efflux using continuous measurements of CO_2 profiles in soils with small solid-state sensors, *Agric. For. Met.*, *118*(3-4), 207-220, doi:10.1016/S0168-1923(03)00112-6.

Townend, J. (2002), *Practical statistics for environmental and biological scientists*, John Wiley and Sons, Chichester.

Vogt, R. D., and I. P. Muniz (1997), Soil and stream water chemistry in a pristine and boggy site in mid-Norway, *Hydrobiologia*, *348*(1-3), 19-38, doi:10.1023/A:1003029031653.

Waldron, S., E. M. Scott and C. Soulsby (2007), Stable isotope analysis reveals lower-order river dissolved inorganic carbon pools are highly dynamic, *Environ. Sci. Technol., 41*, 6156-6162, doi:10.1021/es0706089 S0013-936X(07)00608-6.

8. Paper IV

Transfer of carbon dioxide and methane through the soil-water-atmosphere system at Mer Bleue peatland, Canada

Kerry J. Dinsmore, Michael F. Billett, Tim R. Moore

Published in 'Hydrological Processes', 23: 330-341 (2009)
(doi:10.1002/hyp.7158)

Transfer of carbon dioxide and methane through the soil-water-atmosphere system at Mer Bleue peatland, Canada

Kerry J. Dinsmore, Michael F. Billett, Tim R. Moore

Carbon Dioxide, Methane, Evasion, Supersaturation, Diurnal cycles

Abstract:

Surface waters associated with peatlands, supersaturated with CO_2 and CH_4 with respect to the atmosphere, act as important pathways linking a large and potentially unstable global repository of C to the atmosphere. Understanding the drivers and mechanisms which control C release from peatland systems to the atmosphere will contribute to better management and modelling of terrestrial C pools. We used non-dispersive infra-red (NDIR) CO_2 sensors to continuously measure gas concentrations in a beaver pond at Mer Bleue peatland (Canada); measurements were made between July and August 2007. Concentrations of CO_2 in the surface water (10 cm) reached 13 mg C L^{-1} (*ep*CO_2 72), and 26 mg C L^{-1} (*ep*CO_2 133) at depth (60 cm). The study also showed large diurnal fluctuations in dissolved CO_2 which ranged in amplitude from ~1.6 mg C L^{-1} at 10 cm to ~0.2 mg C L^{-1} at 60 cm depth. CH_4 concentration and supersaturation (*ep*CH_4) measured using headspace analysis, averaged 1.47 mg C L^{-1} and 3252, respectively; diurnal cycling was also evident in CH_4 concentrations. Mean estimated evasion rates of CO_2 and CH_4 over the summer period were 44.92 ± 7.86 and 0.44 ± 0.25 μg C m^{-2} s^{-1}, respectively.

Open water at Mer Bleue is a significant summer hotspot for greenhouse gas emissions within the catchment. Our results suggest that CO_2 concentrations during the summer in beaver ponds at Mer Bleue are strongly influenced by biological processes within the water column involving aquatic plants and algae (*in-situ* photosynthesis and respiration). In terms of carbon cycling soil-stream connectivity at this time of year is therefore relatively weak.

Introduction:

In the northern hemisphere peatlands are estimated to represent a sink of approximately 23 g C m^{-2} yr^{-1} (Gorham, 1991). In light of current climate change predictions, it is becoming increasingly important to both understand and quantify C fluxes in various parts of the peatland system, and to assess their stability as long-term C sinks. The availability of eddy covariance techniques allowing long term, high frequency measurements of net ecosystem exchange (NEE), have meant that many published C budgets focus primarily on soil-atmosphere uptake/emissions (Ball *et al.*, 2007; Miglietta *et al.*, 2007; Nagy *et al.*, 2007; Syed *et al.*, 2006). However, ignoring C fluxes through the aquatic pathway can lead to a significant underestimation of total catchment C loss (Figure 1) (Billett *et al.*, 2004; Hope *et al.*, 2001; Jonsson *et al.*, 2007; Richey *et al.*, 2002).

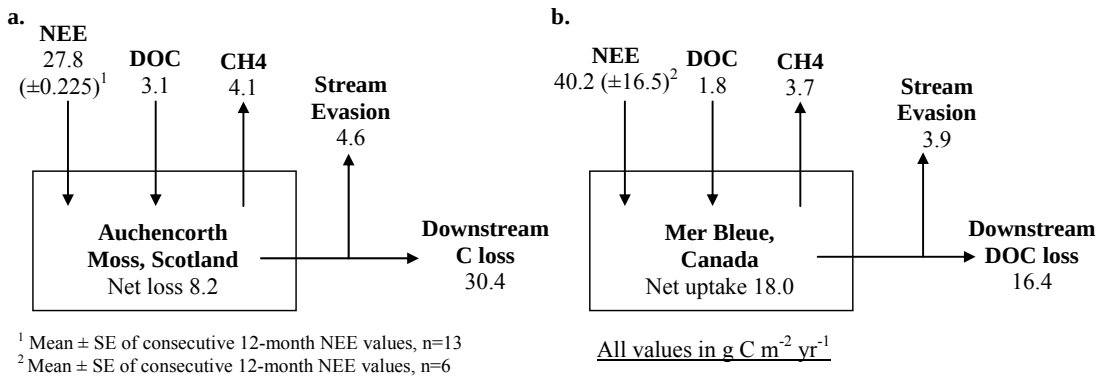

Figure 1. Carbon budgets of 2 ombrotrophic peatlands a) Auchencorth Moss, Scotland and b) Mer Bleue, Canada (Billett and Moore, 2008; Billett *et al.*, 2004; Roulet *et al.*, 2007)

In aquatic systems C is present as dissolved organic C (DOC), dissolved inorganic C (DIC), free CO_2/CH_4 or particulate organic C (POC). The dissolved gaseous forms of C are the least well understood due to the difficulty in making sufficient measurements both temporally and spatially. Both organic and inorganic forms of C can be derived from autochthonous sources attributed to biotic or abiotic production in-stream or allochthonous sources derived from elsewhere in the ecosystem and transported, most likely via water movement, into the surface drainage system. The dominant source of aquatic C varies widely between climatic zones. High CO_2 concentrations in the Amazon are thought to be primarily the result of *in situ* respiration of organic C (Mayorga *et al.*, 2005), whilst in many northern temperate

peatlands, low temperature and water pH restrict in-stream C processing, hence CO_2 is mainly allochthonous in origin (Hope *et al.*, 2004).

Many studies have found surface waters draining peatlands to be highly supersaturated in CO_2 and CH_4 with respect to the atmosphere (Billett and Moore, 2008; Dawson *et al.*, 1995; Hope *et al.*, 2001; Jones and Mulholland, 1998; Kling *et al.*, 1991; Kling *et al.*, 1992; Raymond *et al.*, 1997). This disequilibrium between water and atmospheric concentrations causes degassing (evasion). Evasion rates depend on the concentration gradient across the degassing interface, and the gas transfer coefficient and solubility of the particular gas. The solubility of any gas in fresh water is negatively correlated with temperature. Therefore under most conditions, as temperature increases, gas dissolution and hence evasion also increases (MacIntyre *et al.*, 1995). Both CO_2 and N_2O have a similar solubility in fresh water (0.039 and 0.029 mol L^{-1} atm^{-1} at 20°C respectively) (Weiss, 1974; Weiss and Price, 1980), whereas CH_4 is a relatively insoluble gas (0.0015 mol L^{-1} atm^{-1} at 20°C) and is often released to the atmosphere as bubbles (ebullition) (Wiesenburg and Guinasso, 1979). Methods which indirectly calculate CH_4 evasion may underestimate actual fluxes by ignoring bubbles which would be accounted for in direct chamber measurements (Billett and Moore, 2008).

Studies aimed at quantifying fluxes to the atmosphere have previously had to rely on a relatively small number of isolated concentration or flux measurements to calculate long-term evasion rates (Billett and Moore, 2008; Frankignoulle *et al.*, 1998; Hope *et al.*, 2001; Jones and Mulholland, 1998; Kling *et al.*, 1991). These are unable to capture diurnal, daily and in many cases weekly variability in concentrations due to the physical limitations of having to manually collect spot samples. In this study we use submerged non-dispersive infra-red (NDIR) CO_2 sensors to make continuous summer concentration measurements giving much better temporal resolution.

This study aims to contribute to our understanding of CO_2 and CH_4 dynamics in peatlands based on the hypothesis that the aquatic system plays a major role in greenhouse gas (GHG) release. Specifically we aim to a) study small-scale variability in dissolved CO_2 and CH_4 concentrations at a diurnal rather than seasonal

timescale, b) relate cycles in the water column to cycles elsewhere in the peatland ecosystem and in doing so understand what drives variability, and c) estimate the importance of summer time evasion to both the C and the GHG budget of the catchment as a whole.

Site Characteristics:

Mer Bleue peatland (45.40 °N, 75.50 °E) is located approximately 10 km east of Ottawa, Ontario, and is the site of the Eastern Peatland flux station for Fluxnet Canada (http://www.fluxnet-canada.ca, 2008). Mer Bleue contains an ombrotrophic raised bog with an average elevation of 69 m a.s.l. The bog, which formed *circa* 6000 years BP succeeding a fen formed *circa* 8500 years BP, covers approximately 2800 ha. Peat depth ranges from 1-2 m near the edges to 5-6 m near the centre, underlain by continuous marine clay deposits (Billett and Moore, 2008). The bog surface has a typical hummock-hollow microtopography covered in vascular ericaceous (*Chamaedaphne calyculata, Ledum groenlandicum, Kalmia augustifolia*) and deciduous shrubs (*Vaccinium myrtilloides*) and sedges (*Eriophorum vaginatum*), with an understorey of *Sphagnum* mosses. Trees such as *Picea mariana*, *Larix laricina* and *Betula populifolia* occur in patches across the peatland. The margin of the peatland, where it abuts gravel and sand ridges, comprises open-water beaver ponds, with inundated transition zones of *Typha latifolia* and floating mats of mosses and sedges leading into the bog.

A series of raised peat domes has lead to the formation of 3 distinct drainage 'fingers', which drain the peatland from east to west into the Ottawa river valley with a gradient of approximately 0.0008 (Billett and Moore, 2008). Unlike the spring and autumn periods, during the summer months ground and surface water flow is slow through the centre of the bog moving into a low-energy continuous network of beaver dams at the perimeter.

The climate of the region is defined as mid-continental cool. Mean annual temperature and precipitation are 5.8°C and 910 mm respectively and the growing season lasts from May to September. During the period of this study (July and August 2007) mean temperature was 19.8ºC, compared to a 29 yr (July/August)

average of 20.2ºC; total precipitation over the 2 months was 256 mm compared to a 29 yr average of 178 mm (http://www.climate.weatheroffice.ec.gc.ca, 2008). The precipitation: runoff ratio is 0.4 with more than 55% of annual runoff occurring during spring snowmelt (Roulet *et al.*, 2007).

Materials and Methods

A combination of continuous and single point measurements were made throughout July and August 2007 in open water and at 3 locations at the bog-pool interface (Figure 2). Data collected from a flux tower site located approximately 250 m from the pond, was also used to aid interpretation of the beaver pond data (Humphreys, unpublished data).

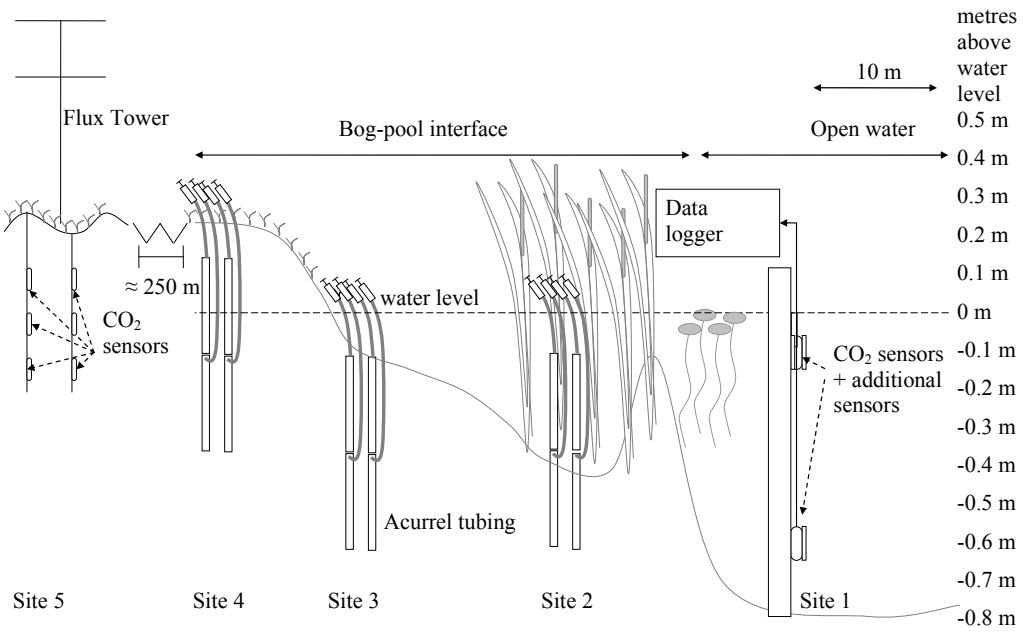

Figure 2 Schematic of sampling setup. Site 1 is referred to in the text as the open water/pond site; sites 2-4 are described as the bog-pool interface; site 5 is approximately 250 m from the pond and is referred to as the flux tower site (not to scale)

Field measurements

At the open water site (site 1, Figure 2) continuous measurements of dissolved CO_2 were made using 2 Vaisala CARBOCAP® (transmitter series, GMT220), non-dispersive infra-red absorption (NDIR) CO_2 sensors. The sensors were enclosed within water tight, gas permeable membranes and connected to a Campbell Scientific CR1000 datalogger (Johnson *et al.*, 2006). The sensors were installed at the site at

the beginning of July 2007 and ran until the end of August 2007. Sensors were placed at depths of 10 cm and 60 cm below the water surface. For 2 weeks during August 2007 CO_2 concentrations were measured using a third sensor, held approximately 10 cm above the water surface. Additional sensors were used to measure water depth (PDCR 1830 series pressure transducer), temperature at 60 cm depth (CS 108), and conductivity, temperature (CS547A) and pH (CSIM11) at 10 cm depth. Measurements were made once per minute with 10 minute averages recorded.

In addition to the continuous measurements at the open water site, single spot measurements of CO_2, CH_4 and N_2O concentrations at 10 cm and 60 cm depths were made using the headspace technique (Billett and Moore, 2008; Billett *et al.*, 2004; Hope *et al.*, 2001; Kling *et al.*, 1991). A 20 ml sample of pond water was equilibrated with 20 ml of gas standard (CO_2 380 ppm, CH_4 0 ppm, N_2O 0 ppm) by shaking under water for 1 minute; the headspace was then transferred to gas-tight syringes and transported back to the laboratory for analysis. To investigate gas concentration gradients within the water column, headspace measurements were made on 4 separate occasions at incremental 10 cm intervals throughout the water profile. Water samples were collected at the same time as the headspace measurements for analysis of DOC. Spot measurements were made weekly between July-August and every other day between 26th July and the 6th August. In addition, hourly samples were collected between 13:00 h 30th July and 12:00 h 31st July to investigate diurnal variation.

Along the bog-pool interface (sites 2-4, Figure 2) soil atmosphere wells were installed, and spot samples collected at the same frequency as samples in the open water site. The soil-atmosphere wells consisted of water tight, gas permeable tubing (ACCUREL® PP V8/2 HF) inserted into the soil at 2 different depths (10-50 cm and 50-90 cm), and in replicates of 2.

Data utilised from the Flux tower site (site 5, Figure 2) included NEE, meteorological data, soil temperature and soil CO_2 concentration. Soil CO_2 was measured *in situ*, using a total of 5 NDIR CO_2 sensors, 3 installed above the water table at depths of 5, 10 and 20 cm below a hummock and 2 at depths of 5 and 10 cm

in a hollow (Roulet, unpublished data). Soil temperature was measured adjacent to each CO_2 sensor. For the purpose of this study, an average CO_2 concentration and average soil temperature is calculated from all 5 sensors. Measurements were made once per minute and a half hourly average recorded.

Short-wave radiation was recorded at the flux tower as part of the meteorological dataset. Radiation entering the water column was estimated as total short-wave radiation minus surface reflectance calculated using the Fresnel equations (Kirk, 1983).

Analytical methods

CO_2 concentrations from the headspace samples and soil atmosphere wells were determined using a Shimadzu Mini-2 gas chromatograph (GC) with a flame ionisation detector (FID) and methanizer (99% reduction efficiency). A separate Shimadzu GC with FID was used to measure CH_4; column and detector temperatures for the two GCs were 45 and 100°C, respectively. N_2O concentrations were determined on a Shimadzu 14-A GC using an electron capture detector (ECD). Ultra high purity N_2 was used as the carrier gas for the 14-A GC with column and detector temperatures of 50°C and 315°C, respectively. Coefficients of variation and detection limits for the GCs were: CO_2 1-3% and 15 ppm, CH_4 1-3% and 0.3 ppm, and N_2O 1-5% and 0.2 ppm. Gas concentrations are expressed in units of partial pressure (pCO_2, pCH_4 and pN_2O), mg L^{-1} or excess partial pressure ($epCO_2$, $epCH_4$ and epN_2O), defined as the partial pressure of gas in solution divided by the partial pressure of the gas in equilibrium with the atmosphere. Continuous concentrations of atmospheric CO_2 were modelled by fitting a sine wave function to the data collected using the third NDIR sensor located 10 cm above the pond surface. Parameter values for the amplitude, height and offset of the sine function were determined by minimising the sum of squared differences using the Excel Solver program. Samples of ambient air were collected and analysed alongside headspace samples, and these values used in the subsequent calculation of gas concentrations using Henry's Law for the spot samples.

Water samples were analysed for DOC on a Shimadzu TOC-VCsn analyzer using high-temperature (720°C) catalytic oxidation and measurement with a NDIR detector. Ultra-Zero Air was used as both carrier and reference gas. The coefficient of variation in detection accuracy was ~3-5%.

Calculation of evasion

To avoid systematic error in the sensor reading, the volume fraction output of the NDIR sensors was corrected for variations in temperature and pressure. The reference temperature and pressure for the sensors were 22.5ºC ± 1% and 100.7 kPa ± 1% respectively. Concentrations were corrected using the method described in Tang *et al.* (2003).

Evasion from the water surface was calculated indirectly using wind speed to predict gas transfer velocity, combined with the partial pressure difference across the air-water interface. The method is based on established relationships between wind speed and gas transfer velocity (MacIntyre *et al.*, 1995; Wanninkhof, 1992). The equation used to calculate gas fluxes ($FCO_2/FCH_4/FN_2O$) is described below for CO_2 (Equation 1) (Billett and Moore, 2008; Borges *et al.*, 2004), where k is the gas transfer velocity (cm hr^{-1}), α is the solubility coefficient and ΔpCO_2 is the difference in partial pressure between the surface water and the atmosphere. The solubility coefficient (α) is temperature and salinity dependent. Values of α for CO_2, CH_4 and N_2O were derived from Weiss (1974), Wiesenburg and Guinasso (1979), and Weiss and Price (1980), respectively.

The transfer velocity (k) is a function of turbulence, the kinematic viscosity of the water, and the molecular diffusion coefficient of the gas. In equation 2 (MacIntyre *et al.*, 1995) wind speed (m s^{-1}) at 10 m above the water surface (u_{10}) is used to describe turbulence, and the Schmidt number (Sc) is a function of the latter 2 terms. The equation is derived from a least squares power law fit through the results of lake experiments using SF_6 as a deliberate tracer. $k(600)$ refers to the transfer velocity normalised to $Sc = 600$, the Schmidt number of CO_2 at 20°C in freshwater. Values

of Sc used in equation 2 for CO_2, CH_4 and N_2O are taken from MacIntyre *et al.* (1995).

Wind speed at 10 m (u_{10}) is calculated using the semi-empirical log wind profile relationship shown in equation 3 with the assumption of atmospheric stability (Monteith and Unsworth, 1990). Friction velocity (u_*) was measured at the flux tower site (site 5, Figure 2). k describes the von Karman's constant (0.41), d is the zero plane displacement calculated as 0.65 times the height of the roughness elements (0.2 m) and z_0 is the surface roughness calculated as 0.077 for Mer Bleue (Lafleur *et al.*, 2005). It is assumed that the wind speed at 10 m above the flux tower is representative of wind speed above the open water site. Laboratory measurements of CO_2 flux suggest that k becomes independent of u_{10} at low wind speeds (Ocampo-Torres *et al.*, 1994). MacIntyre *et al.* (1995) therefore suggest using a u_{10} value of 1.5 m s^{-1} for all values of equal to or less than 1.5 m s^{-1}.

$$FCO_2 = k\alpha\Delta pCO_2 \qquad \text{Equation 1}$$

$$k(600) = 0.45u_{10}^{1.6}(Sc/600)^{-0.5} \qquad \text{Equation 2}$$

$$u_z = \frac{u_*}{k}\ln\left(\frac{z-d}{z_0}\right) \qquad \text{Equation 3}$$

Statistical analysis

Datasets with measurement frequencies of less than 1 hour were treated as time series and suitable statistical methods applied (see below). No significant autocorrelation was found in datasets with measurement frequencies of 1 hour or more. As part of the exploratory analysis into the CO_2 cycles, time series datasets were adjusted, where necessary, for autocorrelation and seasonality (in this case diurnal fluctuations) using autoregression (up to order 2) and a cosine wave function. The adjusted data sets were then compared using cross-correlation analysis to establish maximum correlation lag times. The direction of the lag was used to

eliminate variables that followed CO_2 concentrations, so that only variables presumed to have a causal correlation to CO_2 were included in subsequent models. Relationships between water column and soil CO_2 concentrations, and water column CO_2 and CH_4 concentrations with various independent variables, were modelled using stepwise regression with the inclusion of an autocorrelation term (< order 2) where appropriate. Both forward and backward selection stepwise regressions were performed and compared to aid selection of the most appropriate explanatory model. Where average values are quoted the ± refers to 95% confidence intervals unless stated otherwise. In datasets which display significant autocorrelation and hence the assumption of independence is not met, standard errors and t-statistics are calculated using the effective rather than the real sample size.

Results

Comparison of pCO_2 headspace and NDIR values

The pCO_2 values calculated from the headspace measurements were compared to the corresponding 10-minute mean pCO_2 values calculated using the NDIR sensor. The results were then compared using a paired t-test with a 95% confidence limit. Mean pCO_2 at 10 cm was 11786 ± 4838 µatm and 17323 ± 1450 µatm measured using the headspace and NDIR methods, respectively. Despite headspace measurements averaging ~30% less than NDIR measurements, due to the high variability in the headspace samples the difference was not statistically significant ($t = 1.89$, $p = 0.09$, $n = 13$). Concentrations at 70 cm were significantly different with mean headspace and NDIR pCO_2 values of 17371 ± 1681 and 50137 ± 211 µatm respectively ($t = 40.2$, $p < 0.01$, $n = 11$). A more detailed comparison between measurement methods is discussed in Johnson *et al.* (manuscript in preparation for Limnology and Oceanography: Methods).

To quantify the bias introduced by collecting headspace samples only during daylight hours, and to assess the importance of sampling frequency, a series of manipulations were carried out on the NDIR dataset. One $epCO_2$ value was randomly selected from the continuous NDIR dataset for each day between 09:00 h and 17:00 h, and a mean July and August $epCO_2$ value calculated. This process was repeated to simulate

measurement frequencies of twice weekly, weekly and fortnightly. The process was repeated until 10 mean July and August *ep*CO_2 values were calculated for each measurement frequency. The results were then compared to the mean July and August *ep*CO_2 calculated from the full continuous dataset. Across all measurement frequencies, the mean overestimation in *ep*CO_2 caused by daytime sampling was approximately 3.5%. Although the magnitude of the mean did not change with sampling frequency, the width of the confidence intervals increased significantly as sampling frequency decreased.

July and August concentrations

During July and August 2007, *p*CO_2 concentrations at 10 cm, measured continuously using the NDIR sensors, ranged from 10472 µatm ([C] = 5.01 mg L^{-1}) to 26616 µatm ([C] = 14.2 mg L^{-1}) with a mean of 16268 ± 1700 µatm ([C] = 7.64 ± 0.80 mg L^{-1}). This corresponds to *ep*CO_2 values of between 28.2 and 71.5, with a mean of 43.6 ± 4.60. From the headspace spot samples over the same period, mean *p*CO_2 concentration was 11786 ± 4838 µatm ([C] = 5.38 ± 2.21 mg L^{-1}) (n = 13) corresponding to an *ep*CO_2 of 31.5 ± 12.9. Deep water CO_2 concentrations were around 3 times greater than surface water concentrations. *p*CO_2 concentrations ranged from 49286 µatm to 51420 µatm ([C] = 23.3 to 25.1 mg L^{-1}) with a mean of 49946 ± 165 µatm ([C] = 23.9 ± 0.22 mg L^{-1}). The mean *ep*CO_2 value at 60 cm was 128 ± 0.31.

pCH_4 over the summer period (n = 13) ranged from 249 µatm ([C] = 0.1 mg L^{-1}) to 7795 µatm ([C] = 3.7 mg L^{-1}) with a mean of 3210 ± 1002 µatm ([C] = 1.5 ± 0.5 mg L^{-1}). *ep*CH_4 reached a maximum of 7795, with a mean of 3252 ± 1589. Similar to CO_2, deep water CH_4 concentrations were approximately 3 times greater than surface water concentrations with a mean pCH_4 at 60 cm of 10669 ± 6252 µatm ([C] = 5.21 ± 3.30 mg L^{-1}) and *ep*CH_4 8937 ± 3900. N_2O concentrations in the water column were very low and no significant difference was observed between the 2 measured depths. Mean pN_2O (n = 9) for the summer was 0.66 ± 0.43 µatm. The mean *ep*N_2O was 1.68 ± 1.63; on 2 of the 9 sampling occasions water column N_2O concentrations were below atmospheric concentrations. The mean DOC concentration in the open

water over July and August was 113 ± 4.80 mg L^{-1}. Individual values ranged from 67.1 to 125 mg L^{-1}.

The results from the depth profile measurements in the open water for CO_2, CH_4 and N_2O (Figure 3), showed that on 3 out of 4 sampling occasions CO_2 concentrations increased with depth, with a pronounced increase at a depth of 40 cm. On both the 6th and 9th of August, a peak was also observed at 30 cm. Similar to the CO_2 profiles, on 3 out of 4 sampling occasions, CH_4 concentrations showed a dramatic increase at approximately 40 cm depth. No clear pattern was evident in the N_2O profiles.

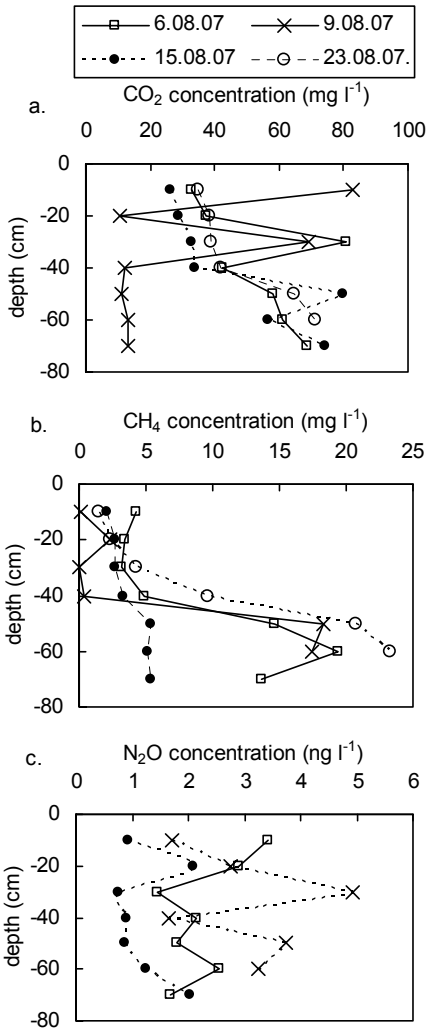

Figure 3 Concentration profiles of (a) CO_2-C, (b) CH_4-C and (c) N_2O-N through the water column on separate sampling occasions. Note the different units used to express N_2O concentrations

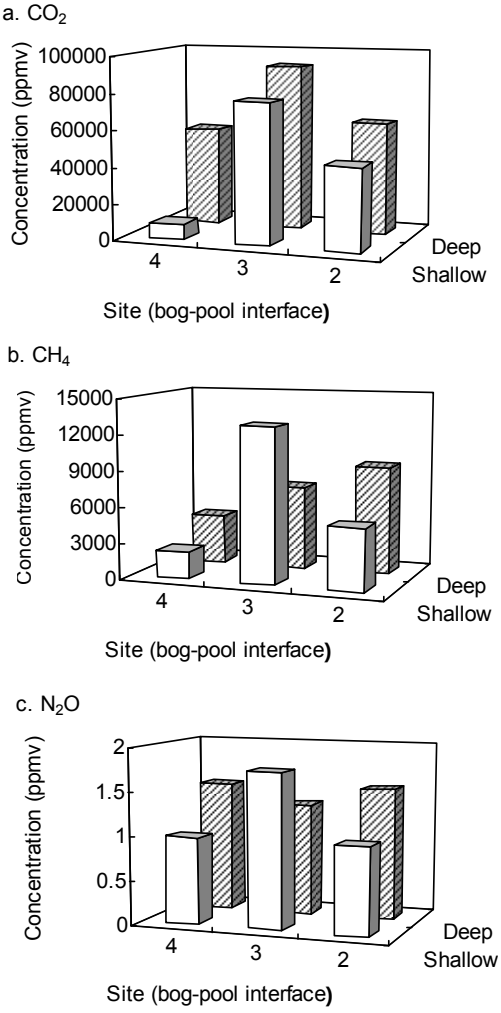

Figure 4 Concentrations (ppmv) of (a) CO_2, (b) CH_4 and (c) N_2O measured in the soil atmosphere wells at 2 depths at sites 2-4 at the bog-pool interface. Shallow and deep refer to wells at 10-50 cm and 50-90 cm depths respectively

Soil CO_2 concentrations measured using NDIR sensors installed at the flux tower site (site 5, Figure 2), ranged from 161 to 2032 ppmv with a mean of 885 ± 103 ppmv. Measurements made by manually sampling the soil atmosphere wells at the bog-pool interface showed significantly higher concentrations. The mean soil atmosphere CO_2 concentration ranged from approximately 8418 ppmv in the site 4 shallow well to >90000 ppmv in the site 3 deep well (Figure 4). In general, CO_2 concentrations in the soil atmosphere wells appeared to be higher in the deep (50-90 cm) wells than in the shallow wells (10-50 cm) (Figure 4a). Mean summer CH_4 concentrations ranged from 2279 ± 667 ppmv in the site 4 shallow well to 7052 ± 909 ppmv in the deep well at site 3 (Figure 4b). The mean N_2O concentration across all wells was 1.33 ± 0.32 ppmv (Figure 4c). For both CH_4 and N_2O, mean concentration at sites 1 and 3 were highest in the deep wells, with the opposite true of site 2. To test the significance of these observed patterns, a 2-way ANOVA was carried out on log-transformed concentrations of each gas using depth and site as independent variables. For both CO_2 and CH_4 concentrations site was the only significant variable at the 95% confidence limit (CO_2: $F = 5.22$, $p = 0.01$; CH_4: $F = 4.50$, $p = 0.02$). Neither site nor depth had a significant effect on N_2O concentration

Diurnal cycles

From the continuous CO_2 measurements in the open water (site 1, Figure 2), clear diurnal cycles were evident in both the surface and deep water concentrations (Figure 5 a and b). Concentrations of CO_2 in the surface water had a diurnal range of approximately 3136 ppmv. Deep water CO_2 cycles were much steadier and more consistent, with a diurnal range ~1 order of magnitude lower than the surface (320 ppmv). Peak CO_2 concentration in deep water was at 16:00 h with a minimum concentration at approximately 06:00 h. Near-surface water concentrations often showed 2 distinct daytime peaks at approximately 10:00 h and 19:00 h with the minimum occurring during darkness at approximately 02:00 h (Figure 5a). The soil CO_2 concentrations also showed a diurnal pattern, but unlike water concentrations, the peak occurred at around midnight with the minimum at approximately 13:00 h (Figure 5c).

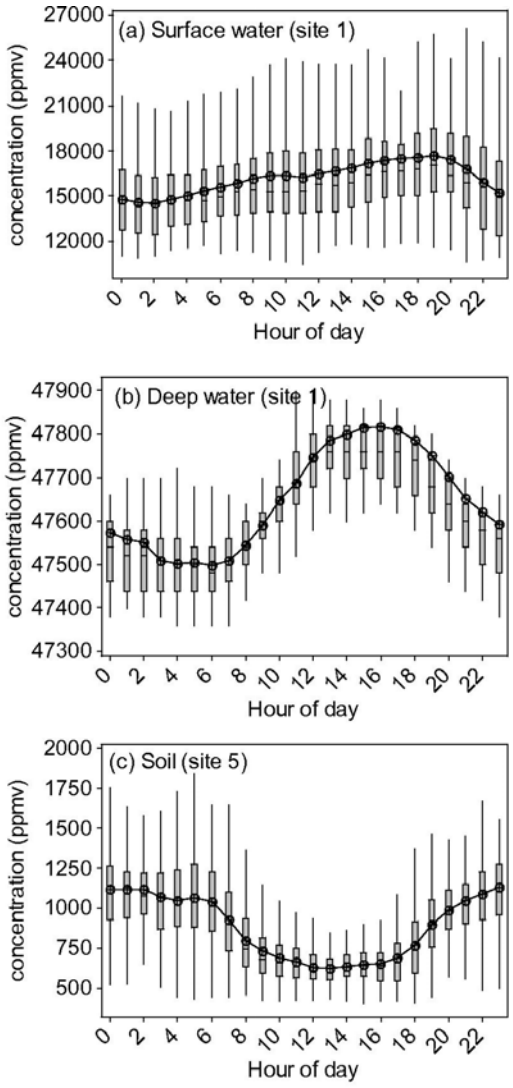

Figure 5 Boxplots illustrating diurnal variation in a) surface water, b) deep water and c) adjacent peat (ppmv CO_2) during July and August 2007

From the 24 hour spot sampling regime, a diurnal pattern was found in the surface water CH_4 concentrations (Figure 6) with minimum values between 00:00 and 04:00. The pattern of near surface CO_2 concentrations was consistent with that observed from the NDIR sensors, minimum CO_2 concentrations were between approximately 00:00 h and 03:00 h. A weak diurnal pattern was also found in the DOC concentrations with the peak concentration occurring at approximately 05:00 h (Figure 6). No diurnal pattern was visible in either deep water CH_4 concentrations or water column N_2O concentrations.

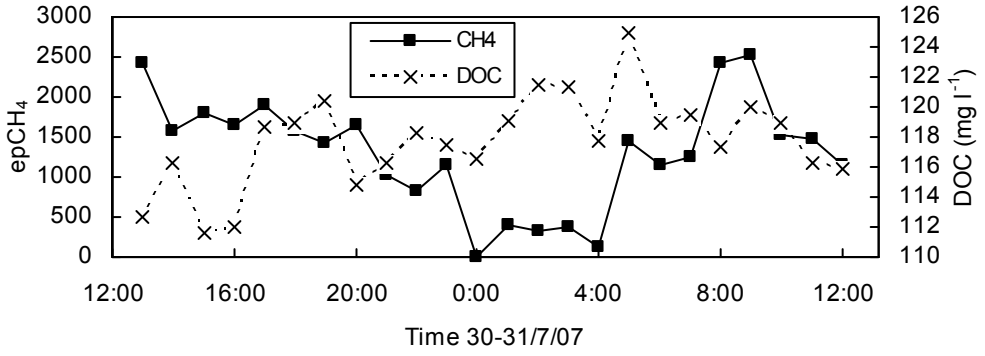

Figure 6 Diurnal variation in surface water (~10 cm) CH_4 and DOC concentrations, calculated using hourly headspace and water samples from 13:00 h on 30th July to 12:00 h on 31st July 2007

Drivers of cycles

To gain a better understanding of what drives aquatic cycles of CO_2, concentrations were compared to other cycles within the peatland ecosystem. Figure 7 shows the cycles of surface water, soil and air CO_2 concentrations over a 4-day period. It is clear that although the cycles were similar, particularly between the soil and surface water where the double peaks described earlier can be seen, there was a lag in the system. After correcting for autocorrelation and seasonality, cross-correlation analyses were carried out between surface water, deep water and soil CO_2 concentrations and against other explanatory variables. Explanatory variables included air and soil temperature, air pressure, surface and deep water temperature, short-wave radiation, short-wave radiation adjusted for surface reflectance, wind speed, 24, 48 and 72 hour antecedent rainfall, water depth, pH and conductivity.

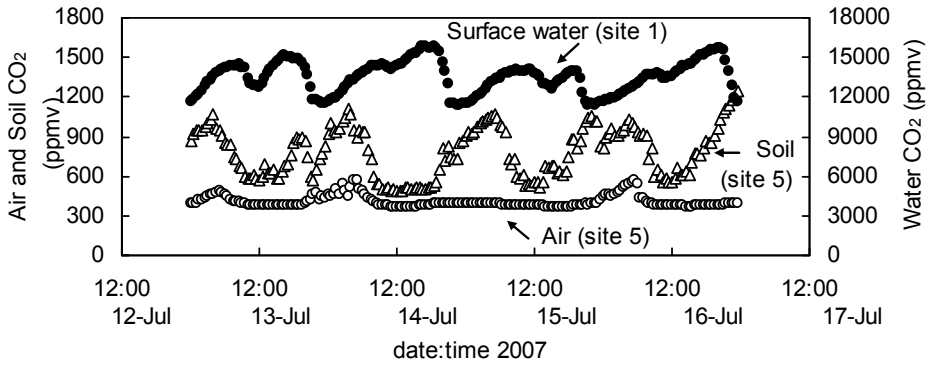

Figure 7 Continuous CO_2 concentrations in soil, air and surface water over a 4 day period illustrating lag in CO_2 cycles. Note separate axis for surface water concentrations

Significant correlation peaks for surface water CO_2 concentration (site 1, Figure 2) with soil concentration (site 5, Figure 2) occurred at lags of -4.5, -32.0 and -40.5 hours. The negative sign indicates that soil concentrations lag behind water concentrations. No significant correlation peaks were identified between deep water and soil CO_2 concentrations.

Where significant positive lags were found for concentration against an explanatory variable, the data set was adjusted before further analysis was carried out. Where significant negative lags were found, as for surface water CO_2 versus conductivity (lag = -4.5 hours), the variable was omitted from further calculations. Variables which could potentially drive CO_2 cycles were therefore separated and modelled independently from variables responding to CO_2 changes.

The remaining variables along with autocorrelation terms of up to order 2 were then used to model CO_2 concentrations with stepwise regression (Table 1). The best model for surface water CO_2 concentration included autocorrelation factors up to order 2, positive coefficients for short-wave variation and air temperature, and negative coefficients for adjusted short-wave radiation and surface water temperature (r^2 = 0.97). Deep water concentrations could be modelled (r^2 = 0.98) using short-wave radiation as the only independent variable.

Table 1 Results from stepwise regression on July and August CO_2 concentrations. Water CO_2 concentrations are expressed in units of mg L^{-1}, soil concentrations are in volume fractions (ppmv).

Dependent variable	Independent variables	Lag (hr)	Coefficient	T	P
(a) Surface water	Intercept	-----	$4.6 * 10^{-2}$	3.51	<0.01
(total r2=0. 97)	Autoregressive term (1º)	-----	1.64	66.8	<0.01
	Autoregressive term (2º)	-----	-0.66	-21.7	<0.01
	Short-wave radiation	3.5	$7.2 * 10^{-5}$	3.7	<0.01
	Air temperature	0	$1.1 * 10^{-4}$	3.2	<0.01
	Adjusted short-wave radiation	3.5	$-1.5 * 10^{-4}$	-2.7	0.01
	Surface water temperature	4.5	$1.5 * 10^{-3}$	-2.7	0.01
(b) Deep water	Intercept	-----	0.39	2.11	0.04
(total r2=0. 97)	Autoregressive term (1º)	-----	0.99	211.1	<0.01
	Short-wave radiation	0	$7.5 * 10^{-5}$	2.4	0.02

Stepwise regression was also used to model CH_4 concentrations from 10 cm and 60 cm depths (Table 2) with the addition of DOC as an independent variable. Autoregressive terms were not included as no significant autocorrelation was found in the CH_4 dataset. Concentrations throughout July and August could be modelled using the variables 24-hour antecedent rainfall and adjusted shortwave radiation (r^2 = 0.73). Diurnal CH_4 concentrations in the surface water from 30th to 31st July were modelled using both surface and deep water temperature (r^2 = 0.78). Using the complete dataset both summer and diurnal variation in CH_4 could be modelled from rainfall, radiation and adjusted radiation with r^2 = 0.63.

Table 2 Results from stepwise regression on July and August CH_4 concentrations. Water CH_4 concentrations are expressed in units of mg L^{-1}, soil concentrations are in volume fractions (ppmv).

Dependent variable	Independent variables	Coefficient	T	P
(a) Surface water CH_4				
July/August dataset	Intercept	-0.2518	-0.32	0.76
(total r^2= 0.73)	Antecedent rainfall (24hr)	0.30	4.20	<0.01
	Adjusted short-wave radiation	0.0064	2.24	0.05
Hourly dataset	Intercept	-226	-3.72	<0.01
(total r^2= 0.78)	Temperature (surface water)	-0.83	-6.11	<0.01
	Temperature (deep water)	13.61	3.96	<0.01
Full dataset	Intercept	0.70	4.77	<0.01
(total r^2= 0.63)	Antecedent rainfall (24hr)	0.25	4.73	<0.01
	Short-wave radiation	0.0032	2.97	<0.01
	Adjusted short-wave radiation	-0.0061	-1.98	0.05
(b) Deep water CH_4				
July/August dataset	Intercept	1159		
(total r^2= 0.66)	Deep water CO_2	-113	-1.97	0.09
	Water depth	-84	-1.97	0.09
Hourly dataset	Intercept	-285.4		
(total r^2= 0.23)	Temperature (deep water)	16.1	2.78	0.01

Evasion from water surface

Mean instantaneous CO_2 evasion from the water surface, calculated from the continuous NDIR sensor data over the summer period, was 165 ± 28.8 μg m^{-2} s^{-1} (Table 3). From the spot headspace measurements, mean CO_2 evasion was 86.2 ±

52.1 μg m^{-2} s^{-1}. These correspond to C losses of 44.9 ± 7.86 μg C m^{-2} s^{-1} and 23.7 ± 14.2 μg C m^{-2} s^{-1}, respectively. As direct measurements of CH_4 could not be made continuously, concentrations were predicted at half hourly intervals for the whole 2 months using the full dataset model and environmental variables measured continuously during July and August. Using these modelled values, the mean summer instantaneous CH_4 evasion rate from the water surface was 0.59 μg m^{-2} s^{-1}. The standard error in the evasion calculations as a result of the modelled CH_4 concentrations equates to ± 0.09 μg m^{-2} s^{-1}. This value in addition to the 95% confidence interval of the mean evasion rate (± 0.33) gives a total standard error in the summer CH_4 flux of ± 0.42 μg m^{-2} s^{-1}. Using only the spot sampled headspace measurements, the mean instantaneous CH_4 flux is calculated as 0.35 ± 0.20 μg m^{-2} s^{-1}. These values correspond to instantaneous C losses of 0.44 ± 0.25 μg C m^{-2} s^{-1} and 0.26 ± 0.15 μg C m^{-2} s^{-1} for the modelled and headspace methods, respectively.

Table 3 Annual (in terms of total catchment budget) and instantaneous (from water surface) exchange of carbon and GHGs using different measurement techniques. Error terms represent standard error of the mean unless otherwise stated

	Method	Global warming potential (CO_2-eq)		Carbon loss	
		mean instantaneous flux (water surface)	monthly summer catchment flux	mean instantaneous flux (water surface)	monthly summer catchment flux
		μg m^{-2} s^{-1}	g m^{-2} $month^{-1}$	μg m^{-2} s^{-1}	g m^{-2} $month^{-1}$
Water surface Evasion					
CO_2	NDIR	164.71 ± 28.3	2.17 ± 0.37	44.92 ± 7.86	0.59 ± 0.10
	Headspace	86.23 ± 52.1	1.14 ± 0.69	23.68 ± 14.22	0.31 ± 0.19
CH_4	Modelled	14.71 ± 8.29	0.19 ± 0.11	0.44 ± 0.25	0.006 ± 0.004
	Headspace	8.12 ± 4.64	0.11 ± 0.06	0.26 ± 0.13	0.003 ± 0.002
N_2O	Headspace	0.32 ± 0.35	0.004 ± 0.004	-------	-------
Vegetated surface					
CO_2	Eddy Covariance[a]	-------	-15.3	-------	-4.17
CH_4	Static chambers[b]	-------	19.2 ± 2.60	-------	0.63 ± 0.08

[a] Values based on six year mean of summer values in Figure 6 from Roulet *et al.* (2007)
[b] Values based on six year annual mean ± standard deviation from Roulet *et al.* (2007) accounting for assumed emission period of 180 days

Discussion

GHG concentrations in the aquatic system

Surface waters at Mer Bleue were consistently and highly supersaturated in CO_2 and CH_4 with respect to the atmosphere. The mean summer CO_2 concentration measured using the headspace technique (pCO_2 = 11786 ± 4838 µatm) was just over 70% of that calculated from the NDIR sensors (pCO_2 = 16268 ± 1700 µatm). However, considering the large confidence intervals associated with both measurements, this difference is not statistically significant. The depth profile experiments showed significant stratification in CO_2 concentrations (Figure 3), with concentrations increasing with depth. Although every effort was made to minimize mixing within the water column during sampling, a degree of mixing is inevitable and may have caused an increase in variation and decrease in the magnitude of the headspace CO_2 concentrations. Mixing within the water column is likely to be greater when headspace samples are collected from depth. This may also partly explain the much larger discrepancy between measurement methods at 60 cm. A similar method comparison was carried out using data collected from the Black Burn, a small peatland draining stream in south east Scotland (Dinsmore, unpublished data). Mean pCO_2 concentrations measured using the 2 different methods in the Black Burn were much more similar than those from Mer Bleue (Headspace: 4330 ± 468 µatm; NDIR: 4007 ± 326 µatm). The Black Burn is a shallow, turbulent stream with a well mixed water column; water disturbance during manual sampling is therefore unlikely to affect measured pCO_2 concentrations. This adds further support to the suggestion that the large differences observed between the 2 measurement methods at Mer Bleue is primarily due to disturbance within the water column during headspace sampling.

The method comparison also suggested that the influence of daytime sampling could lead to a ~3.5% overestimation in the mean headspace concentration. From the direct method comparison, headspace concentrations at 10 cm depth were approximately 30% less than NDIR concentrations. The discrepancy in the July and August means

is therefore likely to be due primarily to differences in measurement method rather than differences in sampling frequency.

A similar study carried out by Billett and Moore (2008) using a small number of headspace spot samples found a mean *ep*CO_2 value of 24.1 ± 10.9 (n=3) at the same pond site between July and August 2005 (Billett, unpublished data). This is within the 95% confidence limits of the mean *ep*CO_2 calculated from headspace measurements in this study (31.5 ± 12.9). Since 2005 when Billett and Moore carried out their study, water levels have dropped allowing wetland vegetation to encroach on the pond. As water levels rose again due to beaver activity the vegetation became immersed. By the summer of 2007 when this study was carried out, the pond contained much more plant and algal life than in 2005. The increase in plant and algal respiration is likely to be the primary cause of the higher dissolved CO_2 levels found in 2007. In the same study by Billett and Moore (2008), mean *ep*CH_4 between July and August 2005 was 1310 ± 2732 (n = 3), compared to 3210 ± 1589 in July and August 2007 (this study). Again, as seen from the overlapping confidence intervals, variation was high and the difference in *ep*CH_4 between 2005 and 2007 was not statistically significant.

Controls on aquatic GHG concentrations

A number of studies have suggested that dissolved CO_2 in aquatic systems is allochthonous in nature, produced within the soil system and transported via ground water or through-flow to surface water courses (Hope *et al.*, 1997; Kling *et al.*, 1991; Palmer *et al.*, 2001; Worrall *et al.*, 2005). In the cross-correlation analyses, soil concentrations were seen to lag behind water concentrations indicating that it is unlikely CO_2 produced in the adjacent peat is influencing concentrations in the water column. It is more likely that the correlation between soil and water column concentrations is the result of a common driving variable e.g. temperature which was seen to be important in driving surface water cycles (Table 1). The observed lag might then be explained by the different thermal properties of soil and water.

The key drivers of aquatic CO_2 cycles in surface water at Mer Bleue during this study appeared to be short-wave radiation, adjusted shortwave radiation and both air

and surface water temperature. These factors suggest a biological control on concentrations through aquatic plants or algae, both of which were visibly plentiful in the pond. The influence of aquatic plant and algae is once again seen in the shape of the diurnal cycles. The double peaks seen in the surface waters were absent in the deep water cycles where light does not penetrate, and are likely to result from high photosynthetic rates during peak daylight hours. We hypothesize that CO_2 is produced by both autotrophic and heterotrophic respiration, similar to findings from studies on the Amazon basin (Mayorga *et al.*, 2005; Richey *et al.*, 2002). Considering the low soil-water connectivity at Mer Bleue, it is likely that autochthonous DOC forms the primary substrate for CO_2 production, making this system comparable to many northern lake systems (Karlsson *et al.*, 2007). During higher flow periods, such as snow melt, the C dynamics are likely to change significantly to more closely resemble the functioning of river ecosystems with dissolved CO_2 being flushed into the water course from adjacent peat. Hence the system may be dynamic, with seasonal variation in the form of the ecosystem functioning reflected in the sources of CO_2 and DOC. Longer term measurements are needed to test this hypothesis.

Diurnal variation in CH_4 concentrations during this study appeared to be driven primarily by the temperature cycle. The longer term summer dataset responded to both short-wave radiation in the water column and rainfall. As with the CO_2, CH_4 concentrations showed significant stratification in the water column with higher concentrations below approximately 40 cm. Although not statistically significant, on a number of occasions a drop in the CH_4 concentration in the soil atmosphere wells can be seen to coincide with a rainfall event, especially at site 2 on the edge of the pond. The increased flow of water during rainfall may flush CH_4 from the adjacent soil or pond fringes, where high CH_4 concentrations were measured (Figure 4), into the open water. Alternatively the physical turbulence caused by heavy rainfall may be enough to raise surface water concentrations by mixing with deeper water containing higher concentrations of CH_4.

GHG release from the aquatic system

CO_2 evasion rates per unit area of water surface, based on headspace samples and NDIR sensors, were 86.2 μg m^{-2} s^{-1} and 164.7 μg m^{-2} s^{-1}, respectively. The NDIR sensor provided a more direct measurement than the headspace technique and was not subject to sampling disturbance, it is therefore likely to be the most reliable method. Both the above values are at the upper end of evasion rates reported in the literature for rivers and lakes. Kling *et al.* (1991) calculated mean CO_2 evasion for arctic tundra rivers and lakes as 3.62 ± 1.53 μg m^{-2} s^{-1} and 10.6 ± 1.68 μg m^{-2} s^{-1} respectively. Evasion from the Hudson River, New York, ranged from 8.19 to 18.8 μg m^{-2} s^{-1} (Raymond *et al.*, 1997). Evasion rates for the Brocky Burn and Black Burn, streams draining 2 separate Scottish peatland catchments, were more similar to the Mer Bleue rates than other non-peatland sites geographically closer to Mer Bleue. Evasion at Brocky Burn ranged from 76.4 μg m^{-2} s^{-1} in the lower reaches to 1213 μg m^{-2} s^{-1} closer to its source (Hope *et al.*, 2001). Evasion from the Black Burn ranged from 162 μg m^{-2} s^{-1} to 1098 μg m^{-2} s^{-1} (Billett *et al.*, 2004).

Mean CH_4 evasion from the water surface was calculated as 0.59 μg m^{-2} s^{-1} and 0.32 μg m^{-2} s^{-1} from the modelled and headspace data, respectively. CH_4 evasion rates in Arctic rivers and lakes and the Hudson River, have been measured as 0.07 μg m^{-2} s^{-1} and 0.09 μg m^{-2} s^{-1}, respectively (Kling *et al.*, 1992; Raymond *et al.*, 1997). In Brocky Burn, evasion rates reached 4.81 μg m^{-2} s^{-1} in the upper stream sections; in the Black Burn, the mean CH_4 evasion rate was 2.12 μg m^{-2} s^{-1} (Billett *et al.*, 2004; Hope *et al.*, 2001). Although evasion from Mer Bleue surface water is at the upper end of all CH_4 rates reported in the literature, it is low in comparison with other peatland sites.

In terms of the relative importance of C evasion to the total catchment budget it is important to accurately assess the proportion of open water in the system. In this instance an estimated value of 0.5% open water in the 4.8 km^2 catchment is used (Billett and Moore, 2008). Evasion rates have be extrapolated to the catchment scale to assess their potential contribution to the overall catchment budget (Table 3). Evasion for CO_2 and CH_4 is expressed both in terms of C losses from the ecosystem

and, using the global warming potentials listed in the IPCC 4th assessment report (IPCC, 2007), as gains to the atmosphere of CO_2 equivalents. In terms of C losses CO_2 is approximately 2 orders of magnitude greater than CH_4. The monthly catchment C loss during the summer season through CO_2 evasion was 0.59 ± 0.10 g C m^{-2} $month^{-1}$ (NDIR measurements); C loss through CH_4 evasion was only 0.006 ± 0.004 g C m^{-2} $month^{-1}$ (modelled dataset). In terms of their global warming potential, CO_2 is approximately 1 order of magnitude greater than CH_4 (Table 3). Even with a global warming potential of 298 (IPCC, 2007), N_2O evasion is negligible (0.004 ± 0.004 g CO_2-eq m^{-2} $month^{-1}$). Billett and Moore (2008) calculated an annual CO_2 evasion rate at Mer Bleue of 3.1 g C m^{-2} yr^{-1} based on measurements made in spring 2005, and assuming evasion only occurred during a 250-day ice-free period. This represents a monthly value of 0.37 g C m^{-2} $month^{-1}$ for the ice-free season. Although this value is significantly less than the value calculated in this study using the NDIR sensor concentrations, it is comparable to the catchment flux of 0.31 g C m^{-2} $month^{-1}$ calculated from headspace measurements. In this case the differences due to measurement method are greater than differences due to inter-annual variability. Using instantaneous NEE rates from July and August, losses through evasion represented 1.3% of the C captured by NEE during the summer months and 1.4% in terms of CO_2-equivalents.

Mean dissolved CO_2-C and CH_4-C concentrations over the measurement period were 7.6 and 1.4 mg L^{-1} from the NDIR CO_2 data and modelled CH_4 values respectively. Roulet *et al.* (2007) published a 6-year mean annual runoff value for the catchment of 391 mm. Using this value and assuming summer concentrations are representative of the whole year, downstream export of dissolved CO_2 and CH_4 represents a loss of 2.97 and 0.56 g C m^{-2} yr^{-1}, respectively. More realistically, as summer concentrations are likely to be higher than the rest of the year (Billett and Moore, 2008; Kling *et al.*, 1991), these values represent the upper limits of our best estimate and are useful only as a comparison to evasion losses calculated in the same way. The annual C loss through CO_2 evasion, assuming summer fluxes are representative of the 250-day ice-free period, is approximately 4.85 g C m^{-2} yr^{1}, almost double that of downstream export. However, downstream losses of CH_4 are much more important to the C budget than losses through CH_4 evasion (0.05 g C m^{-2} yr^{1}). Even assuming a 40%

increase in CH_4 evasion to account for losses through ebullition (Billett and Moore, 2008), downstream export for CH_4 was still significantly more important than evasion.

Significant annual temporal variability in dissolved gas concentrations was observed by both Billett and Moore (2008) and Kling *et al.* (1991). The decrease in CO_2 and CH_4 solubility with high temperatures and solute concentrations (Wiesenburg and Guinasso, 1979; Weiss, 1974) could contribute to a summer evasion peak during July and August. The combination of high flow rates and gas concentrations building up under the winter ice is likely to produce an additional large evasion peak during the spring snow melt period. Caution is therefore needed when up-scaling summer measurements to annual evasion rates. A method comparison carried out by Billett and Moore (2008) showed CH_4 evasion rates calculated from static chambers were on average 40% higher than those calculated indirectly using the method described in this study. As CH_4 is a relatively insoluble gas, a significant proportion may be lost to the atmosphere via ebullition, which is not accounted for in indirect evasion calculations. Hence CH_4 evasion in this study may be an underestimate of actual losses to the atmosphere.

In addition to the temporal variation, significant spatial heterogeneity was measured by Billett and Moore (2008). Along the 4 km hydrological continuum, large variation was found especially between open pools and flowing water. Turbulence created as water flows over beaver dams leads to the formation of degassing hotspots. The seasonal dynamics of Mer Bleue may cause a shift in the location of evasion hotspots throughout the year. Summer evasion hot spots appear to relate to *in-situ* respiration and are therefore likely to occur in stagnant water with a high plant and algal biomass, while spring and autumn evasion hot spots relate to turbulence generated by seasonal high flow (Billett and Moore, 2008).

Conclusions

In conclusion, the study showed extremely high concentrations of both dissolved gaseous C and DOC in the drainage waters of Mer Bleue during the summer season. The high temporal resolution obtained using NDIR sensors allowed us to examine in

much more detail the patterns of CO_2 concentration in the water column. Clear diurnal cycles were evident both in the surface water and near the sediment-water interface. Our results suggest a strong influence of aquatic plants and algae on CO_2 concentrations, and relatively weak soil-stream connectivity. We conclude that during the study period aquatic CO_2 is most likely produced via *in-situ* respiration. Diurnal cycling was also seen in CH_4 concentrations, which could be modelled using rainfall and short-wave radiation ($r^2 = 0.63$). During summer months at Mer Bleue CO_2 production by *in-situ* respiration is more closely related to the C dynamics of Amazonian drainage systems (Mayorga *et al.*, 2005) or northern lakes (Karlsson *et al.*, 2007; Kling *et al.*, 1991). This contrasts to the way many northern river systems function, where CO_2 is produced predominantly within the adjacent peat (Billett *et al.*, 2004; Dawson *et al.*, 2004; Hope *et al.*, 2004).

High summer concentrations of both CO_2 and CH_4 led to extremely high estimated evasion rates at Mer Bleue peatland. Per unit area, summer surface water CO_2 evasion was ~2.5 times higher than CO_2 uptake via NEE. Only when percent open water in the catchment is taken into account does this become less important. Within the ecosystem, surface drainage water therefore represents a significant hotspot for GHG emissions, which is often overlooked when studies rely solely on flux tower measurements.

Acknowledgements

Thanks to Mike Dalva and Allison DeYoung for assistance with field measurements and laboratory analysis; and to Nigel Roulet and Elyn Humphreys for supplying data from soil CO_2 sensors and the flux tower. The work was funded by the UK Natural Environment Research Council (NERC) through an algorithm PhD studentship grant. Infrastructural facilities were supported by the Fluxnet Canada Research Network.

References

Ball T, Smith KA, Moncrieff JB. 2007. Effect of stand age on greenhouse gas fluxes from a Sitka spruce [*Picea sitchensis* (Bong.) Carr.] chronosequence on a peaty gley soil. *Global Change Biology* **13**: 2128-2142.

Billett MF, Moore TR. 2008. Supersaturation and evasion of CO_2 and CH_4 in surface waters at Mer Bleue peatland, Canada. *Hydrological Processes* **22**: 2044-2054.

Billett MF, Palmer SM, Hope D, Deacon C, Storeton-West R, Hargreaves KJ, Flechard C, Fowler D. 2004. Linking land-atmosphere-stream carbon fluxes in a lowland peatland system. *Global Biogeochemical Cycles* **18**: GB1024. DOI:10.1029/2003GB002058.

Borges AV, Vanderborght JP, Schiettecatte LF, Gazeau F, Ferrón-Smith S, Delille B, Frankignoulle M. 2004. Variability of gas transfer velocity of CO_2 in a macrotidal estuary (the Scheldt). *Estuaries* **27**: 593-603.

Dawson JJC, Billett MF, Hope D, Palmer SM, Deacon CM. 2004. Sources and sinks of aquatic carbon in a peatland stream continuum. *Biogeochemistry* **70**: 71-92.

Dawson JJC, Hope D, Cresser MS, Billett MF. 1995. Downstream Changes in Free Carbon-Dioxide in an Upland Catchment from Northeastern Scotland. *Journal of Environmental Quality* **24**: 699-706.

Frankignoulle M, Abril G, Borges A, Bourge I, Canon C, Delille B, Libert E, Theate J. 1998. Carbon Dioxide emission from European estuaries. *Science* **282**: 434-436.

Gorham E. 1991. Northern peatlands: role in the carbon-cycle and probable responses to climatic warming. *Ecological Applications* **1**: 182-195.

Hope D, Billett MF, Cresser MS. 1997. Exports of organic carbon in two river systems in NE Scotland. *Journal of Hydrology* **193**: 61-82.

Hope D, Palmer SM, Billett MF, Dawson JJC. 2001. Carbon dioxide and methane evasion from a temperate peatland stream. *Limnology and Oceanography* **46**: 847-857.

Hope D, Palmer SM, Billett MF, Dawson JJC. 2004. Variations in dissolved CO2 and CH4 in a first-order stream and catchment: an investigation of soil-stream linkages. *Hydrological Processes* **18**: 3255-3275.

IPCC. 2007. Technical Summary. In *Climate Change 2007: The Physical Science Basis. Contribution of Working Group 1 to the Forth Assessment Report of the Intergovernmental Panel on Climate Change,* Solomon S, Qin D, Manning M, Chen Z, Marquis M, Averyt KB, Tignor M, Miller HL (eds). Cambridge University Press: Cambridge, United Kingdom and New York, NY, USA.

Johnson MS, Lehmann J, Couto EG, Novaes JP, Riha SJ. 2006. DOC and DIC in flowpaths of Amazonian headwater catchments with hydrologically contrasting soils. *Biogeochemistry* **81**: 45-57.

Jones JB, Mulholland PJ. 1998. Methane input and evasion in a hardwood forest stream: effects of subsurface flow from shallow and deep pathways. *Limnology and Oceanography* **43**: 1243-1250.

Jonsson A, Algesten G, Bergström A-K, Bishop K, Sobek S, Tranvik LJ, Jansson M. 2007. Integrating aquatic carbon fluxes in a boreal catchment carbon budget. *Journal of Hydrology* **334**: 141-150.

Karlsson J, Jansson M, Jonsson A. 2007. Respiration of allochthonous organic carbon in unproductive forest lakes determined by the Keeling plot method. *Limnology and Oceanography* **52**: 603-608.

Kirk JTO. 1983. *Light and Photosynthesis in Aquatic Ecosystems*. Cambridge University Press: Cambridge.

Kling GW, Kipphut GW, Miller MC. 1991. Arctic lakes and streams as gas conduits to the atmosphere - implications for tundra carbon budgets. *Science* **251**: 298-301.

Kling GW, Kipphut GW, Miller MC. 1992. The Flux of CO_2 and CH_4 from lakes and rivers in arctic Alaska. *Hydrobiologia* **240**: 23-36.

Lafleur PM, Hember RA, Admiral SW, Roulet N. 2005. Annual and seasonal variability in evapotranspiration and water table at a shrub-covered bog in Southern Ontario, Canada. *Hydrological Processes* **19**: 3533-3550.

MacIntyre S, Wanninkhof R, Chanton J. 1995. Trace gas exchange across the air-water interface in freshwater and coastal marine environments. In *Biogenic Trace Gases: Measuring emissions from soil and water,* Matson PA, Harriss RC (eds). Blackwell Science Inc.: Cambridge, MA; 52-97.

Mayorga E, Aufdenkampe AK, Masiello CA, Krusche AV, Hedges JI, Quay PD, Richey JE, Brown TA. 2005. Young organic matter as a source of carbon dioxide outgassing from Amazonian rivers. *Nature* **436**: 538-541.

Miglietta F, Gioli B, Hutjes RWA, Reichstein M. 2007. Net regional ecosystem CO2 exchange from airborne and ground-based eddy covariance, land-use maps and weather observations. *Global Change Biology* **13**: 548-560.

Monteith JL, Unsworth MH. 1990. *Principles of Environmental Physics*. Edward Arnold: London.

Nagy Z, Pinter K, Czobel S, Balogh J, Horvath L, Foti S, Barcza Z, Weidinger T, Csintalan Z, Dinh NQ, Grosz B, Tuba Z. 2007. The carbon budget of semi-arid

grassland in a wet and a dry year in Hungary. *Agriculture Ecosystems & Environment* **121**: 21-29.

Ocampo-Torres FJ, Donelan MA, Merzi N, Jia F. 1994. Laboratory measurements of mass transfer of carbon dioxide and water vapour for smooth and rough flow conditions *Tellus, Series B. Chemical and Physical Meteorology* **46**: 16-32.

Palmer SM, Hope D, Billett MF, Dawson JJC, Bryant CL. 2001. Sources of organic and inorganic carbon in a headwater stream: evidence from carbon isotope studies. *Biogeochemistry* **52**: 321-338.

Raymond PA, Caraco NF, Cole JJ. 1997. Carbon dioxide concentration and atmospheric flux in the Hudson river. *Estuaries* **20**: 381-390.

Richey JE, Melack JM, Aufdenkampe AK, Ballester VM, Hess LL. 2002. Outgassing from the Amazonian rivers and wetlands as a large tropical source of atmospheric CO_2. *Nature* **416**: 617-620.

Roulet N, Lafleur PM, Richard PJH, Moore TR, Humphreys ER, Bubier J. 2007. Contemporary carbon balance and late Holocene carbon accumulation in a northern peatland. *Global Change Biology* **13**: 397-411.

Syed KH, Flanagan LB, Carlson PJ, Glenn AJ, Van Gaalen KE. 2006. Environmental control of net ecosystem CO2 exchange in a treed, moderately rich fen in northern Alberta. *Agricultural and Forest Meteorology* **140**: 97-114.

Tang J, Baldocchi DD, Qi Y, Xu L. 2003. Assessing soil CO_2 efflux using continuous measurements of CO2 profiles in soils with small solid-state sensors. *Agricultural and Forest Meteorology* **118**: 207-220.

Wanninkhof R. 1992. Relationship between wind speed and gas exchange over the ocean. *Journal of Geophysical Research* **97**: 7373-7382.

Weiss RF. 1974. Carbon dioxide in water and seawater: the solubility of a non-ideal gas. *Marine Chemistry* **2**: 203-215.

Weiss RF, Price BA. 1980. Nitrous oxide solubility in water and seawater. *Marine Chemistry* **8**: 347-359.

Wiesenburg DA, Guinasso NL. 1979. Equilibrium solubilities of methane, carbon monoxide, and hydrogen in water and sea water. *Journal of Chemical and Engineering Data* **24**: 356-360.

Worrall F, Burt T, Adamson J. 2005. Fluxes of dissolved carbon dioxide and inorganic carbon from an upland peat catchment: implications for soil respiration. *Biogeochemistry* **73**: 515-539.

9. Results and Discussion

This section of the thesis begins by describing losses from Auchencorth Moss via the aquatic pathway. This includes information which has not been presented in the earlier papers and forms an important part of the final Auchencorth Moss flux budget. Concentrations of solutes in the Black Burn, analysed using the methods described in papers III and IV and Appendix A (POC), are converted to downstream fluxes using discharge and the interpolative 'Method 5' of Walling and Webb (1985, described in Hope *et al.*, 1997a). Concentrations of CO_2, CH_4 and N_2O dissolved in the stream water are then modelled from aquatic and catchment variables and these concentrations used to calculate evasion from the stream surface using the reaeration equation (section 4.2.6.). Both concentrations and fluxes are then compared to similar studies in the literature and to values presented in Papers III and IV.

Concentrations in the terrestrial and aquatic systems at Auchencorth Moss are compared using both this new data and the various papers which make up the body of the thesis. Two complete flux budgets for Auchencorth Moss are then presented, one in terms of catchment carbon and the other in terms of CO_2-equivalents. The section concludes with a discussion on the relative importance of the different flux pathways and the importance of the findings in a broader context.

9.1. Stream fluxes

9.1.1. Solute and particulate concentrations

Total organic carbon concentration in the Black Burn averaged 32.3 ± 2.44 mg L^{-1}, slightly lower than the 40.7 mg L^{-1} measured by Billett *et al.* (2004). Approximately 4% of TOC was particulate (POC) with the remaining 96% (30.8 ± 2.5 mg L^{-1}) as DOC. The mean DIC concentration was 4.33 ± 0.71 mg L^{-1} and the mean NO_3^- and NH_4^+ concentrations were 0.10 ± 0.01 and 0.19 ± 0.02 mg N L^{-1}, respectively. Concentrations of CO_2, CH_4 and N_2O are considered in a later section (9.1.3.).

Both particulate and dissolved forms of organic carbon were positively correlated to discharge (Table 5), consistent with previous studies which link an increase in DOC

with a shift in the dominant flow-path from the lower, DOC absorbing, mineral-rich horizons to the surface organic horizon where much of the DOC is produced (McDowell *et al.*, 1988; Fiebig *et al.*, 1990). DIC concentrations were negatively correlated with discharge (Table 5), suggesting that the deep peat/ground water which sustains base flow is the primary source of DIC. However, the slope of the logarithmic plot was <1 (0.49), indicating that although the overall concentration decreased with increasing discharge, the actual load increased, i.e. input water at high flows still contained DIC although it was lower in concentration than base flow. Paper III concluded that deep peat/groundwater was also the primary source of dissolved CO_2, and that pH was negatively correlated with discharge. Considering the carbonate equilibria system, in which the dominant form of inorganic carbon shifts towards free CO_2 as pH decreases (section 2.3.), it is likely that deep peat/ground water is enriched in the non-gaseous forms of inorganic carbon. Upon contact with the acidic stream water much of this DIC is then likely to be converted to free-CO_2.

Both NO_3^- and NH_4^+ concentrations were positively correlated with discharge (Table 5), indicating a source area in the upper layers of peat which is accessed when the primary flow path switches during periods of high flow.

Table 5 Results from regression analysis on logged solute concentrations against logged discharge

	T	P
POC	2.20	0.03
DOC	3.13	< 0.01
DIC	-4.44	< 0.01
NO_3-N	3.51	< 0.01
NH_4-N	4.04	< 0.01

9.1.2. Solute and particulate downstream export

As sampling frequency was relatively low, the interpolative 'Method 5' of Walling and Webb (1985, described in Hope *et al.*, 1997a) was used to estimate annual loads (Table 6). As continuous discharge data were only available from March 2007 until June 2008, average annual loads were also calculated from the mean of the instantaneous data which spanned a longer (22 month) time period. The actual loads are similar using both methods, however as method 5 incorporates a more realistic

range of annual discharge values, the method 5 results will be used in subsequent calculations.

Table 6 Annual downstream export from the Black Burn, up-scaled to catchment level (kg ha^{-1} yr^{-1})

	Method 5	Mean
POC	20.3 ± 3.41	20.7 ± 8.23
DOC	264 ± 159	271 ± 64.8
DIC	14.6 ± 4.05	15.2 ± 3.02
NO3-N	0.62 ± 0.003	0.70 ± 0.17
NH4-N	1.59 ± 0.006	1.78 ± 0.42

The largest carbon export was in the form of DOC, this is in agreement with previous work which has shown that peatlands are a major source of riverine DOC (Hope *et al.*, 1997b). Total organic carbon export, measured from 1996 -1998 in the Black Burn, was 283 ± 57 kg C ha^{-1} yr^{-1} (Billett *et al.*, 2004), very similar to the 264 ± 159 kg C ha^{-1} yr^{-1} measured in this study, although the standard error in this study is significantly larger than the previous estimate. Annual streamwater losses of DIC were also very similar between the two studies (1996 – 1998: 12 ± 3 kg C ha^{-1} yr^{-1}).

9.1.3. Dissolved CO_2, CH_4 and N_2O concentrations

Mean dissolved concentrations of CO_2, CH_4 and N_2O in the Black Burn were 2.71 ± 0.13 mg C L^{-1} (*ep*CO_2 11.0 ± 0.63), 6.13 ± 0.51 µg C L^{-1} (*ep*CH_4 85.3 ± 5.40) and 0.52 ± 0.02 µg N L^{-1} (*ep*N_2O 1.05 ± 0.07), respectively. The use of the NDIR sensor concentrations at Mer Bleue to calculate evasion rates showed the benefit of having a continuous dataset. However, the sensor was only employed in the Black Burn for a small portion of the study period. In order to estimate evasion using the full set of continuous discharge values, and hence provide a better estimate of annual evasion, best-subset regression modelling was used to interpolate between sampling occasions.

Dissolved concentrations of CO_2, CH_4 and N_2O could be modelled using the variables antecedent rainfall (24-hour and 7-day), stream temperature and discharge (Table 7). Modelled compared to measured values generally lay close to the 1:1 line, though both CH_4 and N_2O models underestimated the highest measured concentrations. As the full set of available data was used to derive the model, no independent observations were available for model validation; hence the applicability

of the model to other sites is unknown. Furthermore, the empirical nature of the model limits its use as a means of predicting responses outside the range of environmental conditions experienced during this study. The model is therefore used primarily as a means of interpolation in the following text.

Table 7 Models describing temporal variability in dissolved concentrations of CO_2, CH_4 and N_2O in the Black Burn

	Coefficient	T	P
$LnCO_2$			
Discharge > 40 L s^{-1} (r^2 = 0.50)			
Intercept	5.53	---	---
Antecedent rainfall (7day)	-0.01	-4.45	< 0.01
Stream temperature	0.03	2.62	0.01
Ln[Discharge]	-0.06	-1.30	0.10
Discharge < 40 L s^{-1} (Paper III)			
Intercept	12.7	---	---
Ln[Discharge]	-0.43	---	---
$LnCH_4$ (r^2 = 0.33)			
Intercept	-0.93	---	---
Antecedent rainfall (7day)	-0.01	-3.08	< 0.01
Ln[Antecedent rainfall (24 h)]	-0.19	-2.44	0.02
Stream temperature	0.05	2.37	0.02
LnN_2O (r^2 = 0.36)			
Intercept	-3.66	---	---
Antecedent rainfall (7day)	0.01	2.80	< 0.01
Ln[Antecedent rainfall (24 h)]	0.04	1.53	0.10
Stream temperature	-0.03	-3.13	< 0.01

Using half-hourly data collected on-site, individual time-series of the dissolved gas concentrations were calculated and compared to measured concentrations (Figure 14). The calculated CO_2 time-series was compared to both routine headspace samples and data collected using the NDIR sensor (Paper III). The NDIR sensor showed that CO_2 concentrations in the stream water increased during periods of low flow when discharge was maintained primarily by inputs from groundwater and deeper peat layers (Paper III). The initial model underestimated CO_2 concentrations during these base-flow conditions but provided a relatively good estimate of concentrations during higher flows. The best correlation between measured and modelled concentrations was achieved by splitting the model into 2 separate sub-models. When discharge was greater than 40 L s^{-1} the original model as described

above was used, when discharge fell below 40 L s^{-1}, the concentration discharge relationship described in Paper III was used (Table 7).

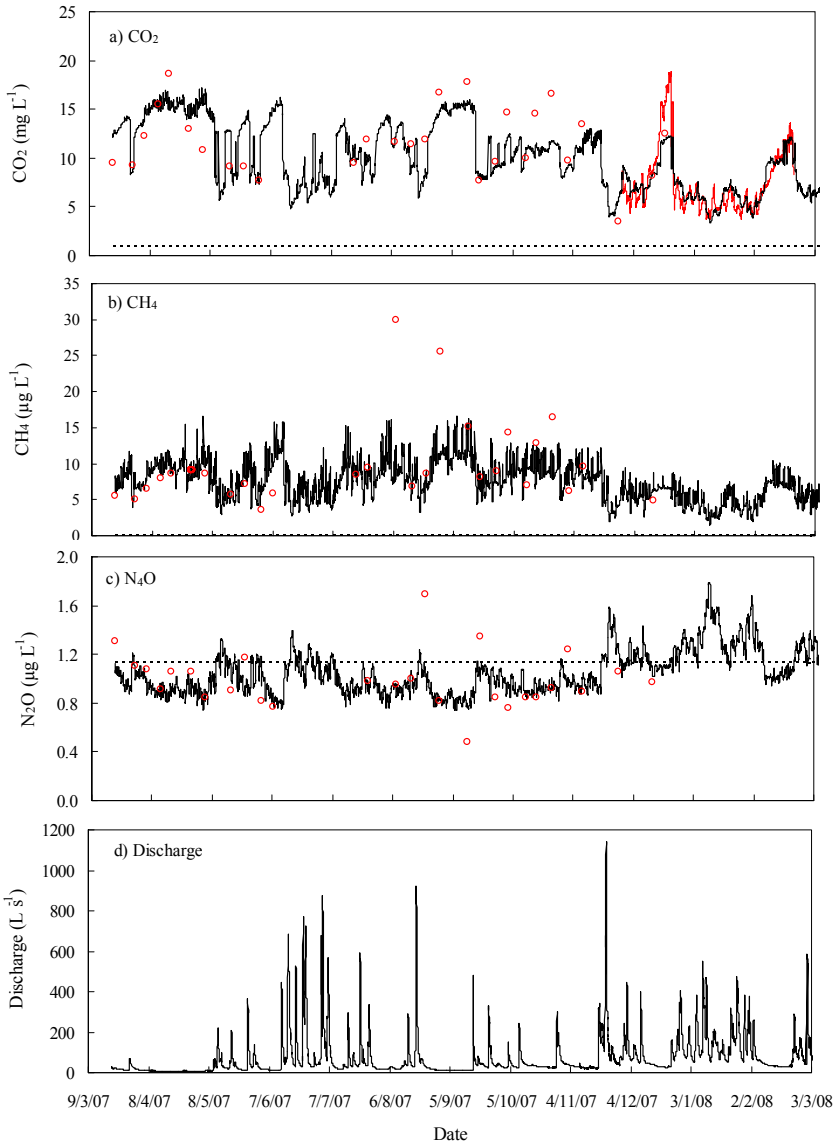

Figure 14 Comparison between modelled (Table 7) and measured concentrations of a) CO_2, b) CH_4 and c) N_2O. Red circles represent concentrations measured using the headspace technique; the red solid line (a) represents concentrations measured using the NDIR sensor. The dotted line (not visible in (b) as it equals only 0.07 µg L^{-1}) represents the average concentration in equilibrium with the atmosphere over the study period. Temporal changes in discharge are shown in (d)

Both CO_2 and CH_4 concentrations showed similar temporal variability with concentrations decreasing with increasing discharge. Similarly both sets of modelled data appear to underestimate concentrations during periods of low flow. It is likely that a sub-model approach similar to that used for CO_2 concentrations, may improve the CH_4 model, however sufficient data was not available to test this approach.

Unlike CO_2 and CH_4, N_2O concentrations were positively correlated to antecedent rainfall, hence the highest concentrations coincided with high discharge. This suggests that unlike CO_2 and CH_4, surface and near-surface flow which dominates water input during high-flow conditions, is the major source of stream water N_2O. It is also during these high flow conditions that the model error is greatest. Concentration-discharge hysteresis was evident in the modelled CO_2 concentrations in agreement with the stormflow data presented in Paper III. However, the direction of the hysteresis loop was not always consistent (Figure 15); the modelled data showed a clockwise rather than anticlockwise loop for storm 5 (Figure 6, Paper III).

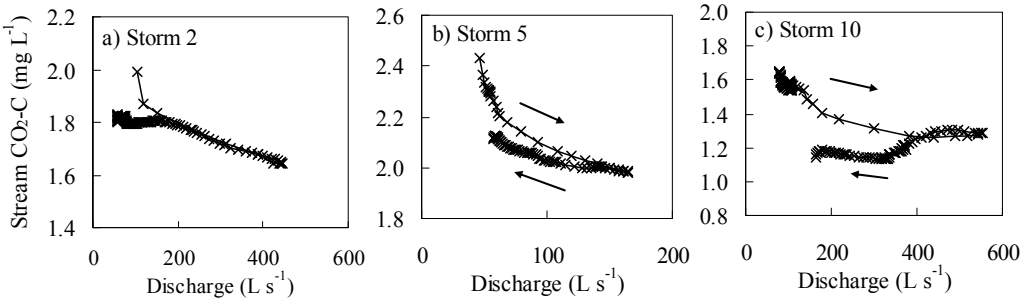

Figure 15 Hysteresis in modelled concentration-discharge relationships. Storms are labelled as in Paper III; figures a, b and c above are directly comparable to a, c and e in Paper III, Figure 6, respectively.

Mean CO_2, CH_4 and N_2O concentrations calculated using only the headspace data were 2.71 ± 0.13 mg C L^{-1}, 6.13 ± 0.51 µg C L^{-1} and 0.52 ± 0.02 µg N L^{-1}, respectively. From the modelled data, the mean concentrations were 2.88 ± 0.09 mg C L^{-1}, 5.71 ± 0.20 µg C L^{-1} and 0.67 ± 0.02 µg N L^{-1}, respectively. Hence there is relatively little difference between the mean of modelled and measured values. CO_2 and CH_4 concentrations in the Black Burn measured from October 1996 to September 1998 averaged 2.06 mg C L^{-1} and 2.07 µg C L^{-1}, respectively (Billett *et al.*, 2004). Although CO_2 concentrations are of a similar magnitude, CH_4 concentrations in this study are more than double these previous measurements, possibly a result of a recent increase in peat extraction upstream. Mean CO_2 concentrations measured here were also significantly higher than either the Brocky Burn or Water of Dye, 2 Scottish upland peatland streams measured during 1997-1998, which had mean CO_2 concentrations of 0.38 and 0.40 mg C L^{-1}, respectively (Dawson *et al.*, 2001). However, CO_2 concentrations closer to the source of the Brocky Burn over the same period ranged from 0.77 – 3.35 mg C L^{-1}, indicating

significant within stream variability (Dawson *et al.*, 2004). CH_4 concentrations in the upper reach of the Brocky Burn ranged from 3 – 91 µg C L^{-1}, with a mean of 25 µg C L^{-1}, approximately 5 times the concentration in the Black Burn (Dawson *et al.*, 2004). Concentrations of CH_4 in the soil and soil-atmosphere fluxes from the adjacent peat were extremely low in comparison to other peatland catchments (Paper I). The low CH_4 concentration in the Black Burn compared to the upper reaches of the Brocky Burn may result from the inherently low measured concentrations associated with the soil/plant system at Auchencorth Moss. Concentrations of both CO_2 and CH_4 in the Black Burn were significantly less than concentrations measured in the surface waters of Mer Bleue during summer 2007, which were 7.64 ± 0.80 mg C L^{-1} and 1.5 ± 0.5 mg C L^{-1}, respectively (Paper IV). Using the modelled concentration dataset, annual downstream export of CO_2 and CH_4 was calculated as 15.4 ± 1.70 and 0.83 ± 0.03 kg C ha^{-1} yr^{-1}; export of N_2O was much smaller at 1.00 ± 0.04 g N ha^{-1} yr^{-1}.

9.1.4. CO_2, CH_4 and N_2O fluxes

Evasion rates were calculated for CO_2, CH_4 and N_2O using the reaeration equation (Young *et al.*, 1998) and the modelled concentrations (Figure 16). Gas transfer coefficients were estimated from the co-injection of conservative solute (NaCl) and volatile gas (propane) tracers as described earlier (Section 4.2.7.) (Billett, unpublished data). Mean instantaneous CO_2 and CH_4 evasion from March 2007 – June 2008 were 785 ± 17.9 and 1.39 ± 0.05 µg C m^{-2} s^{-1}, respectively; mean instantaneous N_2O evasion was 0.08 ± 0.008 µg N m^{-2} s^{-1}. The spiky nature of the instantaneous evasion rates reflects the flashy hydrological regime of the Auchencorth Moss catchment and the close correlation between evasion and discharge. As we have seen (section 9.1.3.), both CO_2 and CH_4 concentrations correlate negatively with discharge, the spikes in evasion rate being primarily a consequence of the increased gas transfer coefficients, highlighting the importance of turbulence as a driver of evasion in stream systems. Relative to the mean, the discharge related spikes in the N_2O time series are the largest of the 3 gases measured, as high concentrations and high gas transfer velocities caused by turbulence coincide.

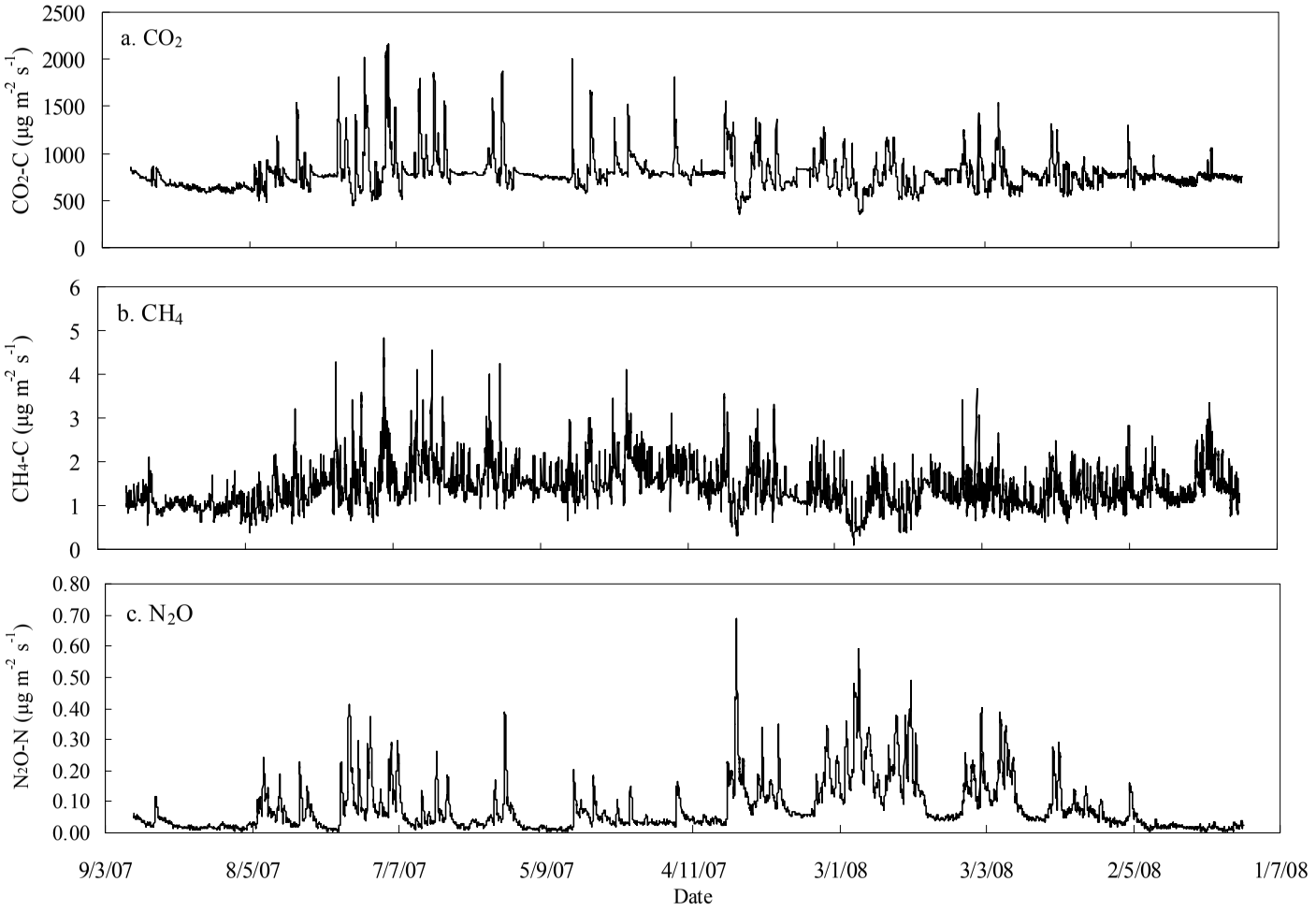

Figure 16 Modelled time-series (30-minute) of a) CO_2, b) CH_4 and c) N_2O evasion from the Black Burn

Due to the nature of the equations used to calculate CO_2 evasion, there appears to be a definite plateau from which evasion rates spike or drop below depending on the conditions (Figure 16a). As discharge decreases, the rate of gas transfer (represented by the k-value in the reaeration equation) decreases causing a decrease in evasion. However, as the discharge decreases, the concentration in the stream water and therefore the strength of the water-atmosphere concentration gradient increases causing an increase in evasion. As these 2 influences are working in opposite directions, there appears to be a range of discharge rates (up to ~25 L s^{-1}) over which evasion is relatively steady, hence the plateau in the plotted time series. The plateau is not as prominent in the CH_4 plot as the model does not fully capture the high concentrations associated with low flow. The dip in both CO_2 and CH_4 evasion rates below this plateau level after a storm has passed (e.g. after the peak on 22/11/07) is due to low concentrations remaining in the stream water. This is in agreement with Paper III where it was shown that after dilution had been accounted for, storms led to a deficit in stream water CO_2 attributed to high evasion caused by greater turbulence during the storm event.

Evasion rates calculated for the single sampling location were upscaled to full stream reach using data from floating chamber measurements made at 5 separate points along the stream on 4 sampling dates in 2005 (Billett, unpublished data, 2008). Although studies have indicated that floating chambers underestimate fluxes in turbulent stream environments (Hlavacova *et al.*, 2006), they are still useful for showing inter-site variability and spatial trends and can therefore be used to aid up-scaling (MacIntyre *et al.*, 1995). CO_2 evasion at the location used in this study was 152 ± 20.7% of the mean calculated from all 5 sampling locations (Figure 17). It is assumed that CH_4 evasion follows a similar downstream pattern to that of CO_2 as concentrations appear to be highly correlated; however no account has been made for differences in gas solubility and evasion through ebullition. As no data is available on the spatial pattern of N_2O concentrations, and the justification that concentrations are highly correlated does not apply, N_2O evasion at the sampling location is assumed to be representative of the whole stream reach. Using the spatial variability identified at the 5 sampling locations to upscale, the mean instantaneous CO_2 and

CH_4 evasion rates for the whole stream reach are estimated as 516 ± 71.7 and 0.92 ± 0.13 μg C m^{-2} s^{-1}, respectively. As the standard error due to upscaling is much greater than the standard error associated with evasion at the single sampling location, the values quoted here represent only that due to upscaling. Assuming that open water represents 0.054% of the total catchment area (Billett *et al.*, 2004), evasion rates can be expressed in terms of total catchment emissions and therefore compared to both soil-atmosphere fluxes and downstream export. Catchment scale evasion of CO_2 and CH_4 are therefore 88.0 ± 12.3 and 0.16 ± 0.02 kg C ha^{-1} yr^{-1}; catchment scale evasion of N_2O is 0.01 ± 0.001 kg N ha^{-1} yr^{-1}.

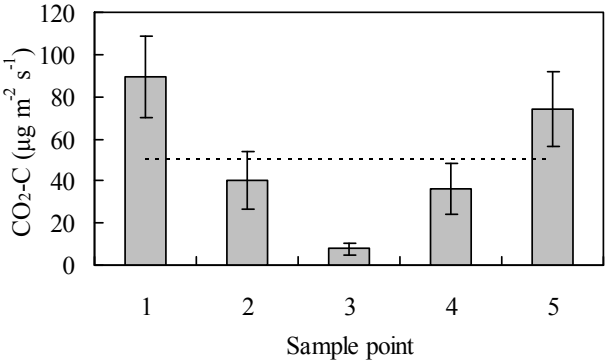

Figure 17 Evasion rates (± SE) of CO_2 from 5 different sampling locations along the Black Burn measured using floating chambers (Billett, unpublished data, 2008). Site 1 is nearest the stream source with sites 2, 3, 4, and 5 located sequentially downstream, site 5 corresponds to the sampling location used in this study. The dashed line represents the average stream evasion rate.

Instantaneous CO_2 and CH_4 evasion rates from the literature and from this study are shown in Table 8. Both CO_2 and CH_4 emissions from the Black Burn are high in comparison to previous studies, and in terms of CO_2 comparable only to the upper reach of the Brocky Burn, another peat dominated site. Emissions from Mer Bleue are also at the high end of the literature values; however despite the much higher CO_2 and CH_4 concentrations, evasion is still significantly less than from the Black Burn. The drainage system at Mer Bleue, during the summer when sampling occurred, was characterised by a series of beaver ponds containing almost static water and low soil-stream connectivity. Turbulence and hence the gas transfer rate across the water-atmosphere boundary, was controlled primarily by wind speed. Conversely, the Black Burn is a fast flowing, shallow and extremely turbulent stream, with high connectivity to the adjacent peat. Despite a weaker water-atmosphere gradient, the much higher gas transfer rate has led to a much higher calculated evasion rate.

Table 8 Summary of CO_2 and CH_4 stream/river evasion data from the literature. Where ± is shown, the number refers to the standard error.

Study site		Method	Drainage Basin Description (Soil Type/Land Use)	Evasion rate CO_2-C ($\mu g\ m^{-2}\ s^{-1}$)	Evasion rate CH_4-C ($\mu g\ m^{-2}\ s^{-1}$)	Reference
Kuparuk river, Alaska		Indirect calculation	Arctic tundra	1.65 ± 0.21	0.05	(Kling *et al.*, 1991; Kling *et al.*, 1992)
Sycamore Creek, Arizona		Static Chambers	Woodland/Desert Scrub;	----	0.18[1]	(Jones *et al.*, 1995)
Hudsen River, USA		Indirect calculation	Forestry/Agriculture/Urban	2.23 – 5.14	0.07	(Raymond *et al.*, 1997)
European (Inner) Estuaries[2]		Indirect calculation/ Floating Chambers	See individual estuaries for more information	6.94 – 105	----	(Frankignoulle *et al.*, 1998)
Walker Branch, Tennessee		Indirect calculation	Hardwood forest; Deep Ultisol soils	20.3 – 49.0	0.003 – 0.11	(Jones et al., 1998a; Jones et al., 1998b)
Brocky Burn, Glen Dye Catchment, Scotland	Upper site	Indirect calculation	Organic rich upland catchment; Histosols, Spodosols, inceptisols, fluvents	331	3.61	(Hope *et al.*, 2001)
	Middle site			126	0.60	
	Lower site			20.8	----	
Amazonian rivers		Indirect calculation	Tropical Rainforest	263 ± 76.1	----	(Richey *et al.*, 2002)
Black Burn, Auchencorth Moss, Scotland		Indirect calculation	Lowland Peatland; 85% Histosols	44.2 – 300	1.59	(Billett *et al.*, 2004)
Sitka Stream, Czech Republic		Eddy model	Rises in mountains, flows through agriculture; Alder Willow and Ash riparian strip	28.6 ± 2.33	0.34 ± 0.03	(Hlavacova *et al.*, 2006)
		Floating Chambers		11.6 ± 0.95	0.14 ± 0.03	
		Static Chambers		3.29 ± 0.33	0.06 ± 0.01	
Mer Bleue, Canada	Open water	Indirect calculation	Raised Ombrotrophic peatbog	7.50 – 86.0	0.01 – 0.12	(Billett et al., 2008)
	Flowing water			7.20 – 81.5	0.01 – 0.09	
Mer Bleue, Canada[3]	Open water	Indirect calculation	As above	44.9 ± 7.86	0.44 ± 0.25	Paper IV (this study)
Black Burn, Auchencorth Moss, Scotland		Indirect calculation	As above	516 ± 71.7	0.92 ± 0.13	This study

[1] More than 80% of this total stream emission was from bank sediments, included as part of the active channel.
[2] Estuaries include Elbe (Germany), Ems (Germany/Netherlands), Rhine (Netherlands), Scheldt (Netherlands/Belgium), Tamar and Thames (UK), Gironde (France), Douro and Sado (Portugal).
[3] Summer fluxes only

Relatively little work has previously been done quantifying evasion from peatland drainage systems, and that which has been done has focussed primarily on gaseous carbon (Hope *et al.*, 2001; Billett *et al.*, 2004; Hope *et al.*, 2004). However, despite very low concentrations of N_2O, with a global warming potential of 298 (IPCC, 2007), it may still have a significant impact on the greenhouse gas balance and therefore should be quantified. Literature values for N_2O evasion include <0.005 μg N m^{-2} s^{-1} from English and Welsh coastal rivers (Dong *et al.*, 2004), 0.002 – 0.23 μg N m^{-2} s^{-1} from suburban and agricultural drainage waters in New Jersey (Laursen *et al.*, 2004), and 0.04 ± 0.006 μg N m^{-2} s^{-1} from a primarily agricultural stream in the Czech Republic (Hlavacova *et al.*, 2006). Reay *et al.* (2003) found evasion rates of up to approximately 0.28 μg m^{-2} s^{-1} from a Scottish agricultural stream, and found a positive relationship between the spatial variability in evasion rates and NO_3^- concentrations. The mean evasion rate of 0.08 μg N m^{-2} s^{-1} in this study is well within these limits despite much lower concentrations of NO_3^- in the stream water; mean NO_3^- concentration in the Black Burn was 0.10 mg N L^{-1} compared to between 0.34 – 8.33 mg N L^{-1} in English and Welsh coastal rivers and <14.0 mg N L^{-1} in the New Jersey drainage waters (Dong *et al.*, 2004; Laursen *et al.*, 2004). Mean NH_4^+ concentration in the Black Burn (0.19 mg N L^{-1}) was however within the limits of that measured in English and Welsh rivers (0.0.8 – 0.38 mg N L^{-1}) (Dong *et al.*, 2004), no information was available on the other systems.

9.2. Comparison between terrestrial and aquatic systems

Mean monthly NEE was estimated from eddy covariance measurements made from 2005-2007 (Helfter, unpublished data, 2008) and compared to monthly mean concentrations of carbon in the Black Burn (Figure 18). The NEE pattern of winter CO_2 loss coupled with summer uptake is typical of peatland sites (e.g. Roulet *et al.*, 2007). The low uptake via NEE in June is primarily due to the unusually wet summer of 2007 (Figure 3b). Similarly, it is likely that dilution due to high discharge during summer 2007 is responsible for the mid-summer dip in dissolved gaseous forms of carbon in the Black Burn (Figure 18b). NEE and stream CO_2 concentrations therefore appear to follow correlated seasonal cycles, and assuming a correlation

between NEE and soil CO_2 concentrations there is likely to be a link between soil and stream CO_2.

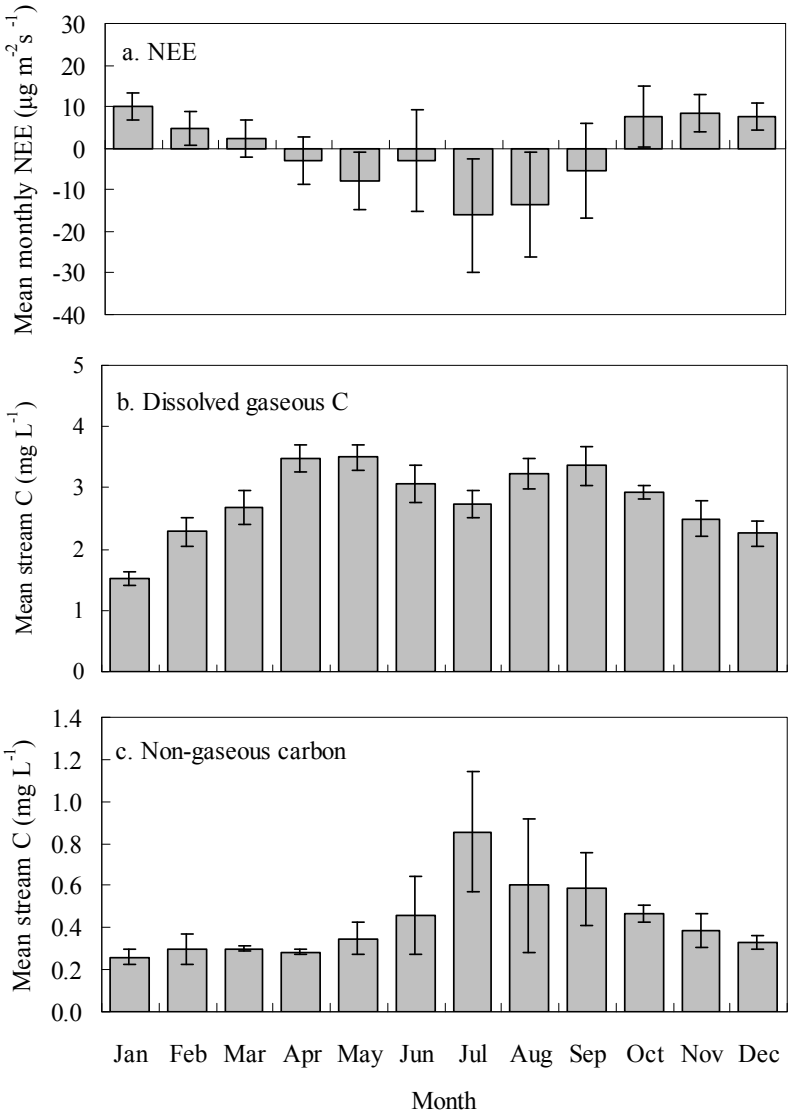

Figure 18 Mean monthly a) catchment NEE (2005 – 2007), b) dissolved gaseous carbon in the Black Burn (March 2007 – June 2008) and c) non-gaseous forms of aquatic carbon (April 2006 – December 2007).

Similar correlations between soil and stream CO_2 concentrations were described in Papers 3 and 4. Although correlations were considered over shorter time periods the use of the NDIR sensors provided a better temporal resolution and therefore a much greater confidence in the relationship, helping the interpretation of the data. Despite a correlation being apparent in both systems the actual nature of the relationship differed considerably. Cross-correlation analysis of the Mer Bleue dataset (Paper IV)

indicated that the correlation was indirect and due primarily to common driving variables. However, in the Auchencorth Moss catchment, soil-stream connectivity was shown to be much greater (Paper III) and the correlation was therefore more likely to be caused by the direct leaching and release of carbon derived from the soil-plant system.

The flashy discharge regime of the Black Burn, caused by both the intrinsic catchment characteristics and presence of overgrown drainage ditches, indicated a strong hydrological connectivity between the catchment and drainage system. Hence the potential for dissolved gas and solute transport from Auchencorth Moss catchment was high. The average lag between peak rainfall and peak discharge during storm events was only 3.3 ± 0.3 hours (Paper III) and during the period over which evasion rates are calculated, the precipitation/runoff ratio was ~0.7. In contrast to this the precipitation/runoff ratio at Mer Bleue was only ~0.4 (Roulet *et al.*, 2007), therefore evapotranspiration played a much greater role in the hydrology of Mer Bleue than in Auchencorth Moss. The average discharge lag of 5 rainfall events at Mer Bleue during summer 2007 was 7.5 ± 2.0 hours, again indicating a much lower hydrological connectivity. In terms of CO_2 source areas, Paper III also showed that soil-stream connectivity was greatest during storm events. The much lower frequency of storm events experienced during the measurement campaign at Mer Bleue may further explain the lower soil-stream connectivity at the site.

Papers I and II described the spatial heterogeneity in both surface GHG emissions and below-ground GHG concentrations which can lead to significant uncertainty in catchment scale budgets. In systems such as Auchencorth Moss where soil-stream connectivity is strong, aquatic concentrations represent an integrated catchment signal. Hence long-term monitoring of aquatic concentrations may indicate changes within the catchment, in response to climate change or management practices, which might otherwise be missed due to natural variability or uncertainty in terrestrial measurements. Furthermore, making measurements in the aquatic system, either by repeated headspace sampling or the installation of NDIR sensors, is both cheaper and less time consuming than making measurements in the terrestrial system and therefore has the potential to be more widely applied. In the event that a significant

shift in aquatic carbon concentrations was identified, in-depth terrestrial studies would still be required to confirm the change in catchment carbon storage and identify the likely causes. The potential of stream CO_2 monitoring as a means to identify changes within the catchment requires significant further study.

9.3. Auchencorth Moss budgets

The carbon budget for Auchencorth Moss (Figure 19) was calculated by combining the estimated Black Burn evasion rates and downstream (lateral) exports with the terrestrial CH_4 emissions calculated in Paper I and the estimated mean annual NEE (Helfter, unpublished data, 2008). To avoid bias towards growing seasons, the CH_4 and N_2O emission estimates are based on a weighted average which assumes the winter season estimates (Paper 1) are representative of both winter 2006-2007 and winter 2007-2008. This process was repeated to calculate the GHG flux budget in terms of CO_2-equivalents (Figure 20). CO_2-equivalents were calculated by multiplying the fluxes of N_2O and CH_4 by their 100-year GWP, as listed in Table 1 (IPCC, 2007).

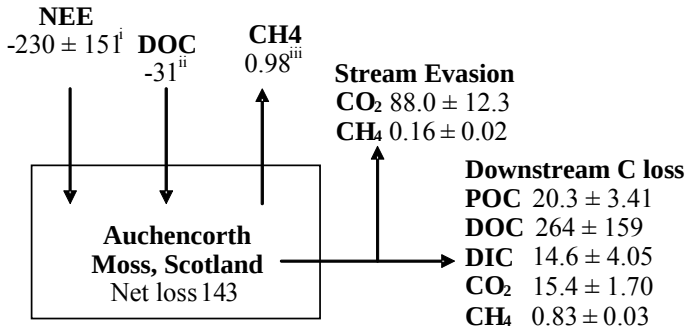

[i] Mean of annual NEE from 2005-2007 (Helfter, personal communication, 2008)
[ii] Billett et al. (2004)
[iii] Paper 2

All values in kg C ha^{-1} yr^{-1}

Figure 19 Carbon fluxes to and from Auchencorth Moss, Scotland.

The catchment carbon budget (Figure 19) suggests an annual loss of 143 kg C ha^{-1} yr^{-1}, primarily via downstream export of DOC. This is in agreement with Billett *et al.* (2004) who estimated a net loss of 83 kg C ha^{-1} yr^{-1} for Auchencorth Moss. The budget assumes that no carbon entered the catchment via external groundwater or through-flow. The water tightness of the catchment was considered by equating

water input via precipitation with losses through discharge and evapotranspiration (calculations were based on 2008 data when evapotranspiration was calculated). Evapotranspiration (Helfter, personal communication 2008) and discharge combined accounted for ~92% of precipitation input suggesting water input from outside the catchment is likely to be minimal.

The fate of the exported organic carbon after leaving the study area is uncertain and represents an area which deserves further consideration. The river continuum concept (Vannote *et al.*, 1980) suggests that in-stream processing becomes increasing important with distance downstream, hence DOC may be respired and lost through evasion. Furthermore, research has shown that despite a very large export of riverine carbon, the contribution of terrestrial carbon to the marine dissolved organic matter pool is relatively small (e.g. Meyers-Schulte *et al.*, 1986). This would again imply a loss of DOC either along the stream length through microbial degradation (Hansell *et al.*, 2004) or in the estuarine environment via flocculation or absorption onto suspended sediments (Uher *et al.*, 2001; Amon *et al.*, 2004; Spencer *et al.*, 2007). If this is the case, DOC exported via the Black Burn, which is currently not included in the GHG budget for Auchencorth Moss, may ultimately act as a CO_2 source further downstream. However, Dawson *et al.* (2004) found no significant loss of DOC with distance downstream within the drainage network of the Glen Dye catchment, Scotland. Clearly more work is required to fully understand the fate of exported DOC.

Auchencorth Moss represents a GHG sink of 382 kg CO_2-eq ha^{-1} yr^{-1} (Figure 20). The largest GHG flux is uptake via NEE. Terrestrial emissions of CH_4 and N_2O combined returned only ~5% of the NEE uptake to the atmosphere; the individual contributions of terrestrial CH_4 and N_2O were ~4% and ~1%, respectively. Hence despite the large uncertainty surrounding their calculation, their actual contribution in terms of the total GHG budget for Auchencorth Moss was minor. Evasion from the stream channel, often ignored in GHG studies, represents a return to the atmosphere of ~40% of the NEE CO_2-equivalent uptake. This assumes that the eddy covariance footprint, over which NEE is calculated, does not include stream evasion; a reasonable assumption given the prevailing wind is from the south west (Figure 2).

Stream evasion fluxes are only included in NEE measurements when the wind comes from the NW sector.

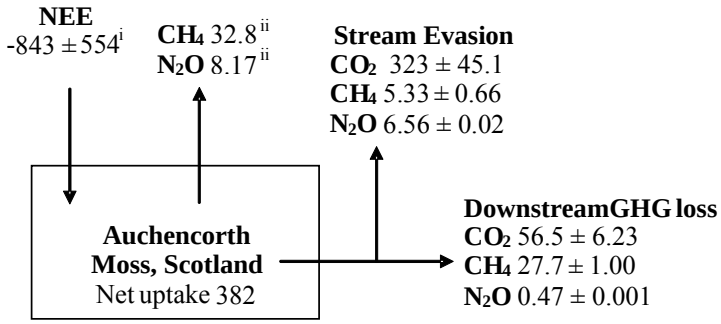

[i] Mean of annual NEE from 2005-2007 (Helfter, personal communication, 2008)
[ii] Paper 2

All values in $kgCO_2$-eq ha^{-1} yr^{-1}

Figure 20 GHG fluxes to and from Auchencorth Moss, Scotland.

The estimated annual budget for Auchencorth Moss described by Billett et al (2004) suggests a NEE uptake of 1019 ± 91.7 kg CO_2-eq ha^{-1} yr^{-1}, offset by a terrestrial CH_4 emission of 1367 kg CO_2-eq ha^{-1} yr^{-1} (estimated from literature), and a CO_2 stream evasion loss of 169 kg CO_2-eq ha^{-1} yr^{-1}. Papers I and II showed that terrestrial CH_4 emissions, and hence the relative contribution of CH_4 to the total budget at Auchencorth Moss, was low in comparison to other peatland sites. Hence in contrast to previous work, and possibly in contrast to other peatlands, stream CO_2 evasion plays a much greater role in the GHG budget than terrestrial CH_4 emissions.

9.4. Implications of study

The above budgets clearly highlight the importance of including aquatic fluxes in calculated budgets. Ignoring riverine evasion from Auchencorth Moss would have led to falsely assuming a GHG sink strength almost twice as high as that calculated here. Furthermore, ignoring the riverine fluxes would have led to the conclusion that Auchencorth Moss was a carbon sink rather than a carbon source. The importance of both CO_2 and CH_4 as atmospheric GHGs means that the global GHG and carbon budgets are intrinsically linked. Although the results of this study showed that Auchencorth Moss was acting as a net sink for GHGs, it also represented a net loss of carbon. The importance of this net carbon loss in terms of climate change depends

on the ultimate fate of the exported carbon. If the carbon is transported downstream to be incorporated into estuarine or ocean sediments, it will not affect the atmospheric radiative balance. However, if in-stream processing leads to evasion downstream of the study site, calculated GHG budgets are likely to underestimate the total influence that peatland catchments have on the global GHG budget. Furthermore, increased precipitation and increased temperatures due to climatic change could potentially increase the volume of DOC exported and increase the likelihood of in-stream processing, respectively. Hence the effect of climate change on the exported carbon is also of major importance.

The rate of increase in atmospheric CO_2 emissions is approximately half the rate implied by fossil fuel and land-use emissions (IPCC, 2007), indicating the importance of land and ocean sinks. However, recent work has indicated a long-term (50-yr) increase in the airborne fraction of CO_2 emissions, implying a decrease in the strength of CO_2 sinks (Canadell *et al.*, 2007). The response of peatlands to changes in global precipitation and temperature regimes may partly explain the apparent weakening of total sink strength. Both Papers I and II showed the importance of water table and temperature in controlling emissions from the terrestrial environment, with lower water tables leading to a net increase in the emission of CO_2-equivalents. Paper II in particular, also showed significant pulses of CH_4 and N_2O in response to sudden changes in water table depth. Although the relative importance of these pulses to annual emission estimates could not be derived from the available data, with a predicted increase in the frequency and intensity of rainfall events (IPCC, 2007), their importance is likely to increase. Paper III suggested that soil-stream connectivity was greater during periods dominated by storm-flow, and also showed the importance of storm-flow in exporting catchment-derived carbon. An increase in both total precipitation and extreme events may therefore also lead to an increase in the relative importance of the drainage system as a pathway for catchment GHG release.

The comparison between the Black Burn and Mer Bleue drainage system showed that the hydrological regime in the catchment and hence the soil-stream connectivity, was an important factor in controlling aquatic losses. Management practices that alter

catchment hydrology, e.g. drainage or drain blocking, may therefore alter the relative importance of aquatic losses. Furthermore, although the influence of peat extraction was not specifically quantified in this study, the disturbance of deep peat could potentially increase the release of carbon from what was previously a relatively stable store, to the drainage network. It is therefore becoming increasingly important to accurately calculate budgets for peatland ecosystems which, as we have shown here, cannot be done without accounting for losses through the aquatic pathway.

The whole-catchment approach and emphasis on developing a process-based understanding of peatland fluxes, has allowed the calculation of a more accurate and complete budget and provided a much stronger basis for predicting the consequences of climate change and management options. Furthermore, the availability of the new methodology for making continuous measurements of CO_2 in aquatic systems has enabled the drivers of aquatic fluxes to be considered in much greater detail than in previous studies. As well as leading to a number of important conclusions, this thesis has also led to a number of new research questions and highlighted various areas where our knowledge and understanding of the system is weak. Questions which have arisen and areas which require future work are described in section 11.

10. Summary and Conclusions

10.1. Terrestrial fluxes

Paper I calculated fluxes of CH_4 and N_2O from Auchencorth Moss of 291 and 5.12 μg m^{-2} d^{-1}, respectively. However, coefficients of variation and hence uncertainty in the estimated fluxes were high. Both Papers I and II illustrated the importance of water table depth in controlling the spatial variability of GHG emissions. Paper I also showed the importance of identifying potential catchment hotspots when designing the layout of chamber studies; the riparian zone alone contributed ~12% of the total catchment CH_4 emission whilst covering only 0.5% of the surface area. Paper II found a strong interaction between water table height and vegetation type. In contrast to much of the current literature, it was found that CH_4 emissions were suppressed by the presence of aerenchyma-containing vegetation. Paper I found a similar negative influence of aerenchymous vegetation in the field.

The drivers of temporal CH_4 and N_2O emissions were seen to vary across different microtopographic/vegetative ecotopes and it was suggested that a series of sub-models that allowed for these distinct differences might better represent the temporal dynamics of the catchment as a whole. The presence of episodic pulsing after significant shifts in the depth of the water table was examined in Paper II. It was suggested that this pulsing, if not captured by the low frequency sampling regimes typical of chamber studies such as that described in Paper I, could potentially lead to a significant underestimation of up-scaled emission estimates.

10.2. Drainage system fluxes

In Paper IV the continuous monitoring of aquatic CO_2 over a 2-month period showed significant diurnal variability in both surface (~10 cm) and deep (~60 cm) water concentrations. Paper IV only considered evasion from Mer Bleue during the summer. As we have seen from the comparison between Mer Bleue and the Black Burn, in peatland systems where the water-atmosphere CO_2 gradient is already very high, the influence of turbulence on the gas transfer rate is much more important than the actual concentration. Hence although concentrations are at their highest during

the summer months, peak evasion may occur during periods of higher turbulence i.e. during snowmelt. Further work is required to test this hypothesis.

Paper IV identified the primary driver of temporal variability in CO_2 concentrations in Mer Bleue drainage waters as biological activity. The primary driver in the Black Burn during the winter season (Paper III) was dilution due to changes in discharge, and similarly when modelling concentrations from the headspace measurements, rainfall and discharge were again important drivers. Whereas in Mer Bleue in-stream processing was the primary source of CO_2 and soil-stream connectivity was weak, the major sources identified in the Black Burn were ground-water and terrestrial inputs. Mer Bleue and Auchencorth Moss have very different hydrological regimes and may represent the extremes of northern peatland systems. Understanding the drivers of concentrations and evasion rates in these two different systems, provides a very good basis for predicting the drivers of greenhouse gas release from the drainage waters of many other northern peatland catchments.

10.3. Auchencorth Moss budget

Compiling the results from both terrestrial and aquatic fluxes in Auchencorth Moss indicated that the catchment was functioning as a sink for CO_2-equivalents (382 kg CO_2-eq ha^{-1} yr^{-1}). However, the results also indicated a net loss of carbon from the catchment (143 kg C ha^{-1} yr^{-1}); primarily due to a very large downstream export of DOC. The downstream fate of this DOC is currently uncertain and requires further consideration. Aquatic fluxes are undoubtedly an important part of both the carbon and the GHG flux budgets in Auchencorth Moss. In systems such as this where soil-stream connectivity appears to be strong, monitoring aquatic changes may provide an easy and cost-effective means to identify change within the catchment as a whole.

11. Recommended Future Work

- The negative response of CH_4 emissions to the presence of aerenchyma-containing vegetation is contrary to much of the previous literature. Clearly this is an area which requires more study. A more detailed understanding of CH_4 concentrations through the soil profile would indicate whether a significant reservoir of CH_4 for plant roots to tap into exists in the shallow peat at Auchencorth Moss. The oxidation potential within the soil profile and the rhizosphere could be quantified using the methyl fluoride technique described by Lombardi *et al.* (1997). In addition to this, the importance of plants as gas conduits could be assessed by comparing chamber measurements such as those made in this study, with similar measurements where the plant transport route has been restricted. Rather than removing vegetation which would also disturb the soil, the vegetation could be sealed by coating in a material such as Plasti-dip© (Plasti Dip International, Blaine, MN USA), or less destructively, sealed within an airtight bag.

- The contribution of episodic pulsing of GHGs following water level change to annual emission estimates needs to be considered in greater detail; such pulsing may lead to significant error in emission estimates up-scaled from infrequent sampling regimes. Visual examination of the 2008 NEE and water table data (Helfter, unpublished data, 2008) suggests that pulsing can be picked up by continuous field measurements, though further statistical analysis is required to substantiate this observed trend; similarly Shurpali *et al*. (1993) picked up episodic CH_4 pulsing from eddy correlation measurements. Either high-frequency measurements using automatic chambers or micrometeorological techniques, or a sampling regime which allows a quick response to rainfall events in addition to standard periodic measurements may therefore provide a basis for further investigation into the pulsing of CH_4 and N_2O at Auchencorth Moss.

- It is suggested that models simulating temporal change in soil-atmosphere CH_4 and N_2O emissions could be improved by separating into sub-models,

which allow drivers to vary between distinct microtopographic/vegetative ecotopes. Further work is required to test this approach.

- The clear importance of DOC export in the carbon budget at Auchencorth Moss highlights the need to consider the fate of riverine carbon after leaving the study catchment. Is the carbon respired further downstream or does it become integrated into a long term sink? This would require the measurement of DOC concentrations along the full length of the stream continuum from headwater to estuary. In addition to considering the volume of DOC along the length of the continuum, it may also be useful to consider DOC composition; for example if DOC was being processed downstream it may become more recalcitrant with distance from source. Alternatively, isotopic signature which allows the source of DOC to be identified may help distinguish between a dynamic equilibrium, where DOC inputs replace DOC lost via in-stream processing, or the conservative downstream transport of DOC.

- The use of NDIR sensors to monitor aquatic CO_2 concentrations has allowed a much greater insight into what drives temporal variability in drainage waters. By pairing in-stream sensors with sensors within the soil profile they also have the potential to greatly improve our understanding of the sources of aquatic carbon. As the Mer Bleue/Auchencorth Moss comparison illustrated, inter-catchment variability is high and there is therefore a need to employ these sensors in a wider range of catchments. This technique has considerable potential and could also be used to consider changes in soil-stream connectivity in response to drainage/peat extraction/forestry.

- Develop a method which would enable the continuous measurement of CH_4 concentrations within aquatic systems, allowing a similar level of understanding to that of CO_2. Although CH_4 flux through the Black Burn was minor in comparison to CO_2, this was most likely connected to the low fluxes in the terrestrial system. Hence in other peatlands where CH_4 production is greater, aquatic CH_4 may play a more important role in the carbon budget.

– Evaluate the relative contribution of aquatic fluxes in a wider range of catchments by extending the whole-catchment approach to similar peatlands; this is one of the aims of the CEH ‘Carbon Catchments’ project.

– Evaluate the use of monitoring concentrations in the aquatic system as a means to identify changes in catchment storage. This could be done by monitoring catchments undergoing changes in management or by comparing the results from Auchencorth Moss with other catchments under different management or climatic influences. Initially the data would be examined for any significant changes in average concentrations or shifts in patterns of variability which may indicate a change in the primary carbon source.

References

Aitkenhead, J.A., Hope, D., Billett, M.F., 1999. The relationship between dissolved organic carbon in stream water and soil organic carbon pools at different spatial scales. Hydrological Processes 13, 1289-1302.

Amon, R.M.W., Meon, B., 2004. The biogeochemistry of dissolved organic matter and nutrients in two large Arctic estuaries and potential implications for our understanding of the Arctic Ocean system. Marine Chemistry 92, 311-330.

Ball, D.F., 1964. Loss-on-ignition as an estimate of organic matter and organic carbon in non-calcareous soils. Journal of Soil Science 15, 84-92.

Ball, T., Smith, K.A., Moncrieff, J.B., 2007. Effect of stand age on greenhouse gas fluxes from a Sitka spruce [Picea sitchensis (Bong.) Carr.] chronosequence on a peaty gley soil. Global Change Biology 13, 2128-2142.

Bartlett, K.B., Harriss, R.C., 1993. Review and assessment of methane emissions from wetlands. Chemosphere 26, 261-320.

Beaumont, L.J., McAllan, I.A.W., Hughes, L., 2006. A matter of timing: changes in the first date of arrival and last date of departure of Australian migratory birds. Global Change Biology 12, 1339-1354.

Beckwith, C.W., Baird, A.J., A. L. Heathwaite, 2003. Anisotropy and depth-related heterogeneity of hydraulic conductivity in a bog peat. I: laboratory measurements. Hydrological Processes 17, 89-101.

Billett, M.F., Moore, T.R., 2008. Supersaturation and evasion of CO_2 and CH_4 in surface waters at Mer Bleue peatland, Canada. Hydrological Processes.

Billett, M.F., Palmer, S.M., Hope, D., Deacon, C., Storeton-West, R., Hargreaves, K.J., Flechard, C., Fowler, D., 2004. Linking land-atmosphere-stream carbon fluxes in a lowland peatland system. Global Biogeochemical Cycles 18.

Bubier, J., Crill, P., Mosedale, A., 2002. Net ecosystem CO_2 exchange measured by autochambers during the snow-covered season at a temperate peatland. Hydrological Processes 16, 3667-3682.

Butterbach-Bahl, K., Papen, H., Rennenberg, H., 1997. Impact of gas transport through rice cultivars on methane emission from rice paddy fields. Plant, Cell and Environment 20, 1175-1183.

Canadell, J.G., Le Quéré, C., Raupach, M.R., Field, C.B., Buitenhuis, E.T., Ciais, P., Conway, T.J., Gillett, N.P., Houghton, R.A., Marland, G., 2007. Contributions to accelerating atmospheric CO_2 growth from economic activity, carbon intensity, and

efficiency of natural sinks. Proceedings of the National Academy of Sciences 104, 18866-18870.

Charman, D., 2002. Peatlands and Environmental Change. John Wiley & sons, Chicester.

Chason, D.B., Siegel, D.I., 1986. Hydraulic conductivity and related physical properties of peat, Lost River Peatland, Northern Minnesota. Soil Science 142, 91-99.

Clayton, H., Arah, J.R.M., Smith, K.A., 1994. Measurement of nitrous oxide emissions from fertilised grassland using closed chambers. Journal of Geophysical Research 99, 16599-16607.

Clymo, R.S., Hayward, P.M., 1982. The ecology of *Sphagnum*. In: Smith, A.J.E. (Ed.), Bryophyte Ecology. Chapman & Hall, London UK, pp. 229-289.

Cole, J.J., Prairie, Y.T., Caraco, N.F., McDowell, W.H., Tranvik, L.J., Striegl, R.G., Duarte, C.M., Kortelainen, P., Downing, J.A., Middelburg, J.J., Melack, J., 2007. Plumbing the global carbon cycle: integrating inland waters into the terrestrial carbon budget. Ecosystems 10, 171-184.

Davidson, E.A., 1991. Fluxes of nitrous oxide and nitric oxide from terrestrial ecosystems. In: Rogers, J.E., Whitman, W.B. (Eds.), Microbial Production and Consumption of Greenhouse Gases: Methane, Nitrogen Oxides, and Halomethanes. American Society for Microbiology, Washington, DC, pp. 219-235.

Dawson, J.J.C., 2000. The controls on concentrations and fluxes of gaseous, dissolved and particulate carbon in upland peat dominated catchments. PhD Thesis, University of Aberdeen.

Dawson, J.J.C., Billett, M.F., Hope, D., 2001. Diurnal variations in the carbon chemistry of two acidic peatland streams in north-east Scotland. Freshwater Biology 46, 1309-1322.

Dawson, J.J.C., Hope, D., Cresser, M.S., Billett, M.F., 1995. Downstream Changes in Free Carbon-Dioxide in an Upland Catchment from Northeastern Scotland. Journal of Environmental Quality 24, 699-706.

Dawson, J.J.C., Billett, M.F., Hope, D., Palmer, S.M., Deacon, C.M., 2004. Sources and sinks of aquatic carbon in a peatland stream continuum. Biogeochemistry 70, 71-92.

Dong, L.F., Nedwell, D.B., Colbeck, I., Finch, J., 2004. Nitrous Oxide Emission from some English and Welsh Rivers and Estuaries. Water , Air, and Soil Pollution: Focus 4, 127-134.

Fiebig, D.M., Lock, M.A., Neal, C., 1990. Soil water in the riparian zone as a source of carbon for a headwater stream. Journal of Hydrology 116, 217-237.

Flechard, C.R., 1998. Turbulent exchange of ammonia above vegetation. PhD Thesis, University of Nottingham.

Frankignoulle, M., Abril, G., Borges, A., Bourge, I., Canon, C., Delille, B., Libert, E., Theate, J., 1998. Carbon Dioxide emission from European estuaries. Science 282, 434-436.

Fray, K.E., Smith, L.C., 2005. Alpified carbon release from vast West Siberian peatlands by 2100. Geophysical Research Letters 32, LO9401.

Gorham, E., 1991. Northern Peatlands: Role in the Carbon-Cycle and Probable Responses to Climatic Warming. Ecological Applications 1, 182-195.

Gut, A., Blatter, A., Fahrni, M., Lehmann, B.E., Neftel, A., Staffelbach, T., 1998. A new membrane tube technique (METT) for continuous gas measurements in soils. Plant and Soil 198, 79-88.

Hansell, D.A., Kadko, D., Bates, N.R., 2004. Degradation of Terrigenous Dissolved Organic Carbon in the Western Arctic Ocean. Science 304, 858-861.

Hejzlar, J., Dubrovský, M., Buchtele, J., Ruzicka, M., 2003. The apparent and potential effects of climate change on the inferred concentration of dissolved organic matter in a temperate stream (the Malse River, South Bohemia). The Science of the Total Environment 310, 143-152.

Hlavacova, E., Rulik, M., Cap, L., Mach, V., 2006. Greenhouse gas (CO_2, CH_4, N_2O) emissions to the atmosphere from a small lowland stream in Czech Republic. Archiv Fur Hydrobiologie 165, 339-353.

Holden, J., 2005a. Controls of soil pipe frequency in upland blanket peat. Journal of Geophysical Research 110, FO1002.

Holden, J., 2005b. Peatland hydrology and carbon release: why small-scale process matters. Philosophical transactions of the royal society. A 363, 2891-2913.

Hope, D., Billett, M.F., Cresser, M.S., 1997a. Exports of organic carbon in two river systems in NE Scotland. Journal of Hydrology 193, 61-82.

Hope, D., Billett, M.F., Milne, R., Brown, T.A.W., 1997b. Exports of organic carbon in British rivers. Hydrological Processes 11, 325-344.

Hope, D., Palmer, S.M., Billett, M.F., Dawson, J.J.C., 2001. Carbon dioxide and methane evasion from a temperate peatland stream. Limnology and Oceanography 46, 847-857.

Hope, D., Palmer, S.M., Billett, M.F., Dawson, J.J.C., 2004. Variations in dissolved CO_2 and CH_4 in a first-order stream and catchment: an investigation of soil-stream linkages. Hydrological Processes 18, 3255-3275.

Hutchinson, G.L., 1995. Biosphere-Atmosphere Exchange of Gaseous N Oxides. In: Lal, R., Kimble, J., Levine, E., Stewart, B.A. (Eds.), Soils and Global Change. Lewis Publishers, Boca Raton, pp. 219-236.

IPCC, 2007. Climate Change 2007: The physical basis. Contribution of working group 1 to the forth assessment report of the intergovernmental panel on climate change. Cambridge University Press.

Joabsson, A., Christensen, T.R., Wallen, B., 1999. Vascular plant controls on methane emissions from northern peatforming wetlands. Trends in Ecology & Evolution 14, 385-388.

Johnson, M.S., Lehmann, J., Couto, E.G., Novaes, J.P., Riha, S.J., 2006. DOC and DIC in flowpaths of Amazonian headwater catchments with hydrologically contrasting soils. Biogeochemistry 81, 45-57.

Jones, J.B., Mulholland, P.J., 1998a. Methane input and evasion in a hardwood forest stream: effects of subsurface flow from shallow and deep pathways. Limnology and Oceanography 43, 1243-1250.

Jones, J.B., Mulholland, P.J., 1998b. Carbon dioxide variation in a hardwood forest stream: an integrative measure of whole catchment soil respiration. Ecosystems 1, 183-196.

Jones, J.B., Holmes, R.M., Fischer, S.G., Grimm, N.B., Greene, D.M., 1995. Methanogenezis in Arizona, USA dryland streams. Biogeochemistry 31, 155-173.

Jonsson, A., Algesten, G., Bergström, A.-K., Bishop, K., Sobek, S., Tranvik, L.J., Jansson, M., 2007. Integrating aquatic carbon fluxes in a boreal catchment carbon budget. Journal of Hydrology 334, 141-150.

Kling, G.W., Kipphut, G.W., Miller, M.C., 1991. Arctic lakes and streams as gas conduits to the atmosphere - implications for tundra carbon budgets. Science 251, 298-301.

Kling, G.W., Kipphut, G.W., Miller, M.C., 1992. The flux of CO_2 and CH_4 from lakes and rivers in arctic Alaska. Hydrobiologia 240, 23-36.

Laine, A., Wilson, D., Kiely, G., Byrne, K., 2007. Methane flux dynamics in an Irish lowland blanket bog. Plant soil 299, 181-193.

Laursen, A.E., Seitzinger, S.P., 2004. Diurnal patterns of denitrification, oxygen consumption and nitrous oxide production in rivers measured at the whole-reach scale. Freshwater Biology 49, 1448-1458.

Likens, G.E., 1985. An ecosystem approach to aquatic ecology. Springer-Verlag, New York.

Linderholm, H.W., 2006. Growing season changes in the last century. Agricultural and Forest Meteorology 137, 1-14.

Livingston, G.P., Hutchinson, G.L., 1995. Enclosure-based measurement of trace gas exchange: applications and sources of error. In: Matson, P.A., Harriss, R.C. (Eds.), Biogenic trace gases: measuring emissions from soil and water. Marston Lindsay Ross International Ltd., Oxford.

Lombardi, J.E., Epp, M.A., Chanton, J.P., 1997. Investigation of the methyl fluoride technique for determining rhizospheric methane oxidation. Biogeochemistry 36, 153-172.

MacDonald, J.A., Skiba, U., Shappard, L.J., Hargreaves, K.J., Smith, K.A., Fowler, D., 1996. Soil environmental variables affecting the flux of methane from a range of forest, moorland and agricultural soils. Biogeochemistry 34, 113-132.

MacDonald, J.A., Fowler, D., Hargreaves, K.J., Skiba, U., Leith, I.D., Murray, M.B., 1998. Methane emission rates from a northern wetland; response to temperature, water table and transport. Atmospheric Environment 32, 3219-3227.

MacIntyre, S., Wanninkhof, R., Chanton, J., 1995. Trace gas Exchange across the air-water interface in freshwater and coastal marine environments. In: Matson, P.A., Harriss, R.C. (Eds.), Biogenic Trace Gases: Measuring emissions from soil and water. Blackwell Science Inc., Cambridge, MA, pp. 52-97.

McDowell, W.H., Likens, G.E., 1988. Origin, composition and flux of dissolved organic carbon in the Hubbord Brook valley. Ecological monographs 58, 177-195.

Meehl, G.A., Washington, W.M., Collins, W.D., Arblaster, J.M., Hu, A.X., Buja, L.E., Strand, W.G., Teng, H.Y., 2005. How much more global warming and sea level rise? Science 307, 1769-1772.

Meyers-Schulte, K.J., Hedges, J.I., 1986. Molecular evidence for a terrestrial component of organic matter dissolved in ocean water. Nature 321, 61-63.

Miglietta, F., Gioli, B., Hutjes, R.W.A., Reichstein, M., 2007. Net regional ecosystem CO2 exchange from airborne and ground-based eddy covariance, land-use maps and weather observations. Global Change Biology 13, 548-560.

Mitchell, G. H., Mykura, W.,1962. The geology of the neighbourhood of Edinburgh, 3rd Ed. H.M.S.O. publishing, Edinburgh.

Milne, R., Brown, T.A., 1997. Carbon in the vegetation and soils of Great Britain. Journal of Environmental Management 49, 413-433.

Minkkinen, K., Laine, J., 2006. Vegetation heterogeneity and ditches create spatial variability in methane fluxes from peatlands drained for forestry. Plant and Soil 285, 289-304.

Nagy, Z., Pinter, K., Czobel, S., Balogh, J., Horvath, L., Foti, S., Barcza, Z., Weidinger, T., Csintalan, Z., Dinh, N.Q., Grosz, B., Tuba, Z., 2007. The carbon budget of semi-arid grassland in a wet and a dry year in Hungary. Agriculture Ecosystems & Environment 121, 21-29.

Payette, S., Delwaide, A., Caccianiga, M., Beauchemin, M., 2004. Accelerated thawing of subarctic peatland permafrost over the last 50 years. Geophysical Research Letters 31.

Pumpanen, J., Kolari, P., Ilvesniemi, H., Minkinnen, K., Vesala, T., Niinisto, S., Lohila, A., Larmola, T., Morero, M., Pihlatie, M., Janssens, I., Yuste, J.C., Grunzweig, J.M., Reth, S., Subke, J.A., Savage, K., Kutsch, W., Ostreng, G., Ziegler, W., Anthoni, P., Lindroth, A., Hari, P., 2004. Comparison of different chamber techniques for measuring soil CO_2 efflux. Agricultural and Forest Meteorology 123, 159-176.

Raich, J.W., Bowden, R.D., Steudler, P.A., 1990. Comparison of two static chamber techniques for determining carbon dioxide efflux from forest soils. Soil Science Society of America Journal 54, 1754-1757.

Raymond, P.A., Caraco, N.F., Cole, J.J., 1997. Carbon dioxide concentration and atmospheric flux in the Hudson River. Estuaries 20, 381-390.

Reay, D.S., Smith, K.A., Edwards, A.C., 2003. Nitrous oxide emission from agricultural drainage waters. Global Change Biology 9, 195-203.

Richey, J.E., Melack, J.M., Aufdenkampe, A.K., Ballester, V.M., Hess, L.L., 2002. Outgassing from Amazonian rivers and wetlands as a large tropical source of atmospheric CO_2. Nature 416, 617-620.

Roulet, N., Lafleur, P.M., Richard, P.J.H., Moore, T.R., Humphreys, E.R., Bubier, J., 2007. Contemporary carbon balance and late Holocene carbon accumulation in a northern peatland. Global Change Biology 13, 397-411.

Ruser, R., Flessa, H., Russow, R., Schmidt, G., Buegger, F., Munch, J.C., 2006. Emission of N_2O, N_2 and CO_2 from soil fertilized with nitrate: Effect of compaction, soil moisture and rewetting. Soil Biology & Biochemistry 38, 263-274.

Russow, R., Sich, I., Neue, H.U., 2000. The formation of the trace gases NO and N_2O in soils by the coupled processes of nitrification and denitrification: results of kinetic 15N tracer investigations. Chemosphere - Global Change Science 2, 359-366.

Segers, R., 1998. Methane production and methane consumption: a review of processes underlying wetland methane fluxes. Biogeochemistry 41, 23-51.

Shurpali, N.J., Verma, S.B., Clement, R.J., Billesbach, D.P., 1993. Seasonal distribution of methane flux in a Minnesota peatland measured by eddy-correlation. Journal of Geophysical Research (Atmosphere) 98, 20649-20655.

Skjelkvåle, B.L., Stoddard, J.L., Jeffries, D.S., Tørseth, K., Høgåsen, T., Bowman, J., Mannio, J., Monteith, D.T., Mosello, R., Rogora, M., Rzychon, D., Vesely, J., Wieting, J., Wilander, A., Worsztynowicz, A., 2005. Regional scale evidence for improvements in surface water chemistry 1990-2001. Environmental Pollution 137, 165-176.

Smith, K.A., Ball, T., Conen, F., Dobbie, K.E., Massheder, J., Rey, A., 2003. Exchange of greenhouse gases between soil and atmosphere: interactions of soil physical factors and biological processes. European Journal of Soil Science 54, 779-791.

Smith, L.C., MacDonald, G.M., Velichko, A.A., Beilman, D.W., Borisova, O.K., Frey, K.E., Kremenetski, K.V., Sheng, Y., 2004. Siberian peatlands a net carbon sink and global methane source since the early Holocene. Science 303, 353-356.

Sottocornola, M., Kiely, G., 2005. An Atlantic blanket bog is a modest CO_2 sink. Geophysical Research Letters 32.

Spencer, R.G.M., Ahad, J.M.E., Baker, A., Cowie, G.L., Ganeshram, R., Upstill-Goddard, R.C., Uher, G., 2007. The estuarine mixing behaviour of peatland derived dissolved organic carbon and its relationship to chromophoric dissolved organic matter in two North Sea estuaries (U.K.). Estuarine, Coastal and Shelf Science 74, 131-144.

Stendel, M., Christensen, J.H., 2002. Impact of global warming on permafrost conditions in a coupled GCM. Geophysical Research Letters 29.

Stoddard, J.L., Kahl, J.S., Deviney, F.A., DeWalle, D.R., Driscoll, C.T., Herlihy, A.T., Kellogg, J.H., Murdoch, P.S., Webb, J.R., Webster, K.E., 2003. Response of surface water chemistry to the Clean Air Act Amendments of 1990. In: U.S. Environemental Protection Agency, Corvallis (OR), pp. 92.

Su, Z., Shi, Y.F., 2002. Response of monsoonal temperate glaciers to global warming since the Little Ice Age. Quaternary International 97-8, 123-131.

Syed, K.H., Flanagan, L.B., Carlson, P.J., Glenn, A.J., Van Gaalen, K.E., 2006. Environmental control of net ecosystem CO_2 exchange in a treed, moderately rich fen in northern Alberta. Agricultural and Forest Meteorology 140, 97-114.

Tang, J., Baldocchi, D.D., Qi, Y., Xu, L., 2003. Assessing soil CO_2 efflux using continuous measurements of CO_2 profiles in soils with small solid-state sensors. Agricultural and Forest Meteorology 118, 207-220.

Uher, G., Hughes, C., Henry, G., Upstill-Goddard, R.C., 2001. Non-conservative mixing behavious of colored dissolved organis matter in a humic-rich, turbid estuary. Geophysical Research Letters 28, 3309-3312.

Vannote, R.L., Minshall, G.W., Cummins, K.W., Sedell, J.R., Cushing, C.E., 1980. River Continuum Concept. Canadian Journal of Fisheries and Aquatic Sciences 37, 130-137.

Walter, B.P., Heimann, M., 2000. A process-based, climate-sensitive model to derive methane emissions from natural wetlands: Application to five wetland sites, sensitivity to model parameters, and climate. Global Biogeochemical Cycles 14, 745-765.

Wanninkhof, R., 1992. Relationship between wind speed and gas exchange over the ocean. Journal of Geophysical Research 97, 7373-7382.

Whalen, S.C., Reeburgh, W.S., 2000. Methane oxidation, production, and emission at contrasting sites in a boreal bog. Geomicrobiology Journal 17, 237-251.

Wolf, I., Russow, R., 2000. Different pathways of formation of N_2O, N_2 and NO in black earth soil. Soil Biology and Biochemistry 32, 229-239.

Worrall, F., Harriman, R., Evans, C.D., Watts, C.D., Adamson, J., Neal, C., Tipping, E., Burt, T., Grieve, I., Monteith, D., Naden, P.S., Nisbet, T., Reynolds, B., Stevens, P., 2004. Trends in Dissolved Organic Carbon in UK Rivers and Lakes. Biogeochemistry 70, 369-402.

Young, R.G., Huryn, A.D., 1998. Comment: Improvement to the diurnal upstream-downstream dissolved oxygen change technique for determining whole-stream metabolism in small streams Canadian Journal of Fisheries and Aquatic Sciences 55, 1784-1785.

Appendix A

Soil soluble carbon extraction

Frozen soil samples were allowed to fully defrost overnight before analysis. Soil samples were thoroughly mixed within the sample bags and 20 g sub-samples weighed into clean plastic pots. The pots were then shaken for 1 hour with 40 ml of deionised water. After shaking, the mixture was allowed to settle and the solution transferred to clean containers and centrifuged until suitable separation was achieved. The supernatant was filtered through 0.45 μm pore size syringe filters before analysis on a Rosemount-Dohrmann DC-80 total organic carbon analyser using the method described in papers I and II.

Soil KCl extractable nitrogen

The method described above for soil soluble carbon extraction was repeated with KCl instead of deionised water, and with a ratio of 10 g of soil to 50 ml KCl. Analysis of the supernatant solution was carried out on a dual channel CHEMLAB continuous flow colorimetric analyser (see Papers I and II).

Loss on ignition for determination of POC

For the purpose of this study, particulate organic carbon is defined as the fraction of organic carbon that will not pass through a 0.7 μm pore size filter paper. Whatman GF/F (0.7 μm pore size) filter papers were pre-ashed by heating at 500ºC for 5 hours; the papers were then weighed (weight 1) and kept in a desiccator until required. Water samples collected in 300 ml glass bottles were filtered through these pre-ashed, pre-weighed filter papers using a vacuum pump. Where possible, filtration was carried out within 24 hours of sample collection. The filter paper, along with the particulate material retained on it, was oven dried at ~100ºC overnight, re-weighed (weight 2) and stored in a dessicater until loss-on-ignition could be carried out. Each filter paper was then combusted in a muffle furnace at 375ºC for 16 hours; the combusted filter papers were again re-weighed (weight 3).

Loss-on-ignition was used to calculate the mass of particulate carbon from each sample using the method of Ball (1964) described in equation A-1, where OC refers to the percent of organic carbon in the sample and LOI is the percent of particulate matter (weight 2 – weight 1) which is lost during combustion at 375ºC (weight 2 – weight 3). The mass of (POC) in the sample can then be calculated and expressed in units of mg L^{-1}.

Equation A-1 $$OC = 0.458 \times LOI - 0.4$$

Approximately 1 from every 10 filter papers was analysed using the same procedure as above, substituting stream water for deionised water to determine additional filter paper weight loss. The mean LOI of these blanks was 0.23 mg, lower than the mean of 0.35 mg calculated by Dawson (2000); the LOI value for individual sample was corrected using this mean blank LOI weight.

Appendix B

Figure B-1 shows the discharge/stage height relationship for the Black Burn sampling location, provided by Billett (unpublished data, 2008). The regression equation ($r^2 = 0.86$) is in the form of the equation B-1, where Q is the discharge in L s^{-1}, H is the stage height in cm, and a and b refer to the constants 0.031 and 2.180, respectively.

Equation B-1 $$Q = aH^b$$

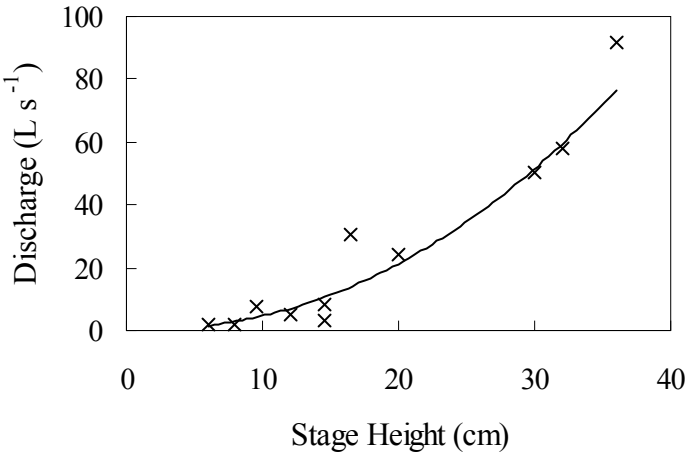

Figure B-1 Discharge/stage height relationship for the Black Burn sampling location (Billett, unpublished data, 2008)

Appendix C

Table C-1 Average (± SE) CH_4 and N_2O fluxes (n=9) alongside auxiliary data from fortnightly measurement campaign (Paper I). Soil temperature data is from the flux tower at Auchencorth Moss (Coyle, unpublished data, 2008). No value indicates missing data.

Sampling Date	CH_4	N_2O	Soil Respiration	Water Table	Soil Moisture	Soil Temperature
	$\mu g\ m^{-2}\ h^{-1}$	$\mu g\ m^{-2}\ h^{-1}$	$g\ m^{-2}\ h^{-1}$	cm	$m^3\ m^{-3}$	°C
18/05/06	35.0 ± 43.1	0.81 ± 2.43	0.60 ± 0.21	-6.41 ± 1.39	0.99 ± 0.01	7.71
14/06/06	19.4 ± 101	-0.76 ± 5.13	0.37 ± 0.03	-47.5 ± 4.63	0.49 ± 0.04	9.36
18/07/06	-0.48 ± 93.2	-25.3 ± 4.70	0.50 ± 0.04	-43.8 ± 3.53	0.44 ± 0.04	11.40
23/08/06	84.8 ± 92.3	10.5 ± 11.1	0.46 ± 0.08	-26.5 ± 2.16	0.60 ± 0.04	12.13
31/08/06	-2.23 ± 4.54	8.03 ± 3.30	0.37 ± 0.06	-28.8 ± 1.69	----	11.61
06/09/06	-4.16 ± 3.19	0.31 ± 1.66	0.19 ± 0.02	-6.53 ± 1.43	----	11.84
13/09/06	7.70 ± 7.82	1.55 ± 1.85	0.30 ± 0.04	-13.9 ± 0.00	----	11.54
19/09/06	105 ± 104	1.80 ± 1.95	0.20 ± 0.04	-20.1 ± 2.53	0.93 ± 0.02	11.45
04/10/06	28.6 ± 14.8	14.5 ± 7.54	0.15 ± 0.03	-9.07 ± 1.55	----	11.12
18/10/06	173 ± 141	0.78 ± 1.89	0.12 ± 0.03	-9.31 ± 1.60	0.84 ± 0.04	9.81
01/11/06	38.8 ± 33.0	-1.60 ± 1.34	----	-6.03 ± 1.50	----	9.08
15/11/06	31.3 ± 26.4	-0.74 ± 0.13	----	-3.31 ± 0.90	0.98 ± 0.01	7.77
29/11/06	41.0 ± 25.7	0.06 ± 0.24	----	-3.56 ± 1.45	0.98 ± 0.02	7.08
19/12/06	23.9 ± 16.0	-0.24 ± 0.53	0.06 ± 0.01	-4.77 ± 1.41	0.99 ± 0.01	6.00
04/01/07	17.5 ± 15.0	0.93 ± 0.38	----	-2.51 ± 1.43	1.00 ± 0.00	5.98
19/01/07	22.7 ± 18.5	1.49 ± 1.44	----	-2.24 ± 1.21	1.00 ± 0.00	5.39
01/02/07	52.6 ± 28.3	0.17 ± 1.26	0.14 ± 0.04	-4.60 ± 1.42	0.99 ± 0.00	5.79
13/02/07	-2.01 ± 7.56	1.98 ± 0.58	----	-3.27 ± 1.31	0.99 ± 0.01	4.79
27/02/07	22.2 ± 12.5	-29.4 ± 14.1	0.07 ± 0.03	-1.30 ± 0.90	1.00 ± 0.00	5.96
14/03/07	18.4 ± 16.5	-6.66 ± 0.96	0.09 ± 0.01	-3.20 ± 1.17	1.00 ± 0.00	6.14
29/03/07	9.21 ± 12.5	-0.95 ± 1.07	----	-2.97 ± 1.02	1.00 ± 0.00	6.04
12/04/07	-8.20 ± 1.35	-0.11 ± 0.78	0.18 ± 0.02	-33.5 ± 3.42	0.90 ± 0.02	6.84
26/04/07	-10.1 ± 2.43	-4.29 ± 1.25	0.24 ± 0.03	-38.3 ± 2.41	0.85 ± 0.03	7.96
14/05/07	-0.41 ± 1.02	2.26 ± 1.19	0.16 ± 0.02	-5.34 ± 1.57	0.99 ± 0.00	7.83
24/05/07	0.98 ± 1.78	-0.49 ± 0.27	0.25 ± 0.02	-15.6 ± 4.08	0.94 ± 0.01	7.08
07/06/07	3.18 ± 3.74	-0.02 ± 0.17	----	-21.6 ± 1.01	0.95 ± 0.02	10.23
21/06/07	36.6 ± 27.4	-0.09 ± 1.04	0.25 ± 0.05	-6.19 ± 1.09	----	10.97
03/07/07	105 ± 70.5	1.56 ± 0.36	0.25 ± 0.05	-3.64 ± 1.03	----	11.26
20/07/07	221 ± 133	1.90 ± 1.99	0.22 ± 0.04	-7.39 ± 1.10	0.98 ± 0.64	12.03
01/08/07	27.0 ± 13.0	1.02 ± 3.18	0.40 ± 0.07	-19.6 ± 1.73	0.96 ± 0.01	11.66
20/08/07	79.9 ± 50.9	0.28 ± 0.40	0.17 ± 0.02	-5.03 ± 1.06	0.89 ± 0.01	11.30
04/09/07	-3.72 ± 2.44	-0.95 ± 0.33	0.43 ± 0.08	-32.8 ± 1.66	0.95 ± 0.01	11.21
18/09/07	-0.42 ± 2.92	-1.06 ± 1.50	0.16 ± 0.02	-9.23 ± 1.25	0.91 ± 0.01	10.88
02/10/07	604 ± 314	-3.59 ± 3.72	0.20 ± 0.06	-11.7 ± 1.04	0.93 ± 0.01	9.59
16/10/07	19.4 ± 22.0	1.16 ± 1.02	0.27 ± 0.09	-9.12 ± 2.15	0.96 ± 0.02	10.54

Table C-2 Particulate, solute and dissolved gas concentrations from routine measurements in the Black Burn. No value indicates missing data.

Sampling date	Discharge	CO_2	CH_4	N_2O	POC	DOC	DIC	NO_3^--N	NH_4^+-N
	L s^{-1}	mg L^{-1}	µg L^{-1}	µg L^{-1}	mg L^{-1}	mg L^{-1}	mg L^{-1}	mg L^{-1}	mg L^{-1}
17/05/06	81.06	1.17	2.13	0.77	5.58	11.41	14.28	0.04	0.00
24/05/06	44.30	1.37	2.12	0.57	1.85	29.04	7.87	0.05	0.00
01/06/06	1.54	----	5.44	0.41	0.99	36.89	0.60	0.04	0.02
06/06/06	3.29	3.15	7.01	0.37	0.20	32.06	0.42	0.01	0.11
14/06/06	3.73	3.54	7.65	0.38	1.27	6.85	18.69	0.01	0.00
22/06/06	3.73	2.68	7.23	0.42	3.73	21.58	7.06	0.01	0.21
27/06/06	4.69	4.03	7.55	0.48	1.49	5.43	18.17	0.03	0.00
05/07/06	8.30	2.49	6.42	0.56	1.86	35.47	1.81	0.03	0.15
17/08/06	6.97	3.52	13.59	0.37	1.33	10.80	9.39	0.01	0.00
23/08/06	28.79	3.38	8.55	0.53	2.19	23.91	0.45	0.04	0.21
31/08/06	13.05	3.73	11.10	0.57	1.95	18.86	2.08	0.02	0.00
19/09/06	33.04	3.07	7.44	0.39	1.35	31.62	1.09	0.01	0.26
26/09/06	98.81	2.29	7.32	0.74	2.29	39.74	1.86	0.08	0.32
25/10/06	67.49	2.34	3.76	----	1.88	34.74	0.67	0.01	0.31
01/11/06	63.24	2.09	5.77	0.63	1.61	32.51	2.65	0.01	0.08
07/11/06	16.87	3.15	6.74	0.49	1.02	25.62	2.06	0.03	0.24
15/11/06	228.52	1.59	3.38	0.60	1.71	25.31	0.57	0.04	0.21
21/11/06	232.72	1.36	2.92	0.61	1.29	18.60	0.30	0.06	0.26
29/11/06	44.20	1.74	3.52	0.50	0.62	32.75	0.94	----	----
05/12/06	362.19	1.29	2.18	0.62	2.99	26.81	0.28	0.00	0.32
18/12/06	31.59	2.11	5.46	0.55	0.66	23.40	0.74	0.00	0.48
04/01/07	159.84	1.34	2.02	0.61	0.94	19.96	0.52	0.00	0.36
09/01/07	245.59	1.26	2.13	0.53	3.62	22.11	0.33	0.00	0.33
19/01/07	236.97	1.08	2.11	0.64	0.74	18.61	0.67	0.13	0.08
24/01/07	28.79	2.15	4.57	0.60	0.06	18.82	0.74	0.12	0.03
01/02/07	28.79	1.92	3.24	0.58	0.68	21.71	1.18	0.15	0.65
08/02/07	11.34	3.54	6.05	0.65	0.45	17.09	4.62	0.10	0.23
13/02/07	91.01	1.53	2.48	0.66	0.91	21.25	0.55	0.20	0.49
23/02/07	30.17	2.24	2.72	0.55	0.42	19.80	0.39	0.15	0.38
27/02/07	320.60	1.57	2.37	0.58	12.60	21.89	0.74	0.20	0.44
07/03/07	47.72	1.84	3.21	0.64	0.66	22.53	1.40	----	----
14/03/07	51.37	2.15	3.41	0.75	0.69	24.42	1.07	0.08	0.29
20/03/07	26.13	2.58	4.13	0.63	0.30	22.09	1.25	0.08	0.18
30/03/07	40.18	2.52	3.80	0.54	0.65	23.88	0.94	0.12	0.20
05/04/07	11.34	3.34	4.84	0.53	0.68	17.85	6.15	0.08	0.13
12/04/07	8.16	4.22	6.00	0.45	0.83	12.04	11.30	0.08	0.10
17/04/07	6.97	5.09	6.42	0.52	0.78	7.89	14.78	0.06	0.06
27/04/07	8.16	3.53	6.86	0.52	0.68	8.85	12.76	0.04	0.03
04/05/07	7.62	2.97	6.49	0.41	1.17	4.26	16.20	0.02	0.04
17/05/07	20.77	2.49	4.29	0.44	0.92	23.56	2.04	0.12	0.32
24/05/07	13.72	2.48	5.32	0.57	0.34	23.70	3.33	0.06	0.06
01/06/07	35.38	2.10	2.72	0.40	1.70	31.25	0.73	0.05	0.09

Table C-2 Continued from previous page

Sampling date	Discharge	CO_2	CH_4	N_2O	POC	DOC	DIC	NO_3^--N	NH_4^+-N
	L s^{-1}	mg L^{-1}	µg L^{-1}	µg L^{-1}	mg L^{-1}	mg L^{-1}	mg L^{-1}	mg L^{-1}	mg L^{-1}
07/06/07	12.53	----	4.42	0.37	0.47	32.83	9.11	0.05	0.04
14/06/07	58.73	2.60	6.36	----	0.04	70.27	3.55	0.08	0.44
06/07/07	453.66	3.25	7.05	----	3.43	61.92	2.02	----	----
18/07/07	29.62	3.19	22.50	----	0.77	87.45	2.08	----	----
24/07/07	61.17	3.11	5.07	0.49	0.82	86.05	1.87	0.23	0.13
22/08/07	62.40	3.26	6.49	0.47	0.87	65.73	1.51	0.14	0.14
07/08/07	25.62	----	----	0.49	1.39	56.34	3.22	----	----
15/08/07	222.70	----	----	0.85	1.71	86.59	1.56	0.20	0.12
29/08/07	15.48	4.56	19.19	0.40	0.57	46.43	12.92	0.07	0.11
12/09/07	32.46	4.85	11.31	0.21	0.64	13.73	24.33	0.03	0.12
18/09/07	36.67	2.08	6.08	0.67	1.34	64.51	2.26	0.16	0.15
26/09/07	41.16	2.63	6.72	0.42	1.91	55.87	1.70	0.16	0.14
02/10/07	23.61	3.99	10.69	0.37	3.96	31.36	----	0.24	0.13
11/10/07	49.89	2.72	5.20	0.41	0.52	38.83	3.36	0.21	0.15
16/10/07	37.04	3.98	9.64	0.41	0.95	35.51	3.27	0.00	0.51
24/10/07	26.44	4.53	12.39	0.45	1.39	23.66	9.97	0.05	0.11
01/11/07	42.47	2.66	4.64	0.62	1.52	38.38	1.44	0.41	0.18
08/11/07	1.24	3.66	7.20	0.44	31.59	4.15	0.23	0.28	----
26/11/07	0.63	0.96	----	----	29.50	1.56	0.45	0.15	----
13/12/07	0.86	2.22	3.71	0.47	25.99	0.72	0.38	0.15	----